THE UNIVERSITY
of EDINBURGH

Adipose tissue macrophage heterogeneity and the role of Tim4^{+} macrophages in lipid homeostasis

Marlène Sophie Magalhaes Pinto

Doctor of Philosophy

The University of Edinburgh

2018

Declaration

I hereby declare that all work carried out during this PhD was performed by myself, unless otherwise stated, under the supervision of Dr. Cécile Bénézech and Prof. Karen Chapman. This thesis has not previously been submitted for any other degree or qualification.

Marlène S. Magalhaes Pinto Date

Acknowledgements

First, I would like to thank Cécile Bénézech for her extraordinary support and trust. Our meetings always nourished my thought process and developed my motivation. You are a true inspiration for everybody, not only by your scientific achievements but also the balance with your personal life, your kindness and your remarkable spirit and intelligence. I would also like to thank Karen Chapman for her great support, help and encouragement. It was greatly appreciated, coming from such a remarkable person.

You can only feel empowered after having such great women surrounding you, but it would not go without a huge thanks to Lucy Jackson-Jones, who was more than a post doc in the #TeamBenezech. She has been an infinite source of science chat, biscuits and someone to look up to. A giant Thanks, you will be a wonderful PI!

I would like to thank all the people that helped me. First Steven Jenkins, whose enthusiasm for science and input of ideas made my PhD reviews very enjoyable. Calum Bain and Ruairi Lynch who showed me the art of mastering BM chimera generation and also how to truly enjoy going to conferences. Thanks to the people in the CVS department, in particular Margaret Heck, Zoi Michailidou, Will Cawthorn and Rod Carter for their expertise and advices. Many thanks to the Flow lab (Shonna, Will) and the CALM facility for their technical help and for their enthusiasm at doing their jobs. Thanks to the Ann Walker Animal Unit, who have been wonderful and always so agreeable to be around, even after some of my last minute requests, or the fact that I did not always understand what they were talking aboot, aye!

Thanks to the Lunch Gang who integrated me into their table since day 1 with a special mention to Kate who stayed to enlighten my coffee breaks with good gossips and laughs. Special thanks to some special people who I have shared more than a bench with: Clare and Raphaël, you showed me how nerve wracking it will be to write a thesis but that if you have good friends to support you, it will be okay. I am very proud of Amelia who lost some hair but has finally finished writing her thesis (almost): we should write a song about this on a Loch. MayfieldCrew: we shared laughs, salads, plagues, bad movies, good movies, first dates (literally)… You showed me how

important it was to know where the bottle opener is, especially for the thesis writing part, and how all these little things combined can create friends for life. Huge thanks to Cat, my favourite partner in crime. You helped me to keep sane with craft beers at Andrew's, music, delicious Chilli and the "bits" of yourself that you added in those moments, you are the best. Thanks also to Loan and Corina (and their new addition little Elliot) who have been my friends way before the start of this PhD and this might not even have happened without them.

To finish I would like to thanks my friends and family. Merci à Cindy, tu comprends ce que sont de longues études et à toi d'écrire ta thèse! Merci à mes potes de toujours en particulier Laeti, Sarah et Ziad (mais si tu lies ça, tu en fait aussi partie). Merci à Laura et Nas, vous m'avez montré la route, et quelle route (la route du Still, du 101 et la route de thèse)! Grand merci à mes 2 super grandes « petites » sœurs Cathy et Patricia, ainsi que ma famille. Votre soutien et confiance a été top même si vous avez essayé de m'inviter à bien trop d'apéro et de vacances… Et enfin, merci à mes parents, Joaquim et Maria, qui sont mes plus grands model. Votre travail acharné et votre vie sont un exemple à suivre. Minha gratidão por vocês jamais poderá ser demonstrada com palavras. Obrigada por fazerem de mim, a pessoa que sou hoje. Et une pensée pour Rosa et José.

TABLE OF CONTENTS

Abstract

Resident macrophages are essential for the maintenance of tissue homeostasis as they participate in clearance of apoptotic cells and tissue remodelling and repair. In recent years, there has been an increased interest in the study of adipose tissue macrophages (ATMs). In lean individuals, ATMs are important for the control of insulin sensitivity, thermogenesis, angiogenesis and adipose tissue development. In obesity, the number and phenotype of ATMs is altered, and is associated with chronic low grade systemic and local inflammation. These "pro-inflammatory" changes are postulated to contribute to the manifestation of metabolic syndrome. These findings have suggested that the pool of ATMs is heterogeneous and may change, especially during obesity. To date, the characterisation of ATMs has been limited largely to the F4/80/CD11b markers, however the hypothesis of this thesis is that ATMs have distinct phenotype and function that could influence, in different ways, tissue homeostasis. This thesis aims to characterise and phenotype ATM subsets in order to better understand their potential specific role in the tissue. During the course of this research, a novel population of $Tim4^+$ resident ATMs were identified. An additional aim of this thesis was to elucidate their role in adipose tissue homeostasis.

Partial bone marrow chimeras were used to identify macrophage origin. The main AT depots were shielded from irradiation and a donor BM was injected intravenously. After 8 weeks, the origin of macrophages was analysed using flow cytometry. Tim4, a phosphatidylserine receptor mediating phagocytosis of apoptotic cells and a marker found on resident macrophages in other tissues, was used for the first time in adipose tissue. Four subsets of ATMs were identified: $F4/80^{high}CD11c^-Tim4^+$, $F4/80^{high}CD11c^-Tim4^-$; $F4/80^{low}CD11c^+Tim4^-$; $F4/80^{low}CD11c^-Tim4^-$. Interestingly, this newly described $F4/80^{high}Tim4^+$ ATM subset showed the lowest non-host chimerism compared to the other ATMs, suggesting this is a main self-replenishing resident ATM population.

To study the impact of obesity on ATM turnover, partial chimeric mice were fed HFD for 8 weeks. This increased the number of macrophages in AT. However, the different subsets of ATMs were differentially affected by the diet. Indeed, only a small proportion of $Tim4^+$ ATMs derived from the bone marrow. In contrast, replenishment

of the 3 other subsets was almost fully dependent on the arrival of monocyte-derived cells from the bone marrow.

TIMD4, the gene encoding for Tim4, has been highlighted in genetic studies as being linked with dyslipidaemia. This suggests that $Tim4^+$ ATMs might play a role in lipid homeostasis. Further characterisation of Tim4 ATMs demonstrated that these $Tim4^+$ ATMs are highly charged in neutral lipid, and also have an increased lysosomal activity (shown by lysotracker staining) compared to the other ATM subsets. Using blocking anti-Tim4 antibodies in vivo, I found that Tim4 contributed markedly to free fatty acid (FFA) release into the plasma after short-term and long term HFD feeding. In addition, in vitro and in vivo experiments demonstrated that Tim4 could be required for the uptake of neutral lipids and their integration into lysosomes for degradation, though this seems to be dependent on the nature of the lipid.

Collectively, these results indicate that Tim4 plays a crucial role in the control of lipid trafficking under conditions when dietary lipid is in excess. Tim4 allows uptake of lipids by $Tim4^+$ ATMs and subsequent release of FFA into the circulation. Finally, the presence of $Tim4^+$ lipid laden ATMs was demonstrated in the human omentum. This finding may lead to the discovery of new targets to improve metabolic health in obese patients.

This work stresses the importance of resident ATM population in body lipid homeostasis as they could be involved in coping with lipid availability in the body and influence the amount of FFA in the plasma.

Lay Summary

Obesity is a worldwide problem. It is associated with other diseases such as type 2 diabetes, cardiovascular problems (atherosclerosis, heart attack) and cancer. During obesity, the dramatic expansion of fat tissue (which stores excess energy in a form of fat called triglyceride) is accompanied by an increase in white blood cells that move into the tissue from the blood in a process called inflammation. Inflammation usually occurs at sites of injury or infection and normally involves the recruitment white blood cells to the injured tissue so they kill the microbes or eliminate dead cells and help repair the tissue. In the context of obesity, the capacity of the fat cells to store excess energy (in the form of triglyceride, a lipid or fat) is exceeded and the fat cells become dysfunctional and die. Macrophages (derived from the Greek meaning big [macro] eater [phage]) are one of the main populations of white blood cells that are recruited to the tissue during inflammation, notably to clear and remove the dead cells. But in this process they also release signals that recruit more white blood cells and by doing so they participate in the inflammatory process.

In order to understand how macrophages work during obesity and what they do in fat tissue, it is important to know what these cells are and if (under the umbrella description of macrophages as a key cell type), subtypes exist with different roles in the tissue. The aim of this thesis was to identify subtypes of macrophages within adipose tissue of mice, using specific cellular tags (markers), and to study the role of one particular macrophage subset that was identified, tagged with Tim4. Tim4 is a marker on the surface of macrophages that is usually involved in the recognition of dead cells.

Normally during inflammation, the bone marrow produces fresh macrophages which travel via the blood to enter the inflamed tissue. Here, using mice as an experimental system, it was found that during the inflammation that is associated with obesity, not all macrophages found in adipose tissue come from the bone marrow. Indeed, macrophages identified by their Tim4 tag were able to multiply themselves in the adipose tissue of mice fed a HFD. Furthermore, these Tim4-tagged cells contained an expansion of structures within cells called lysosomes. Lysosomes are an acidic compartment of the cell which functions as a “recycling centre”, breaking down

protein and lipid molecules for re-use in other parts of the cell. Moreover, these Tim4-tagged macrophages were able to pick up (phagocytose, or "eat") more lipids from the surrounding tissue than other macrophages were.

In experiments in mice, blocking Tim4 activity led to a decrease in macrophage uptake of lipid molecules and the ability of the lysosomes in macrophages to act as recycling centres. The ingestion of a fat-rich meal normally increases lipid (in the form of free fatty acid) in the blood. However, blocking Tim4 activity prevented the normal increase in free fatty acids in the blood, indicating a role for Tim4 in the release of free fatty acids after fat feeding. These observations suggest that Tim4 tagged macrophages in adipose tissue, by virtue of their lysosomes, can break down large lipid molecules (such as triglycerides) into free fatty acids for release into the blood. In conclusion, this research has identified a new pathway controlling the levels of free fatty acid in the blood which could be targeted in the future for the treatment of obesity associated diseases.

Publications

Magalhaes M.S., Jackson-Jones L.H., Bain, C., Hawley, C., Lynch, R., Michailidou, Z., Jenkins, S.J. and Benezech C. (In preparation, 2019) Adipose tissue macrophages and the role of Tim4 in lipid metabolism.

Jackson-Jones L.H., Duncan, S.M., **Magalhaes M. S**., Campbell, S., Maizels, R.M.M., McSorley H.J., Allen, J.E. and Benezech C.B. (2016) Fat Associated Lymphoid Clusters are IL-33R dependent Sites of B Cell Proliferation and local IgM Production. Nature Communications 7, 12651 DOI 10.1038/NCOMMS12651

Jackson-Jones L.H., **Magalhaes M.S.,** Mylonas, K., Garcia, M., Mole, D. and Benezech C. (In preparation, 2018) The omentum is a critical site for neutrophil recruitment and NETosis during peritonitis

Abstracts from thesis

Macrophage satellite symposium 2018 (Edinburgh, UK) (Oral presentation) "Adipose tissue macrophages : hungry for fat"

Edinburgh Immunology Group Summer Symposium 2018 (Oral presentation) "The role of $Tim4^{+}$ adipose tissue macrophages in lipid metabolism"

Keystone Symposia Myeloid cells, 2018 Breckenridge USA (Poster presentation)

Macrophages in the single cell era, 2017 Ghent (poster presentation)

Edinburgh Immunology Group summer symposium, Edinburgh. UK (Poster presentation)

British Society for Immunology Congress, Liverpool, UK, 2016 (Oral presentation) "Defining the heterogeneity of adipose tissue macrophages at homeostasis and during obesity" Keystone Symposia Myeloid cells, 2016 Killarney (Ireland) (Oral presentation)

Abbreviations

AA: amino acid

ABCA1: ATP-binding cassette A1

AGM: aorta-gonad-mesonephros

ALOX: arachidonate lipoxygenase

AMPK: 5′-adenosine monophosphate activated protein kinase

AT: adipose tissue

ATMs: adipose tissue macrophages

ATP: adenosine tri phosphate

BM: bone marrow

BMI: body mass index

BSA: bovine serum albumin

CCL: C-C chemokine ligand

CCR2: C-C chemokine receptor type 2

CD: control diet

CE: cholesteryl esters

CLS: crown-like structures

CM: chylomicrons

CSF1r : colony-stimulating factor receptor

DC: Dendritic cell

EdU: 5-ethynyl-2′-deoxyuridine

EMPs : erythromyeloids progenitors

FA: fatty acid

FABP: fatty acid binding protein

FACS: fluorescence activated cell sorting

FAO: fatty acid oxidation

FL: fetal liver

g: gram

GAT: gonadal adipose tissue

GLUT: glucose transporters

GWAS: genome wide association studies

HDL: high density lipoprotein

HFD: High fat diet

IFN: interferon

IL: interleukin

ip: intraperitoneal

iv: intravenous

LAL: lysosomal acid lipase

LDL: low density lipoprotein

LDLr: low density lipoprotein receptor

LO: lipoxygenase

LpL: lipoprotein lipase

LPS: lipopolysaccharide

M-CSF: macrophage colony-stimulating factor

MCP1: Monocyte chemoattractant protein 1

MERTK: myeloid-epithelial-reproductive tyrosine kinase

MES: mesenteric

NBF: neutral buffered formalin

NF: nuclear factor

oxLDL: oxidised low density lipoprotein

OXPHOS: oxidation phosphorylation

PBS: phosphate buffer saline

PPAR: peroxisome proliferator-activated receptor

PS: phosphatidyl serine

RELMα: Resistin-Like Molecules

SAT: subcutaneous adipose tissue

SR: scavenger receptor

SREBP: sterol regulatory element binding proteins

STAT: Signal transducer and activator of transcription

TG: triglycerides

TGF: transforming growth factor

Tim: T-cell immunoglobulin and mucin domain containing protein

TLR4: toll like receptor 4

TNF: tumour necrosis factor

Treg: T regulatory cell

UCP1: uncoupling protein 1

VLDL: very low density lipoprotein

VLDL: very low density lipoprotein

VLDLr: very low density lipoprotein receptor

WHR: waist to hip ratio

WT: wild type

YS: yolk sac

List of figures

List of tables

CHAPTER 1 INTRODUCTION

1.1 Overview

The last decade brought to macrophage biology a revolution in terms of what researchers thought they knew about these innate immune cells. Historically, macrophages were believed to derive from bone marrow (BM) recruited monocytes differentiating in tissues (Davies et al. 2013). However, astonishingly, studies pointed out that macrophages can proliferate and be maintained independently from the BM, which gave rise to further questions about the initial origin of these resident cells (Davies et al. 2013). Adipose tissue macrophages (ATM) have been highlighted in studies about obesity, both in human and mice, as they represent the main subset of immune cells in the fat tissue and that their increase in number has been linked to the low grade inflammation associated with the metabolic complications of obesity (Weisberg et al. 2003; Carey N Lumeng, Bodzin, and Saltiel 2007). However, ATMs are still lacking from the most recent reviews about resident macrophages in tissues : it is not clear if all macrophages are recruited to the tissue (monocyte derived) or if a resident self-replenishing population exist. Moreover, ATMs fulfil different roles, and their heterogeneity of function in the tissue seem unappreciated(Thomas and Apovian 2017). After defining what is adipose tissue and obesity, this introductory chapter will give an insight into what we know of the role of macrophage in adipose tissue but also what we can learn about macrophage biology, origin and metabolism in other tissues that can be transposed to AT.

1.2 White adipose tissue, lipid homeostasis and obesity

1.2.1 White adipose tissue: localisation and role

White adipose tissue (WAT) is the principal site of energy storage in mammals. In healthy men and women, WAT represent 20 and 30%, respectively, of the body mass (Morigny et al. 2016). The energy is stored as fat in adipocytes, each one containing a unilocular lipid droplet made of triglycerides (TG) which are 3 fatty acids (FA) esterified on 1 glycerol. The rest of the tissue is composed of various other cell types such as preadipocytes, immune cells, endothelial cells, fibroblasts and nerves, collectively named stromal vascular fraction (SVF). WAT depots are found across the human and mouse body, the main depot being the visceral adipose tissue (VAT) and

the subcutaneous adipose tissue (SAT). In mouse, the VAT can be divided into gonadal AT (GAT) also called epididymal AT, mesenteric AT (Mes AT), omental AT, retroperitoneal AT, mediastinal AT and pericardial AT.

If there is a positive energy balance, the role of WAT is to store lipids and avoid ectopic storage. A prolonged excessive energy intake, which exceeds energy expenditure, results in obesity which is defined as an enlargement of the fat mass detrimental to health (WHO definition). The World Health Organisation recognised that in 2016, 650 million adults were obese ("WHO | Obesity and Overweight" 2018). A body mass index (BMI) superior to 30 kg/m^2 is an indicator of obesity, however fat distribution is also an important factor, as measured by the waist to hip ratio (WHR). The "pear shape" characterises people with WAT accumulation around the hips (below the waist) while the "apple shape" is a central accumulation (above the waist). After being adjusted to the BMI, central WAT accumulation (or VAT accumulation in the abdomen), is more often associated with chronic diseases such as type 2 diabetes and cardiovascular diseases (Matsuzawa et al. 1995; Fu, Hofker, and Wijmenga 2015). Indeed, the "Framingham Heart Study" gathered data of around 3000 people and showed a stronger correlation between VAT, compared to SAT, with different health risk factors, such as hypertension and increased fasting glucose (Fox et al. 2007; McLaughlin et al. 2011). As such, obese VAT has been at the centre of numerous studies. In humans the VAT is mostly represented by the omental AT (omentum). In comparison, mouse omental AT is a small tissue that only minimally store fat but have important immunological functions (Benezech et al. 2015; Jackson-Jones et al. 2016). The murine VAT studied during obesity is the GAT, as this is the one expanding the most with high fat diet (HFD) and linked with metabolic disorder (van Beek et al. 2015).

WAT responds to negative energy balance through lipolysis. Lipolysis is an enzymatic process by which AT releases the FFA contained in their lipid droplets to the bloodstream to accommodate organ energy demand. Indeed FA can be oxidised (FAO) by tissues to produce ATP (Stern, Rutkowski, and Scherer 2016; Duncan et al. 2007). How FFA are exported from adipocytes is not very clear yet, but fatty acid binding protein (FABP) 4 guide FFA to the plasma membrane for secretion (Nielsen et al.

2014). Insulin acts as an anti-lipolytic signal, favouring glucose uptake by tissues, by upregulating glucose transporters (GLUT) 1 and 4 (Stern, Rutkowski, and Scherer 2016). Obesity is often associated with insulin resistance and elevated glycemia. Obese individuals have abnormally elevated basal lipolysis which results in elevated circulating FFA (Stern, Rutkowski, and Scherer 2016). But this is not the only lipid found to be in abnormal levels during obesity.

1.2.2 Obesity, lipid metabolism and low grade inflammation

The main dietary lipids found are TG, cholesterols, phospholipids (PL), cholesterols esters (CE) and FFA. FFA are brought to the tissue either directly as short chain, or in chylomicrons (CM) which are synthetized by enterocytes in the small intestine (Feingold and Grunfeld 2000). CMs gain the bloodstream via the lymphatics and once in circulation, go to the peripheral tissues where they are hydrolysed by lipoprotein lipases (LpL) in order to diffuse and be used by the cells (oxidation). The CM remnants (CMr), now richer in cholesterol as they lose TG, go back to the liver, which secretes in exchange very low density lipoproteins (VLDL) back to the circulation. The remnants VLDL are hydrolysed by the liver, to become low density lipoproteins (LDL) very rich in cholesterol and pro-atherogenic if in excess (Figure 1.1). LDL are internalised via binding to the LDL-Receptor (LDL-R) at the cellular membrane before being hydrolysed into cholesterol in acidic organelles, called lysosomes. The transcription factor SREBP (sterol regulatory element binding proteins) will stimulate LDL-R synthesis when low levels of cellular cholesterol are detected (Horton, Goldstein, and Brown 2002). Finally, remaining cholesterol excess is returned to the liver by high density lipoproteins (HDL) in order to be excreted (Feingold and Grunfeld 2000; Jaishy and Abel 2016).

Fifty to 60% of obese patients present dyslipidaemia (increased plasma levels of TG, LDL and VLDL and a decrease in HDL), and this represents a major risk factor for the development of cardiovascular disease (Feingold and Grunfeld 2000) (Mittendorfer 2011). Excess LDL and more generally hyperlipidaemia, can lead to lipid accumulation in arteries that cause fatty steak formation and atherosclerosis. Macrophages in these atherosclerotic plaques form lipid rich cells called foam cells and participate in inflammation (Moore and Freeman 2006). Additionally, the reduced

suppression of AT lipolysis and the increase in FFA coming from the diet results in elevated plasma FFA in obese individuals compared to lean subjects, which is linked with insulin resistance (Boden 2008). Lowering plasma FFA can restore insulin sensitivity (Boden 2008).

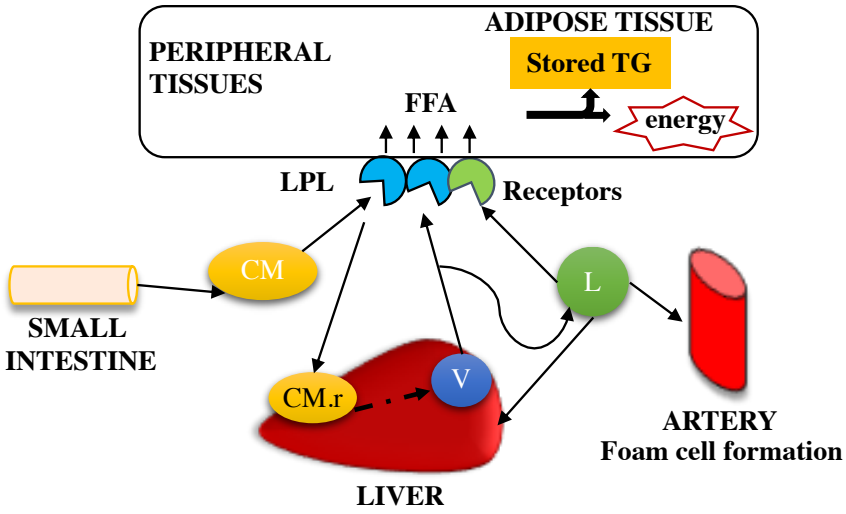

Figure 1.1 Lipoproteins synthesis and use

After a meal, enterocytes synthesize CM which quickly enter the blood circulation to be distributed to organs. The CM remnants go to the liver where they are used to create VLDL. VLDL in the circulation are used as energy or transformed as LDL. Excess lipids are brought to the adipose tissue to be stored as an energy source which can be mobilised when needed. Excessive levels of LDL in the blood can cause accumulation of foam cells in artery walls (atherosclerosis). **CM**: chylomicron; **CM.r**: chylomicron remnant; **V** : VLDL; **L** : LDL;**LPL** : lipoprotein lipases; **FA**: Fatty acid; **TG**: triglycerides

Obesity is also accompanied by a chronic low grade inflammation which favours the development of non-alcoholic fatty liver disease, type 2 diabetes and cardiovascular diseases, all factors linked with an increase in morbidity (Reilly and Saltiel 2017). The primary trigger of inflammation is uncertain and probably multifactorial. Pathological AT expansion, by hypertrophy or hyperplasia, is associated with increased apoptosis, increase release of pro-inflammatory cytokines such as IL-6 and IL1β and a toxic uncontrolled lipid spill over which can then accumulate in other tissues (Kanneganti and Dixit 2012). FFA themselves can trigger

inflammation by binding toll like receptors (TLR) which promotes expression of genes involved in inflammation via the nuclear factor (NF) κB signalling pathway (Reilly and Saltiel 2017). Numerous studies mentioned a drastic upsurge of macrophages in AT that appear to be one driver of inflammation (Weisberg et al. 2003; M. T. A. Nguyen et al. 2007; A. A. Hill, Reid Bolus, and Hasty 2014; Ferrante 2013). The understanding of AT macrophage biology is still in progress and majorly linked to their role during obesity. First I will review some general knowledge about macrophage biology and then focus on adipose tissue macrophages (ATMs), as many elements can be transposed.

1.3 Macrophage heterogeneity

1.3.1 Recruited and resident macrophages

The first description by Elie Metchnikoff of macrophages was simple: large cells (macro) capable of eating (phage). He described those cells as the "balayeur" (translated as "sweeper"), related to their great ability of phagocytosis (Metchnikoff 1892). Traditionally, macrophages were designated as being exclusively derived from blood circulating monocytes coming from the bone marrow (BM) and entering the tissue (van Furth and Cohn 1968). Circulating monocytes are short lived and their number in the blood is dependent on the C-C chemokine receptor type 2 (CCR2). Indeed, *Ccr2*$^{-/-}$ mice have a drastic reduction in circulating monocytes, as they fail to exit the bone marrow upon CCL2/CCL7 (CC-chemokine ligand 2 and 7) mediated recruitment (Tsou et al. 2007). Those 2 chemokines (also known as MCP1 and MCP3), released by tissues, target inflammatory Ly6c^{high} monocytes to go to inflamed sites (Epelman, Lavine, and Randolph 2014a; Shi and Pamer 2011). Infiltrated Ly6c^{+} monocytes downregulate Ly6c and upregulate the major histocompatibility complex class II (MHCII) (Tamoutounour et al. 2012; C C Bain et al. 2013). In Human, 3 subsets of monocytes are characterised using CD14 (LPS co-receptor) and CD16 (FcγRIIIA): classical (CD14^{++}CD16^{-}), intermediate (CD14^{++}CD16^{+}) and non-classical (CD16^{++}CD14^{+}) monocytes (Geissmann, Jung, and Littman 2003). "Recruited" macrophages appear mainly during the innate phase of infection to fight pathogens with, notably, the production of proinflammatory factors (Helming 2011). However, characterising macrophages and macrophage role(s) in tissues and during infection led

to acknowledgement of their heterogeneity and notably the presence of tissue resident macrophages (Wynn and Vannella 2016). For instance, resident macrophages show a distinct gene expression profile compared to BM recruited macrophages, as well as distinct functions (Gundra et al. 2014). Resident macrophages play important roles during wound healing, resolution of inflammation, development, and maintain tissue homeostasis (Epelman, Lavine, and Randolph 2014b). In some cases, monocytes do participate in resident macrophage expansion in tissues, notably in the intestine, dermis and heart in a CCR2 dependent manner (Calum C Bain et al. 2014; Epelman et al. 2014). However the origin of these residents cells in adult tissues has been shown to be more complex than the classical monocyte to macrophage transition as studies showed that macrophages can be maintained independently from the BM and have an intrinsic capacity to self-renew in tissues, notably dependent on IL-4 and colony stimulating factor 1 (CSF1) (Jenkins et al. 2011; Komornik 1985; Davies et al. 2011; Jenkins et al. 2013a). Recently, researchers emphasized the fact that macrophages from a tissue can have various origins but to determine this, distinguishing subsets is primordial (Shaw et al. 2018). Indeed, using CD4 and Tim4 as surface markers, they realised that the gut does have a subset of $CD4^{-}Tim4^{-}$ macrophages highly dependent on the BM, while $CD4^{-}Tim4^{+}$ had a low dependency and the $CD4^{+}Tim4^{+}$ subset was maintained independently from the BM(Shaw et al. 2018). Interestingly, early during the course of inflammation, resident macrophages are partially depleted (known as the "disappearance reaction"), notably in the liver, the epidermis, the lungs and the peritoneal cavity. Surviving macrophages then go through a high proliferative activity to repopulate the tissue (Davies et al. 2013, 2011). During obesity, AT is considered as a site of sterile inflammation, raising the question of whether a disappearance reaction exists too. In the past decade, a paradigm shift occurred in the macrophage field as the embryonic origin of resident tissue macrophages was discovered, first in brain and epidermis (Davies and Taylor 2015). Macrophage tissue origin is a fascinating topic, and most tissues have their ontogeny covered, with the exception of ATMs which are still missing from major recent reviews (Hoeffel and Ginhoux 2015; Ginhoux and Guilliams 2016; Epelman, Lavine, and Randolph 2014b). However, we can still learn from these tissues to grasp an idea of the possible origin of ATMs.

1.3.2 Origin of tissue resident macrophages

Method of study: generation of BM chimeras

To understand the origin of tissue macrophages, during inflammation for example, BM chimeras can be generated. This method consists of the irradiation of a recipient/host followed by intravenous (iv) transplantation of histocompatible donor bone marrow, generally isolated from femurs. The donor's cells re-populate the irradiated hematopoietic system and, after 2 to 3 weeks, leukocytes from the donor are detected in the host (Duran-Struuck and Dysko 2009). Total body irradiation uses a dose of gamma of about 9.5 Gray. A modified protocol includes the protection of body cavities from irradiation, inducing chimerism in blood monocytes, but sparing resident macrophage eradication (Aparicio-Vergara et al. 2010). Engraftment can then be followed over time: if the rates stay low, it is very likely that the macrophage population persists independently from the BM / blood monocytes. Other method of study exists, such as fate mapping, which are more relevant to understand embryonic origins of cells as I will describe in the following paragraph.

Ontogeny

M. Naito and K. Takahashi described immature macrophages (F4/80 "weak" and lacking phagocytic activity) by microscopy, localised in the blood islands of the embryonic mouse yolk sac (YS), a membranous vesicle attached to the embryo, at embryonic day 9 (E9) and the foetal liver (FL), which is the main hemopoietic organ in the embryo, at E10 (K. Takahashi, Yamamura, and Naito 1989). The first fate mapping studies showed that in the adult, brain macrophages (microglia) had a YS origin (Ginhoux et al. 2010) while Langerhans cells (skin macrophages) were coming from the FL, with a minor participation of YS progenitors (Hoeffel et al. 2012). Later on, the embryonic origins of liver, spleen, lung and peritoneal macrophages were also confirmed (Yona et al. 2013). Typically, macrophages issued from the YS acquire a F4/80^{high} (or bright) phenotype in contrast with HSC derived macrophages that are F4/80^{low} (Schulz et al. 2012a). Most tissues retain pre-natal macrophages that persist in the tissue by proliferation. Nonetheless, these populations are replaced in a time, organ and sex dependent manner by HSC derived cells (Perdiguero and Geissmann 2016). In a nutshell, macrophage generation in adults seems to be relying on either YS

erythromyeloid progenitors (EMPs), FL derived monocytes, or embryonic hematopoietic stem cells (HSC) (Gomez Perdiguero et al. 2014; Hoeffel and Ginhoux 2015; Sheng, Ruedl, and Karjalainen 2015) (Figure 1.2).

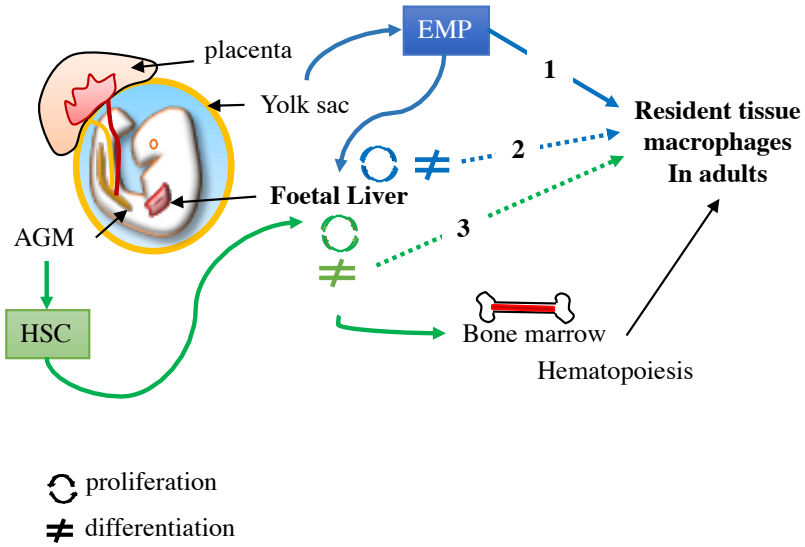

Figure 1.2 Three coexisting models of macrophage origin in adult tissues

Three models of macrophage ontogeny have been hypothesised. Macrophages in adult tissue can originate from (1) YS EMPs (Gomez Perdiguero et al. 2014), (2) FL monocytes (Hoeffel and Ginhoux 2015), or (3) FL HSC (Sheng, Ruedl, and Karjalainen 2015). These embryonically derived macrophages persist in tissues by proliferation. HSCs are generated in the aorta-gonad-mesonephros (AGM) region prior to seed the FL. HSCs colonise the BM at E15, where haematopoiesis is detected from E17 and give rise to monocytes in adults mouse which will replace embryonic derived macrophages in a time and organ specific manner.

1.3.3 Macrophage activation

External stimuli can "activate" macrophages, skewing their response towards the synthesis of pro-inflammatory or anti-inflammatory cytokines. Macrophages are generally classified as M1 (classically activated) or M2 (alternatively activated). The M1/M2 nomenclature comes from older studies which defined macrophage populations based on their cytokine production, mainly done *in vitro* (Mackaness 1962; Stein et al. 1992). M1 polarisation occurs when macrophages are stimulated with LPS or IFN γ. These macrophages produce pro-inflammatory cytokines (e.g.: IL-6, TNFα, IL-1β) and are microbicidal (Martinez and Gordon 2014). On the other hand,

M2 polarisation occurs when macrophages are stimulated with IL-4 or IL-13 which result in anti-inflammatory cytokine production such as IL-10 and TGF. M2 macrophages promote tissue remodelling, angiogenesis and tumour growth (Martinez and Gordon 2014). From there, researchers described macrophages in tissues to be more M1 or M2 like and associate them with specific markers, which are still widely used in AT (Martinez and Gordon 2014). For example the M1/M2 markers applied by flow cytometry and fluorescence activated cell sorting (FACS) to ATMs are represented in the table below (Table 1-1)

Table 1-1 M1/M2 markers associated with ATMs in mouse and human

		ATM (pan markers)	**M1**	**M2**
Mouse	**Proteins**	F4/80; CD64; CD115; CD68	CD11c; TLR4; CCR2; CCL2	CD206 ; CD301 ; Ym1 ;Arg1;
	Genes	*Emr1 CD68*	*Tnfα; Il6; Ccl2, Nos2*	*Il10 ; Arg1, Mrc2, Mgl2, Clec7a, Stat6, Vegf*
Human	**Proteins**	CD14; CD68	CD11c; TLR4; CCR2	CD206; CD163; IL10
	Genes		*Mcp1; Tnfα ;*	*Il10; Tgfβ*

Adapted from Hill *et al.* 2014 (A. A. Hill, Reid Bolus, and Hasty 2014)

However, this convenient nomenclature does not reflect the real complexity of the *in vivo* biology. The entrance in the genomic era and the advance characterisation of macrophages in tissues shows that macrophages can indeed express both “M1” and “M2” markers (Davies and Taylor 2015).

1.4 Adipose tissue macrophages

1.4.1 Maintaining a healthy AT: a balancing act for immune cells

Healthy AT is home to various immune cells that act to remodel the tissue and maintain its functions. Lean AT contains anti-inflammatory (Th2-like) cells such as M2 macrophages, eosinophils, T regulatory cells (Treg) and invariant Natural Killer T (iNKT) cells. They generally produce IL-10 which can repress tumor necrosis factor (TNF) α and control inflammation (Ferrante 2013). Discovered only recently in AT, iNKT are present in the murine and human AT and maintain tissue homeostasis (Lynch et al. 2012). Obesity reduces their number in the tissue but restoring or activating them shows positive outcomes such as insulin and glucose sensitivity improvement (Lynch 2014). AT $Foxp3^{+}CD4^{+}$ Tregs express high levels of peroxisomes proliferator activated receptors (PPAR) γ compared to lymphoid organ Tregs. Their specific deletion inhibits drug-induced insulin sensitizing (Cipolletta et al. 2012). AT Tregs reduce AT inflammation and promote insulin sensitivity notably by their action on macrophages, adipocytes and T cells. Their loss, in obese AT, aggravates insulin resistance (Feuerer et al. 2009; Tiemessen et al. 2007). Eosinophils are important IL-4 producers, link to the promotion of M2 activation via the signal transducer and activator of transcription 6 (STAT6), the improvement of insulin sensitivity (Wu et al. 2011; Odegaard et al. 2007), but also the reduction of AT inflammation, decrease body weight and AT mass (Ricardo-Gonzalez et al. 2010). Surprisingly, helminth infection promotes eosinophilia and M2 macrophages in WAT and consequently improves metabolic function and notably, insulin sensitivity and glucose tolerance in HFD fed mice (Hussaarts et al. 2015).

During obesity, the immune balance is disturbed and leans towards inflammation, notably with a "switch" of macrophage phenotype that I will further describe (Schipper et al. 2012; Ferrante 2013). Figure 1.3 summarises the principal changes in immune cells and cytokines produced during obesity.

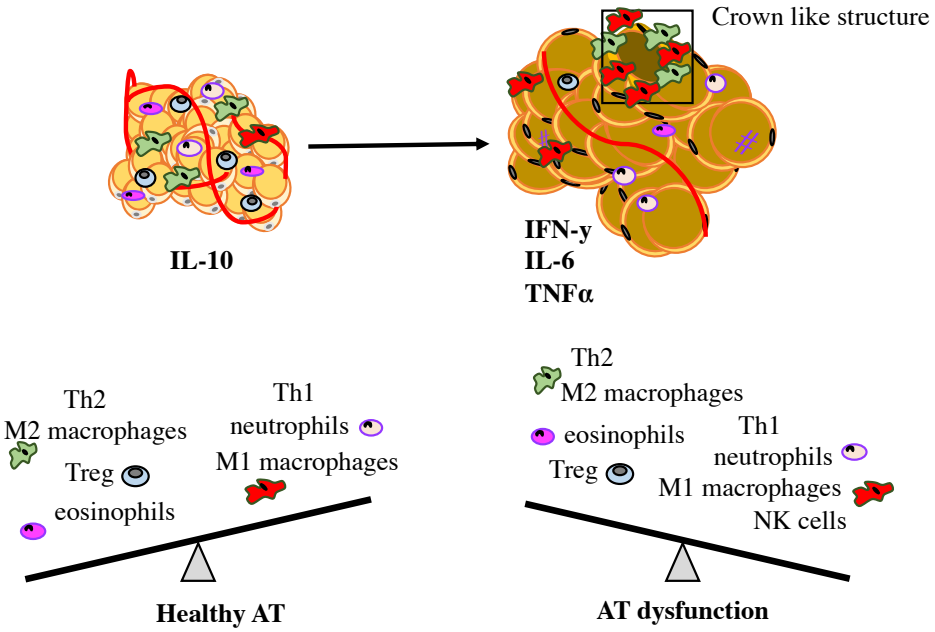

Figure 1.3 Immune cells in AT in lean and obese

Lean AT contains various anti-inflammatory immune cells, such as eosinophils, resident macrophages, Th2 cells, Treg cells important for AT homeostasis. In obese AT, pro-inflammatory immune cells infiltrate the tissue and promote cytokines production that perturb AT functions. Adapted from Choe et. al (Choe et al. 2016).

1.4.2 ATM roles and "switch"

ATMs in lean AT promote insulin sensitivity notably because they are able to secrete IL-10, but also by removing dead cells and maintaining a healthy tissue (Osborn and Olefsky 2012; Lumeng, Deyoung, and Saltiel 2007). Macrophage infiltration in AT during obesity is one of the major elements occurring during the course of fat expansion (Weisberg et al. 2003). Most studies have focussed on ATMs in the context of obesity and on their pro-or anti-inflammatory properties. However, other beneficial roles for ATMs in the maintenance of AT homeostasis have more recently emerged (Figure 1.4)(Thomas and Apovian 2017). ATMs are involved in thermogenesis after cold exposure or β adrenergic stimulation, by promoting FA mobilisation in WAT and increasing uncoupling protein 1 (UCP1) gene expression (Wu et al. 2011; K. D. Nguyen et al. 2011; Qiu et al. 2014). ATMs promote adipogenesis and angiogenesis by secretion of platelet-derived growth factor and vascular endothelial growth factor. Furthermore, depleting macrophages during adipogenesis limits AT development

(Martinez-Santibañez and Nien-Kai Lumeng 2014). Most importantly, recent studies showed a role for ATMs in the control of lipid efflux from AT, highlighting the fact that the net release of FFA from AT might rely on ATMs lipid buffering ability, which will be one of the axis of my thesis (Kosteli et al. 2010a; X. Xu et al. 2013; Boutens and Stienstra 2016).

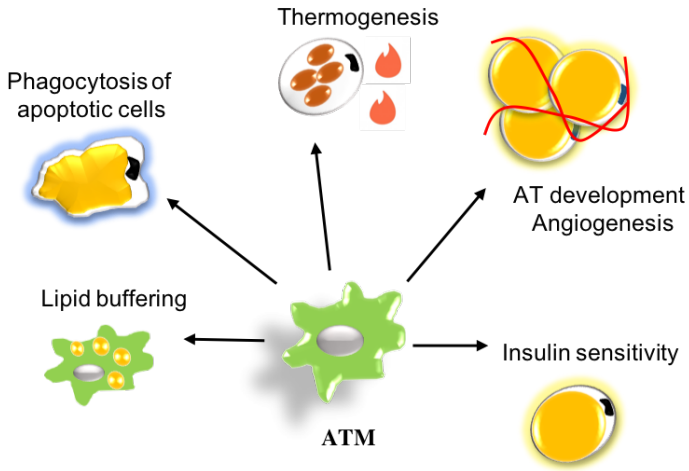

Figure 1.4 ATMs ensure tissue homeostasis
ATMs are involved in lipid buffering, removal of dead cells, thermogenesis in beige subcutaneous adipose tissue, adipose tissue development and insulin sensitivity. Their presence ensures AT homeostasis.

Usually, macrophages represent 5-10% of the stromal vascular fraction (SVF) in lean GAT, but can be multiplied by 5 in obese murine GAT, and by 3 in omental AT in human (from 4% to 12%) (Harman-Boehm et al. 2007; Ferrante 2013). Compared to lean AT, where ATMs are spread out in the tissue, during obesity, 90% of ATMs are regrouped around apoptotic or necrotic adipocytes, in what is called “crown-like” structures (CLS) (Figure 1.5). These structures appear in both mice and humans with obesity (Cinti et al. 2005; Murano et al. 2008; Bigornia et al. 2012).

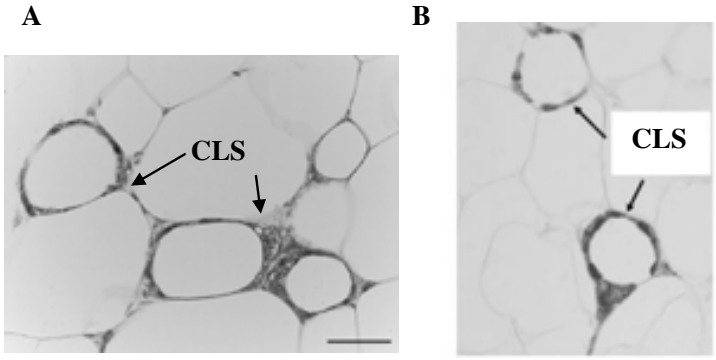

Figure 1.5 CLS in visceral AT in mouse (A) and human (B)
Histological illustrations showing adipocytes surrounded by ATMs, forming CLS (indicated by arrows). **A** From Murano *et al.*, 2008. Scale bar 50 µm **B** From Bigornia *et al.* 2012 (× 40).

As just mentioned, the existence of two states in adipose tissue: lean non inflammatory and obese inflammatory led to the notion of ATM switch from M2 to M1 during obesity (C. N. Lumeng et al. 2008). Lean AT has increased expression of genes associated with an M2 signature such as *Chi3l3, Arg1, Il10.* In contrast, obese AT contains a subset of $CD11c^+$ macrophages, associated with inflammation (*Tnfα*, *Nos2*) (Carey N Lumeng, Bodzin, and Saltiel 2007). Diphtheria toxin (DT) inducible depletion of $CD11c^+$ cells in obese mice reduced inflammation and the recruitment of ATMs in the WAT and ameliorated insulin sensitivity (Patsouris et al. 2008b), thus revealing the role of inflammatory macrophages in the deregulation of insulin sensitivity during obesity. This raised the important question of the exact nature of these ATMs and their origin (recruited or resident).

1.4.3 ATM Recruitment

It was first shown in the early 2000s by Weisberg and colleagues, that in mice prone to obesity, a third of the transcripts coming from the GAT were genes related to macrophages, notably *Csf1r* (also known as CD115) and *Cd68*. By generating fully irradiated chimeric mice, they also showed that 85% of ATMs were coming from the BM (Weisberg et al. 2003). However, full irradiation compromises the tissue as it artificially increases recruitment as explained in 1.3.2. Following this important publication, researchers got interested in the mechanisms controlling macrophage recruitment in obese AT. MCP1 (CCL2) was shown to be elevated in murine obese

GAT (Kanda et al. 2006a). Similarly, in human, several other chemokines, including CCL2, were also found increased in the omentum and serum of obese patients (Huber et al. 2008). MCP1 is produced by a multitude of cells including adipocytes. When FFA arrive in AT, they trigger adipocyte TLR4 activation which initiates an inflammatory response, via NF-κB, and increases MCP1 expression by adipocytes (Reilly and Saltiel 2017). ATMs themselves can produce MCP1 via the same mechanisms (Catrysse and van Loo 2018). MCP1 receptor (CCR2) is expressed by monocytes and recruited macrophages (C. N. Lumeng et al. 2007). Recruitment of monocytes into tissues is CCR2 dependent and *Ccr2*$^{-/-}$ mice exhibit a low monocyte count in their bloodstream, as they fail to exit the bone marrow to be recruited to tissues (Tsou et al. 2007). CCR2 recruited monocytes in AT are pro-inflammatory (M1). They express high level of IL-6, a pro-inflammatory cytokine. However, in *Ccr2*$^{-/-}$ mice, ATMs are still present in the tissue, either as they rely on other recruitment signals or because they could be resident. These cells showed a distinct gene profile (M2-like) compared to the CCR2 recruited macrophages, the latter being more pro-inflammatory (C. N. Lumeng et al. 2007). This study pointed to the fact that ATMs might not all be CCR2 dependent.

1.4.4 ATM Proliferation

Recent studies showed that in addition to increased recruitment of BM derived monocytes, there is an *in situ* proliferation of ATMs during obesity. This was measured by 5-ethynyl-2′-deoxyuridine (EdU) injection, which labelled proliferating cells, 3h before the cull in mice fed with HFD for 7 weeks. EdU labelled 1% of the F480^{+}CD11b^{+} cells (ATMs) in lean AT, whereas it labelled 4.5% in obese AT (Amano *et al.*, 2014). They confirmed this proliferation data by using an intracellular staining of Ki67, a protein expressed during mitosis. Another group strengthened these results and added that the IL-4/STAT6 pathway was one driver of ATM proliferation (Zheng et al. 2016a). Consistently across these publications, proliferating macrophages resided near CLS (Amano et al. 2014; Zheng et al. 2016a). One study showed that these ATMs express M2 (CD206;CD301) rather than M1 markers and the authors found proliferative CD68^{+} ATMs in obese patients, located in CLS (Haase et al. 2014a). The limitation of all these studies is that (i) the relative amount of recruited

and/or proliferative macrophages is hard to determine, (ii) macrophages are analysed as a whole and this does not take into account that ATMs may be heterogenous in terms of their BM dependency and their proliferative capacity. Therefore, there is still clearly a debate about ATM origin during obesity that this thesis will explore.

1.5 Macrophages and lipid metabolism

1.5.1 Lipid buffering properties of macrophages

During fasting, lipolysis is increased to meet organ's demand in energy. (Kosteli et al. 2010b; Fitzgibbons and Czech 2016). Obese mice put on calorie restriction accumulated ATMs at day 3, which was quantified by *CD68* and *Emr1* (F4/80) gene expression, but was not associated with inflammation nor accumulation of pro-inflammatory $CD11c^+$ ATMs or CLS (Kosteli et al. 2010b). ATMs accumulated lipids in response to lipolysis, and became lipid laden, similarly to foam cell formation during atherosclerosis (Babaev et al. 1999). The authors highlighted a relationship between ATM content in GAT and FFA in the plasma of these mice, implying that fasting is linked with a surge in ATMs to respond to the increase in FFA efflux from AT. To support the buffering properties of ATMs, they transiently depleted macrophages via injection of clodronate encapsulated liposomes (i.p.) which increased FFA in the plasma. However, this technique ablates all macrophages, and by doing so it is not clear if all macrophages can buffer lipids or just a specific subset (Kosteli et al. 2010b). As mentioned in 1.2.1, basal lipolysis is also increased during obesity. Staining with Nile red after adherence on plates showed that ATMs can uptake lipids during HFD (C. N. Lumeng et al. 2007). Two other studies demonstrated that, contrary to fasting, $CD11c^+$ ATMs accumulated during HFD feeding and have the highest lipid content when compared to $CD11c^-$ ATMs. $CD11c^+$ ATMs represent, in some cases, 33% of ATMs in the tissue of obese mice, and assessing all $CD11c^-$ ATMs together (67% of all ATMs) might mask a potential subset that would be more efficient than $CD11c^+$ cells at picking up lipids (Prieur et al. 2011; Grijalva et al. 2016). There is thus an urgent need to acknowledge ATM heterogeneity of function.

Xu *et al.* move the concept forward by hypothesising that lysosomal lipolysis (the hydrolysis of TG in FFA by the lysosomal acidic lipase, LAL) in ATMs played an

important role in lipid trafficking (Figure 1.6). To test this, they used chloroquine, a strong inhibitor of lysosomal acidification which impairs LAL activity and thus stop lipid degradation (Emanuel et al. 2014). Chloroquine increased the lipid content in BM-derived-ATMs *in vitro*, and when added to obese AT explants, FFA efflux in media was decreased. First, they concluded that AT lipolysis was ATM dependent. The same observation was observed *in vivo* with decrease of serum FFA after injection of chloroquine in obese mice. This action was totally reversed when macrophages were depleted using clodronate liposomes (X. Xu et al. 2013). They concluded that there is an increased lysosomal activity in ATMs to buffer lipids that are released from apoptotic adipocytes during obesity. However the origin of these lipids was only hypothetical and could be expanded to lipids from the circulation. Moreover, in their model, all macrophages were depleted using chlodronate. Importantly, the authors highlighted that lysosomal activation was not linked with a M1 ATM polarisation state like during obesity (X. Xu et al. 2013). It is thus possible that macrophage origin (recruited vs resident) dictates macrophage lipid handling, one being more metabolically inclined to degrade lipids by fatty acid oxidation (FAO) for example. Also, ATMs contained in CLS can liberate lysosomal enzymes by exocytosis to pre-digest adipocytes needed to be phagocytised and be a source of lipids (Haka et al. 2016).

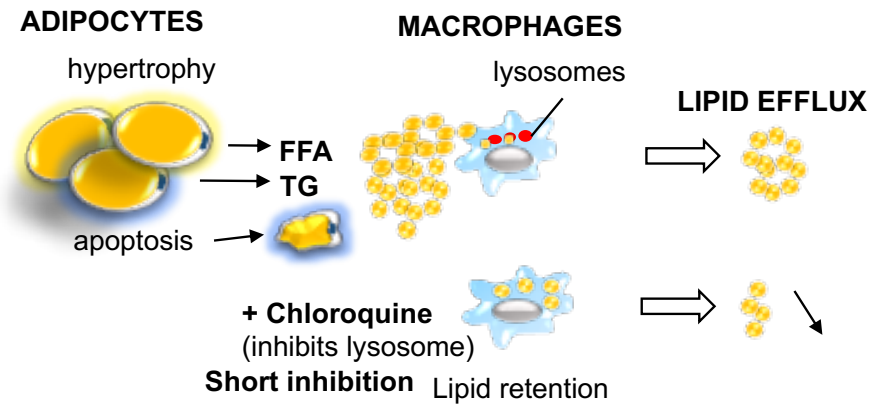

Figure 1.6 ATM lysosomal activity control lipid efflux.

Obese adipose tissue release lipids that can be buffered by ATMs. A short inhibition of lysosomal activity using chloroquine blocks lipid catabolism, induces lipids retention in ATMs, and decreases FFA efflux in the circulation. Adapted from Xu *et al* 2013

1.5.2 Intrinsic lipid metabolism and lysosomes

Experiments in which BM macrophages were polarised toward M2 or M1 demonstrated that the energy need of M2 and M1 are highly different and that their polarisation requires a different type of metabolic adaptation. Indeed, M2 rely heavily on FA uptake and their oxidation in the mitochondria, while M1 favour glycolysis (O'Neill, Kishton, and Rathmell 2016). In M2, FA are obtained by hydrolysis of TG rich lipoproteins such as CM, LDL and VLDL. The scavenger protein CD36, located at the macrophage's surface, internalised TG which are catabolised by LAL in lysosomes as described by Xu et al. (S. C.-C. Huang et al. 2014). CD36 dependent TG uptake leads to increased oxidative phosphorylation (OXPHOS) rates. Blocking with orlistat, a lipase inhibitor, decreases lipolysis and OXPHOS, and leads to a marked reduction of M2 markers (such as CD206, CD301 and RELMα), indicating that M2 polarisation is dependent on lipid oxidation (Heck, Yanovski, and Calis 2000). Targeting LAL induce lipid accumulation in M2 and decreased FAO, as measured by a decrease in oxygen consumption rates (SeaHorse technology) (S. C.-C. Huang et al. 2014).

Lysosomes are abundant and active in ATMs from obese mice. They accumulate in lipid laden macrophages, and do not corelate with a M1 phenotype (X. Xu et al. 2013). A recent publication acknowledge that there rather is a "metabolic activation" of ATMs during obesity, that does not resemble M1 or M activation (Boutens et al. 2018). Interestingly, ATMs contained in CLS upregulate glucose transporter (GLUT) 1 (Appari, Channon, and McNeill 2018). Micro-array analysis of ATMs revealed that during obesity, ATMs showed an enrichment for set of genes involved in carbon metabolism (glycolysis) and OXPHOS (Boutens et al. 2018). Although, this could indicate that different types of ATMs coexist, and this is not as simple as ATMs switching from M2 to M1. The field is thus starting to move forward. In addition, work in the branch of atherosclerosis can give us some insight in the mechanism regulating lipid cellular metabolism in ATMs.

Foam cell formation

Little is known about foam cell biology in ATMs but atherosclerosis has been more largely studied. In atherosclerosis, macrophages uptake lipoproteins from the plaque

and its environment, notably oxidised LDL (oxLDL). LDL oxidation is promoted by free radicals, 12/15-lipoxygenase (LO), and myeloperoxidase present in the arterial wall. Tissue macrophages express scavenger receptors such as SR-A, LOX1, MARCO and CD36 and can internalise and hydrolyse oxLDL in their lysosomes (Kunjathoor et al. 2002). Lysosomes are guarantor of the degradation of vesicles coming from phagocytosis (Jaishy and Abel 2016; Lim and Zoncu 2016). They contain proteases, nucleases and lipases, enabling the digestion a wide range of molecules, including lipids. After lysosomes catabolise lipoprotein into free cholesterol and FFA. FFA are ligands of peroxisomes proliferator activated receptors PPARs (α, γ, δ). *In vitro* activation of PPARs results in a rise in cholesterol efflux via increasing the number of ABCA1 transporters (Rader and Puré 2005). Indeed, cellular free cholesterol can either exit macrophages via these ABCA1 transporters, or traffic to the endoplasmic reticulum (ER) to undergo modifications and form cholesteryl esters (CE) (Figure 1.7) (Jeong, Lee, and Oh 2017). CE are packaged into lipid droplets that can be hydrolysed via creation of autophagosomes, which are fused to lysosomes and hydrolysed by LAL. The free cholesterol can then also exit via ABCA1 transporter (Emanuel et al. 2014). During the progression of atherosclerosis and diabetes, lipids are in excess and more lipid droplets accumulate in the macrophage, but also into dysfunctional lysosomes, which give its “foamy” appearance to the macrophage (Ouimet et al. 2011).

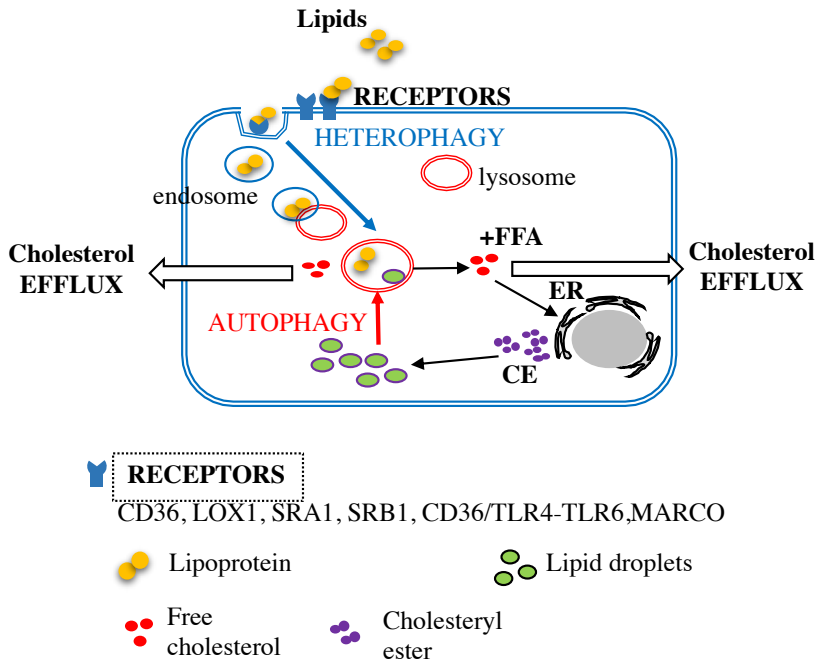

Figure 1.7 Lipid metabolism in macrophages of the atherosclerotic plaque

Uptake of lipids and lipoproteines occurs via multiple receptors. Once in the macrophage, the lipid microparticles are degraded by the lysosomes into free cholesterol and FFA for ABCA1- dependent efflux. Free cholesterol traffic to the ER where it is esterified into CE and packaged into lipid droplets. Lipid droplets are integrated into autophagosome which fuse with lysosomes to be degraded into free cholesterol and FFA which can exit the cell (lipid efflux). Accumuation of CE in the macrophage give it its foamy appearance characteritic of the progress of atherosclerosis. Adapted from Moore, Shedy and Fisher Nat Review Immunology 2013

It is possible that saturation of lysosomal lipolysis in ATMs leads to the formation of foam cells which become more inflammatory. Thus, there is a real importance of studying ATM metabolism to understand obesity, lipid and meta-inflammation. Interestingly, a receptor expressed on murine macrophages and dendritic cells has been linked in numerous studies with dyslipidaemia in human (Kathiresan et al. 2009b; Weissglas-Volkov et al. 2013). However the study of this receptor regarding metabolic disease has been very poor.

1.5.3 *Timd4*, gene coding for phosphatidylserine receptor on macrophages is associated with dyslipidaemia

The phosphatidylserine receptor Tim4 (T-cell immunoglobulin and mucin domain containing protein 4), is present on macrophages of various tissues including spleen macrophages, Kupffer cells in the liver and the resident large peritoneal macrophages (Rosas et al. 2014; Davies and Taylor 2015). When cells die, they expose their phosphatidylserine (PS) on their surface. This "eat me" signal is recognised by Tim4 macrophages for their engulfment (Miyanishi et al. 2007). The "Tim" family plays a role in immune regulation , notably in allergy, asthma and autoimmunity (Freeman et al. 2010). It contains 8 members (Tim1-8) in mouse and 3 in human. The murine Tim4 is an orthologue of the human Tim4. The Tim structure is made of an N immunoglobulin-like extracellular domain, a mucin domain, a transmembrane domain and a cytoplasmic region. The extracellular domain binds PS via a metal ion-dependent ligand-binding site (Santiago et al. 2007). This part of the interaction in hydrophilic, while the fatty acid and glycerol composing the rest of the PS interact with hydrophobic residues on Tim4. The engulfment mediated by Tim4 is an ATP dependent process (Park, Hochreiter-Hufford, and Ravichandran 2009). $Tim4^+$ and $MerTK^+$ (myeloid-epithelial-reproductive tyrosine kinase) are required for the correct engulfment of apoptotic bodies by peritoneal macrophages. Tim4 acts as a tethering receptor and if blocked, the engulfment process is drastically reduced (Nishi et al. 2014). Tim4 resident macrophages in the peritoneal cavity synthesise the enzyme 12/15-lipoxygenase (12/15-LO) which directs the uptake of apoptotic cells towards $Tim4^+$ macrophages themselves and block their uptake by inflammatory monocytes, indicating a key regulatory role for these macrophages in the control of phagocytosis (Uderhardt et al. 2012). The 12/15 LO can oxidase lipids such as LDL, but no link yet has been made between Tim4 and oxLDL uptake or any other lipids. Interestingly, TLR4 activation (which can act with CD36 to uptake lipids) promotes Tim4 expression (Ji et al. 2014). As said, *TIMD4*, the gene coding for Tim4, is found in humans. Genome-wide association study (GWAS) showed association of *TIMD4* (5q23 loci) with blood LDL cholesterol in multiple studies, reviewed in Table 1-2 (Weissglas-Volkov et al. 2013; Kathiresan et al. 2009a; Spracklen et al. 2017; Surakka et al. 2015; Teslovich et al. 2010; Willer et al. 2013). However, these studies do not mention if the

single nucleotide polymorphisms (SNPs) found in the gene modify the protein structure or function. In human, Tim4 macrophages are present in the spleen and tonsil (Kobayashi et al. 2007). But there is no reported studies of human Tim4 ATMs.

Table 1-2 Genome wide association study involving *Timd4*

References	DISEASE/ TRAIT	REPORTED GENE(S)	SNPS	P-VALUE	RISK ALLELE FREQUENCY	OR or BETA
Weissglas-Volkov *et al.*, 2013	Hypertriglyceridemia	TIMD4, HAVCR1, HAVCR2	rs2036402	3.00E-06	0.45	1.23
Kathiresan *et al.*, 2009	LDL cholesterol	TIMD4, HAVCR1	rs1501908	1.00E-11	0.37	0.07 s.d decrease
Spracklen *et al.*, 2017	LDL cholesterol levels	TIMD4	rs6882076	1.00E-33	0.334	0.0456 unit decrease
	Total cholesterol levels	TIMD4	rs6882076	2.00E-43	0.334	0.0508 unit decrease
	Triglyceride levels	TIMD4	rs4704727	3.00E-16	0.313	0.0289 unit decrease
Surakka *et al.*, 2015	Cholesterol, total	TIMD4, HAVCR1	rs1553318	2.00E-21	0.65	0.058 s.d. increase
	LDL cholesterol	TIMD4, HAVCR1	rs1553318	2.00E-15	0.65	0.05 s.d. increase
	Triglycerides	TIMD4, HAVCR1	rs1553318	2.00E-11	0.65	0.042 s.d. increase
Teslovich *et al.*, 2010	LDL cholesterol	TIMD4, HAVCR1	rs6882076	2.00E-22	0.35	1.67 mg/dL decrease
	Triglycerides	TIMD4, HAVCR1	rs6882076	4.00E-12	0.36	2.63 mg/dL decrease
	Cholesterol, total	TIMD4, HAVCR1	rs6882076	7.00E-28	0.35	1.98 mg/dL decrease
(Willer *et al.*, 2013	LDL cholesterol	TIMD4	rs6882076	3.00E-31	0.36	0.046 unit decrease
	Cholesterol, total	TIMD4	rs6882076	5.00E-41	0.36	0.051 unit decrease
	Triglycerides	TIMD4	rs6882076	2.00E-15	0.36	0.029 mg/dL decrease

Single nucleotide polymorphisms (SNPS) reported in the chromosome 5, region 5q33.3, corresponding to *Timd4* have been associated in several studies with traits such as cholesterol, LDL, triglycerides, hypertriglyceridemia. The P-value indicates the genome wide significance, and the OR (odd ratio) or BETA indicates the coefficient.

Contrary to other Tims, Tim4 does not contain tyrosine phosphorylation motif and little is known about the intracellular signalling of this receptor (Freeman et al. 2010). Despite the fact that the study from Park in 2009 showed that Tim4 doesn't have a direct signalling pathway, other studies mention an intracellular interaction between Tim4 and AMPKα1 (Park, Hochreiter-Hufford, and Ravichandran 2009; Baghdadi et al. 2013). Interestingly, AMPKα1 signalling promote M2 activation, reduce the production of pro-inflammatory cytokines by macrophages and a global KO of AMPKα1 enhance lipid accumulation in adipocytes suggesting a role of AMPKα1 in lipid metabolism (W. Zhang et al. 2012). Indeed AMPK activates FAO in cells, indicating that Tim4 macrophages could oxidise lipids (Jeon 2016). The GWAS directed the interest of a team towards Tim4 blockade in atherosclerosis, pathology linked with high level of LDL in the plasma. They showed that in *ldlr*$^{-/-}$ mice fed for 4 weeks with HFD, blocking Tim4, aggravated atherosclerosis as apoptotic cells accumulates in the lesion and the blood, but also increased the proportion of activated T cells in the bloodstream (Foks et al. 2016). This is the only study, to my knowledge, studying the role of Tim4 in the setting of dyslipidaemia. Tim4 macrophages are present in the peritoneal cavity on F4/80^{high} "large" resident population (Rosas et al. 2014; Davies and Taylor 2015), but are also resident in the liver (Kupffer cells) and the gut (Scott and Guilliams 2018; Shaw et al. 2018). At the onset of this PhD, it has not been established if Tim4^{+} macrophages exist in AT (of human and mouse) and if they could play a role in the control of lipid homeostasis which could explain the traits found in GWAS.

1.6 Thesis aim and hypothesis

Defining the origin and the heterogeneity of ATMs is key to identify potential targets against tissue inflammation and dyslipidaemia that occurs during obesity or HFD stress. My overarching hypothesis is that ATMs are an heterogenous population and that it encompasses populations of macrophages with various functions particularly regarding lipid uptake and catabolism.

Therefore, this thesis aims to characterise and phenotype ATM subsets in order to better understand their potential specific role in the tissue in lean (Chapter 3) and obese (Chapter 4) AT. During the course of this research, a novel population of $Tim4^+$ resident ATMs was identified. An additional aim of this thesis is thus to elucidate the role of $Tim4^+$ ATMs and Tim4 in adipose tissue homeostasis (Chapter 5). Finally, the last aim of this thesis is to verify the existence of $Tim4^+$ ATMs in human adipose tissue.

CHAPTER 2 MATERIAL AND METHODS

2.1 *In vivo* experiments

2.1.1 Animal

All animal experiments were carried out in accordance with the Animal (Scientific Procedures) Act, UK 1986 following approval by the University of Edinburgh Animal Ethical Review Committee and Vets through Experimental Request Forms. Mice were housed in standard cages (except stated otherwise) and given food and water *ab libitum.*

2.1.2 Time course experiments

C57BL/6J pups, bred in house, were taken and culled by neck dislocation.

2.1.3 HFD experiments

6-8 week old C57BL/6J males were put on a control diet (CD) (11kcal%Fat and corn starch, Research diet, D12328i) or a high fat diet (HFD) (58Kcal%Fat and sucrose, Research diet, D12331i) for variable periods of time (from 1 day to 14 weeks).

2.1.4 Oral glucose tolerance test (OGTT)

After 8 weeks of CD or HFD, mice were given a bolus of glucose to test their glucose tolerance. Mice were fasted from 5-6 hours and put in the room where the OGTT was conducted to limit stress. First basal fasting glucose was measured after blood was taken by venesection. To read the measure, a commercially available glucometer was used (Roche, Accu-Chek Performa Nano). Then mice were given a bolus of glucose by gavage (2g/kg body mass) and blood was sampled at 15, 30,60 and 120 minutes post-glucose to read the level of glucose.

2.1.5 Generation of chimeras

General

Protected/partial bone marrow irradiation was realised in collaboration with Dr Stephen Jenkins and his team following a protocol they developed (Centre for Inflammation Research, Queen's Medical Research Institute, Edinburgh). First, mice were sedated/anaesthetised and the upper half of the body (head, thorax and front set of legs) exposed to lethal levels of gamma-irradiation (12Gy) for 19 min 30 seconds. Mice were irradiated on a Perspex sheet over laying a 2 inch thick block of lead, with

only the upper half (or the lower half) of the body uncovered, this for the maximum protection of the adipose tissue. After irradiation, the mice were injected s.c. with antisedan to reverse the sedation, and keep in a warm cage (30°C) up until awareness was found again. Then they were randomly put in individually ventilated cages (5 by cage). The next day, mice received 2 to 5 millions donor bone marrow cells iv obtained in house. Mice were kept on mash for 2 weeks then put back on normal diet for 2 weeks. They received baytril for 4 weeks following irradiation to limit infection.

Chimeras and macrophage origin

Eight weeks old C57BL/6J Ly5.1 female mice were partially irradiated as described in 2.1.5. Mice were reconstituted after radiation with congenic CD45.2^{+} WT BM or *Ccr2*$^{-/-}$ BM obtained in house. After 8 weeks' recovery, the gonadal and mesenteric adipose tissue were collected for flow cytometry analysis (Figure 2.1). Irradiations were conducted by Dr Stephen Jenkins lab.

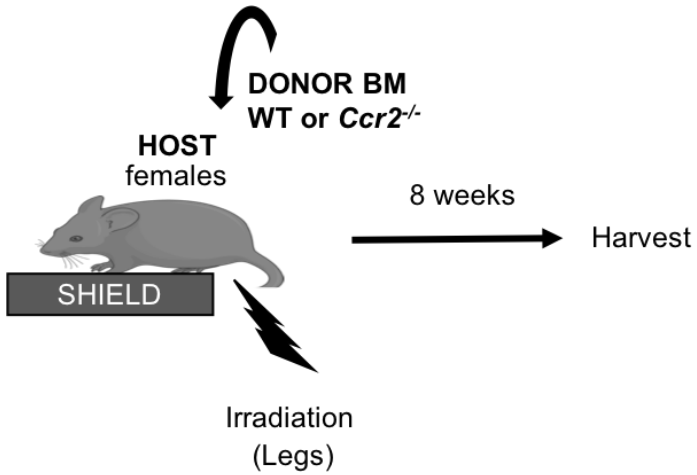

Figure 2.1 Experimental design of partial BM chimeras

After irradiation of the head, Ly5.1 host females (expressing CD45.1 and CD45.2), were injected i.v. with CD45.2^{+} donor BM or *Ccr2*$^{-/-}$ BM. After recovery, mice were then put on a control diet or a HFD (60% fat) for 8 weeks.

Chimeras and HFD

Eight weeks old Ly5.1 male and female mice were partially irradiated as described in 2.1.5, and reconstituted with congenic CD45.2^{+} WT BM. After 4 weeks of baytril and mash + normal diet, mice were put on either a control diet (11kcal%Fat and corn

starch, Research diet, D12328i) or a HFD (58Kcal%Fat and sucrose, Research diet, D12331i). After 8 weeks of diet, mice were sacrificed by exsanguination under terminal anaesthesia (Figure 2.2). Irradiations were conducted by Dr Stephen Jenkins lab.

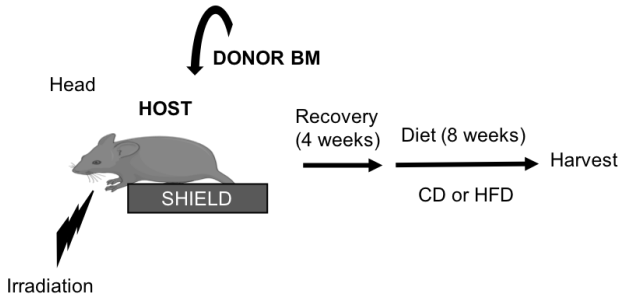

Figure 2.2 Experimental design of partial BM chimeras coupled with diet to study macrophage turn-over during HFD.
After irradiation of the head, Ly5.1 host mice (expressing CD45.1 and CD45.2), both males and females, were injected i.v. with CD45.2^{+} donor BM. After recovery, mice were then put on a control diet or a HFD (60% fat) for 8 weeks.

2.1.6 *In vivo* Tim4 blockade

Mice were i.p. injected with 100µl of PBS containing either 200ng of monoclonal antibody anti mouse Tim4 (aTim4) (clone RMT4-53, Rat IgG2a, BE0171 from BioXCell) or 200ng of of rat IgG2a isotype control (Isotype) (BE0089 from BioXcell). These concentrations were based on a publication from 2016 (Foks et al. 2016). The experiments coupled with HFD were performed as shown in Figure 2.3

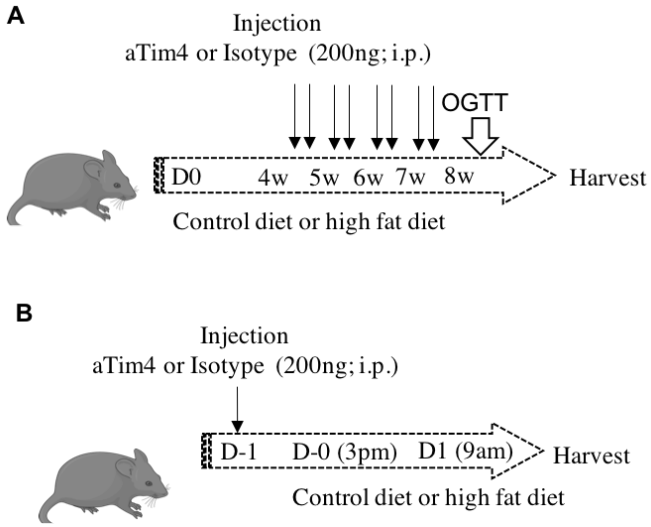

Figure 2.3 Experimental design of Tim4 blockade during long (A) and short HFD (B)

Male mice were given a HFD for 8 weeks (w: weeks) or for a shorter period of time (D: day). **A** After 4 weeks of diet, mice from both groups were i.p. injected twice a week for the rest of the experiment with 100μl of PBS containing either 200ng of blocking anti-Tim4 IgG2a or 200ng of isotype IgG2a control (plain arrow). An oral glucose tolerance test (OGTT) was performed 2 to 3 days before the cull. **B** Short HFD with injection of 100μl of PBS containing either 200ng of blocking anti-Tim4 IgG2a or 200ng of isotype IgG2a control (plain arrow)

2.2 Cell isolation

2.2.1 Human adipose tissue

Omentum or SAT were collected by surgeon in PBS. Shortly after collection ,tissues were digested using the gentleMACS dissociator (Miltenyi Biotec). Tissues were put in tubes containing 5ml of PBS BSA 2% and collagenase I (2mg/ml) (Worthington LS004196), and after mechanical dissociation, were incubated in a water bath at 37°C for 30 minutes, with a shake after 15 minutes. The reaction was stopped by using 25µl of EDTA (0.5M). After filtration (100µm), tubes were spun at 700g for 10 minutes at 4°C to dissociate adipocytes from the stromal vascular fraction.

2.2.2 Murine adipose tissue

Adipose tissue were harvested in RPMI and kept at room temperature. Shortly after the harvest, the tissues were weighed and put into the digestion media (Collagenase D

10mg/ml in RPMI 1% FCS) (500µl/tubes). Each tissue was pre-cut with scissors to facilitate the collagenase digestion, and put at 37°C for 30 minutes to 45 minutes. A gentle mixing with pipetting up and down a few times after 15 minutes of incubation was done. At the end of the incubation, EDTA (50mM) was added to the digests (5µl/ml) to stop the enzyme by ion chelation. RPMI 1% FCS was added on top and the digests were filtered (100µm – 75 µm) and centrifuged at 700g for 10 minutes at 4°C in order to separate the stromal vascular fraction (SVF ; containing leukocytes, pre-adipocytes, fibroblasts) from the floating fraction (containing mainly adipocytes) . If the floating fraction was needed, the centrifugation was done at room temperature to avoid it to freeze. After separation, cells from the SVF was counted in 2 ml of RPMI 1% FCS with the Biorad cell counter.

2.2.3 Peritoneal cavity lavages

In order to retrieve the cells of the peritoneal cavity, mice were euthanised in a CO_2 chamber. Quickly following death, 2ml of RPMI was injected in the cavity of C57BL/6J mice. After a short shake of the cavity, the media was taken back and put in falcon tubes on ice. Cells were then spun at 1200g for 5 minutes at 4°C. The pellet contained immune cells for further analysis.

2.2.4 Liver

Livers were perfused with PBS to eliminate blood from vessels, and put on a tube on ice. Using a razor blade, livers were chopped in small petri dishes with a few drops of RPMI up until full homogenisation. Then, they were put in a 50ml Falcon tube with the cocktail of enzyme described in Table 2-1 prepared in warm RPMI (5ml per liver). The Falcons were placed in a water bath at 37°C for 22 minutes, with vigorous shaking every 5 minutes. At the end of the 22 minutes, cold RPMI (30ml) was poured on top of the liver digest and the mixture was filtered (100µm filter). Tubes were spun at 300g for 5 mins, 4°C. For better results, a second filtration was done with a 70µm filter after cell resuspension in 30ml of RPMI. Tubes were spun again at 300g for 5 mins and the digests were resuspended in 5 to 10 ml and cells were counted.

Table 2-1 Enzymes necessary for liver murine liver digestion

Enzyme	Concentration	Suppliers
Collagnease V	0.8mg/ml	Sigma Cat. No. C9263-1G
Collagenase D	0.625mg/ml	Roche Cat. No. 11 088 882 001
Dispase	1mg/ml	Gibco Cat. No 17105-041
DNase	30mg/ml	Roche Cat. No. 101 104 159 001

2.3 *In vitro* experiments

2.3.1 Fatty acids dosage

Samples of blood were taken from a brachial exsanguination in tubes (BD Vacutained) and spun at 1800g for 10 minutes to separate the plasma from the rest. FFA was measure using a WAKO Kit (reagent 1 : 434-91795; reagent 2: 436-91995) and WAKO standard (4270-77000). A slightly modified protocol was used:

- Add 10µl of plasma in wells after gentle mixing to homogenise the sample
- Add of 150µl of reagent 1 for 3minutes (at 37°C)
- Add 75µl of reagent 2 for 4 minutes (at 37°C)
- Reading at 546nm and 660nm

2.3.2 Adhesion mediated purification of macrophages

Cells obtained from AT, PEC or liver were resuspended in serum free RPMI and placed on a 24 well plate, up to 500 000 cells per well for AT and PEC, 1 million for the liver (due to the fact that more cells (non-macrophages) are in the digests compared to the other tissues). Each well contained a 13 mm coverslip to be able to analyse the cells later by microscopy. After 30 minutes to 1h at 37°C in 5% CO_2, the cells were washed in RPMI (room temperature) 3 times. Macrophages are able to adhere to the coverslip, and other cells are washed away (Davies and Gordon 2005).

2.3.3 In vitro LDL uptake by macrophages

After adhesion mediated purification of macrophages, 300µl of media containing 50ng anti Tim4 or Isotype control for 30 minutes to 1h, then LDL-Bodipy (Invitrogen Bodipy^{TM} FL low-density lipoprotein, 50ng/ml) was added. After 6 hours, lysotracker (DND99) was added (500nM) for 30 minutes at 37°C to stain the lysosomes. The coverslips were washed 2 times in PBS and fixed with 2-5% NBF for 10 min at RT.

2.3.4 Chylomicron uptake by macrophages

After adhesion mediated purification of macrophages, 300µl of media containing 50ng anti Tim4 or Isotype control for 30 minutes to 1 hour, then chylomicrons (Human plasma CM, CMIC15-N from Alpha Diagnostic, 83µg/ml) was added for 3 hours. Before the end of the incubation, Lysotracker (DND99, 500nM) was added for 30 minutes at 37°C to stain the lysosomes. The coverslips were washed 2 times in PBS and fixed with 2-5% NBF for 10 min at RT.

2.4 Techniques of analysis

2.4.1 Flow cytometry

Staining

Cells were plated in 96 well plate and the staining was realised in a total volume of 50µl/well. If no intracellular staining was required, the cells were stained in 2 steps (on ice):

- 10 minutes in blocking buffer (25µl per well)
- 30 minutes in antibody mix (25µl per well), made in FACS buffer
- Wash 2 times in FACS buffer and resuspend in 200µl of FACS
- Add 2µl of DAPI before flow acquisition (Sigma Aldrich;1mg/ml stock)

If fixation and/or intracellular staining was needed, the following steps were followed for each samples:

- 10µl of Live/Dead (Thermofisher) diluted in PBS, 10 minutes at room temperature in the dark

- 15µl of blocking buffer for 10 minutes on ice
- 25µl of antibody mix
- Wash 2 times in FACS buffer
- Fixation/permeabilization 1 hour (eBioscience) or fixation with 5% NBF for 10 minutes followed by permeabilization (eBioscience) 30minutes and intra-cellular staining in permeabilization buffer.

Samples were acquired using a BD LSR 5 Fortessa and analysed with FlowJo software (Tree Star).

Table 2-2 List of buffers

BUFFER NAME	COMPOSITION	Manufacturer
Blocking buffer	1x FACS Buffer 20% rat and mouse serum FcR CD16/32 (1/300)	 Biolegend
10x FACs Buffer	50 ml of PBS 2.5g Bovine Serum Albumin 2 ml of 0.5M EDTA	Sigma Sigma Sigma

2.4.2 Gating strategy

Bone marrow chimeras

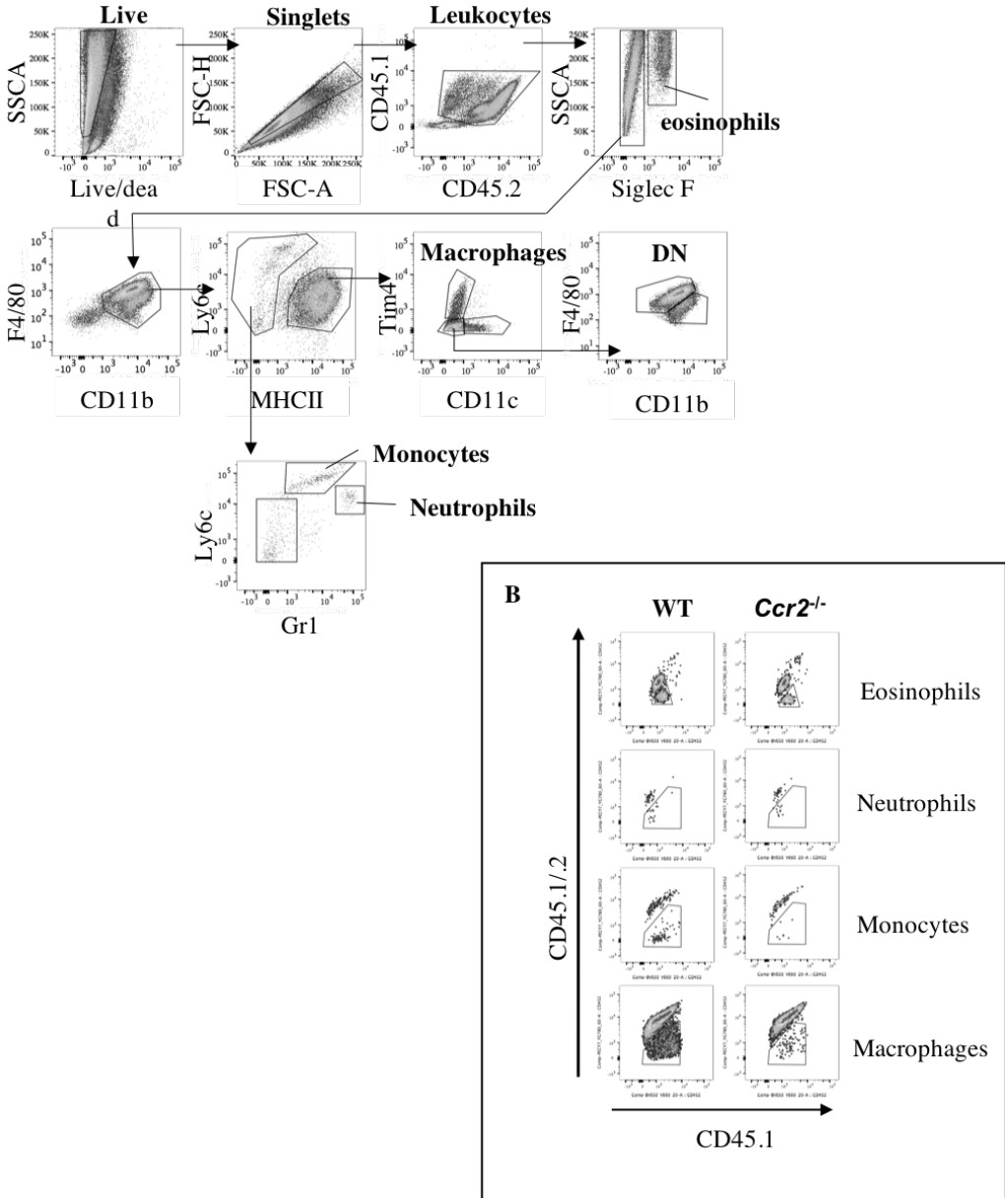

Figure 2.4 Gating strategy used to define immune cells in the GAT after generation of BM chimeric mice.

After generation of BM chimeras as decribed in 2.1.5, GAT and MES imune cells were analysed by flow cytometry and imune subsets were gated as presented (**A**). To define the non-host chimerism, cells were gated on CD45.2^{+} cells as shown in **B.**

Table 2-3 Flow cytometry antibody clones, manufacturer and titration (mouse)

Antigen Name	Conju-gate	Clone	Isotype	Manu-facturer	Concen-tration	Titra-tion
CD11b	PE Dazzle	M1/70	Rat IgG2b	Biolegend	0.2 mg/ml	1/1200
CD11c	BV605	N418	Armenian Hamster IgG	Biolegend	0.2 mg/ml	1/200
CD19	BV421	6D5	Rat IgG2a	Biolegend	0.2 mg/ml	1/200
CD206	FITC	MCA2235 FA	Rat	Miltenyi		1/200
CD45.1	PE/Cy7	A20	Mouse IgG2a	Biolegend	0.2 mg/ml	1/200
CD45.2	BV650	104	Mouse IgG2a	Biolegend	0.2 mg/ml	1/200
F4/80	PE/Cy7	BM8	Rat IgG2a	Biolegend	0.2 mg/ml	1/200
KI-67	FITC	REA183	recombinant human IgG1	Miltenyi	100 tests /ml	
Live/dead (405nm)				Thermo-Fisher	(Stock diluted in 12.5μl DMSO)	1/300
Ly6C	AF700	HK1.4	Rat IgG2c	Biolegend	0.5 mg/ml	1/200
Ly6G	BV421	1A8	Rat IgG2a	Biolegend	0.2 mg/ml	1/200
MHCII IIA/IE	APCe780	M5/114.15.2	Rat / IgG2b	ebiosciences	0.2 mg/ml	1/600
Siglec F	BV421	E50-2440	Rat LOU	BD	0.2 mg/ml	1/200
TCRb	BV421	h57-597	Armenian Hamster IgG	Biolegend	0.2 mg/ml	1/200
Tim4	PE	RMT4-54	Rat IgG2	ebiosciences	0.2 mg/ml	1/1200
Lysotra-cker (DND99)	RED 577/590			ThermoFisher	1mM	1/1500

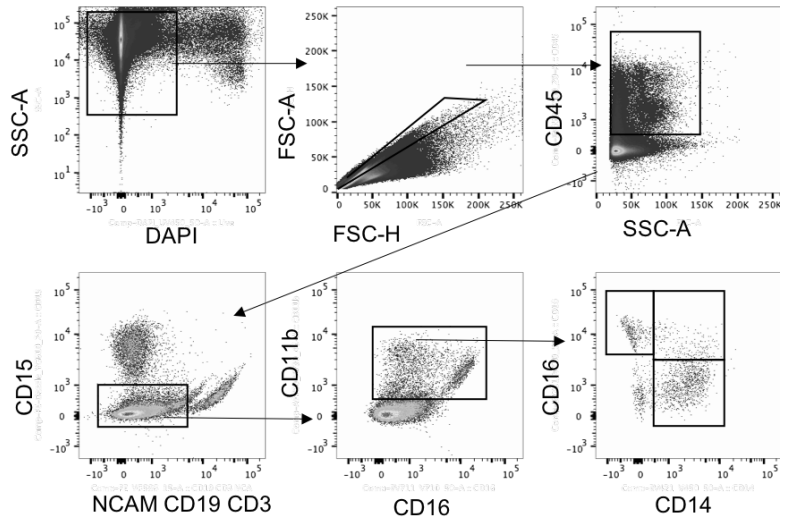

Figure 2.5 Gating strategy used to define macrophages in human visceral AT (omentum).

Flow cytometry plots showing the gating strategy used to define ATM in human. Macrophages were gated on Live cells (DAPI negative), singlets, $CD45^{+}$, $CD15^{-}Lin^{-}$ $CD11b^{+}$ cells then divided according their CD16 and CD14 expression.

Table 2-4 Flow cytometry antibody clones, manufacturer and titration (human)

Antigen Name	Conjugate	Clone	Manufacturer	Isotype	Titration
CD14	e 450	HCD14	Biolegend	Mouse IgG1	1/25
CD163	BV605		Biolegend	Mouse IgG1	1/20
CD45	BV650	HI30	Biolegend	Mouse IgG2a	1/20
Tim4	PE/Cy7	9F4	Biolegend	Mouse IgG1	1/10
HLA-DR	FITC	L243	Biolegend	Mouse IgG2	1/20
CD19	PE	HIB19	Biolegend	Mouse IgG1	1/40
NCAM	PE	MEM-188	Biolegend	Mouse IgG2a	1/40
CD3	PE	HIT3a	Biolegend	Mouse IgG2a	1/40
CD15	PEDazzle 594	W6D3	Biologend	Mouse IgG1	1/40
CD62L	PerCPcy55	DREG-56	Biolegend	Mouse IgG1	1/20
CD16	BV711	3G8	Biolegend	Mouse IgG1	1/20
CD11b	AF700	M1/70	Biolegend	Rat IgG2b	1/200
CD64	APCcy7	10.1	Biolegend	Mouse IgG1	1/20
CD206	AF647	15_2	Biolegend	Mouse IgG1	1/20

2.4.3 Cell sorting and cytospin

Cells were stained as described in 2.4.1. Cells were then sorted (FACS ARIA) in tubes containing RPMI complemented with 10% FCS. 100µl of the cell suspension were transferred to a cytocentrifuge cytofunnel containing a slide and a filter card. Cells were cytospined for 3min at 300g onto the slide (X. Zhang, Goncalves, and Mosser 2008). Shandon™ Kwik-Diff™ (Thermofisher) staining solutions was used to stain the cells according to the manufacturer's instructions.

2.5 Microscopy

2.5.1 Whole mount immunofluorescence staining for confocal microscopy

The samples were fixed in 10% neutral buffered formalin (NBF, Sigma) for 2 hours on ice then transferred in PBS. The tissues were cut in smal pieces to facilitate the staining and the mounting. The staining was realised in 3 steps:

- Permeabilization with Triton 1% (Sigma) for 30 min *
- Antibody mix in 1%Triton*/PBS BSA 1% (1:1) for 2 hours on a shaking plate (room temperature) or overnight at 4°C
- Wash 3 times in PBS

*To visualise lipids or lysosomes in macrophages, triton 0.1% or no triton at all was added.

The tissues were mounted in a mounting media (Fluoromount, Sigma Aldrich) as shown in Figure 2.6 (Wang, Scherer, and Gupta 2014).

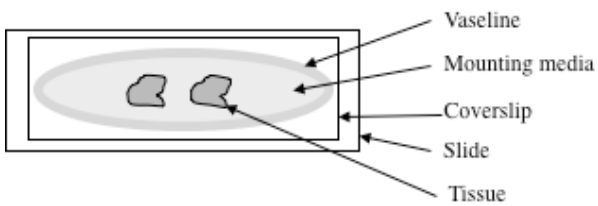

Figure 2.6 Mounting of tissue for microscopy analysis

The tissues were place in the middle with mounting media. Vaseline was placed and a coverslip was added on top. To seal the coverslip, nail varnish was added around, or in some cases superglue.

The antibodies used for immunofluorescence microscopy are listed in the table below

Table 2-5 Antibodies used for immunofluorescence staining

Antigen Name	Conjugate	Manufacturer	Titration
Tim4 anti mouse	APC	Biolegend	1/50
CD11b	PB	Biolegend	1/200
Anti-rat IgG	AF 647	Invitrogen	1/400
Tim4 anti human	APC	Biolegend	1/50
Lysotracker	RED	ThermoFisher	75 to 500nM

2.5.2 Lysotracker and LipidTox staining

Lysotracker staining. Lysotracker red (577/590; Lysotracker red DND99 from TermoFisher) was used on live cells (500nM) and tissues (1/1000). The dye was diluted in warm RPMI, and put with the cells/tissues for at least 30 minutes. Then the tissues were fixed in formalin neutral buffer (10%) followed by wholemount staining. The cells were fixed in formalin neutral buffer 2-5% and kept in PBS in the fridge for following staining.

LipidTox staining. HCS LipidTox Green Neutral lipid stain from Invitrogen was used to stain neutral lipids after fixation. If used on cells the concentration was of 1/500 and on tissues 1/100. Permeabilization reduced the dye intensity, so only a gentle permeabilization (0.1% Triton) should be done or none at all.

2.5.3 Fiji analysis

Intensity measurement in single cell

In order to analyse the intensity of lysotracker and lipid content for each cell, I created a macro to run on FIJI, a free image processing software:

```
run("Duplicate...", "duplicate channels=4");
run("16-bit");
setAutoThreshold("Default dark");
//run("Threshold...");
setThreshold(30, 255);
run("Analyze Particles...", "size=10-Infinity display exclude clear add in_situ");
```

The first step included the duplication of the channel 4 (with Tim4 APC staining), then the identification and count of positive cells, and to finish the measurement of fluorescence intensity. The threshold to identify $Tim4^+$ macrophages was defined on the first image and was not changed. The lysotracker and lipid intensities were measured on raw images, with no change of threshold or image modification (Figure 2.7).

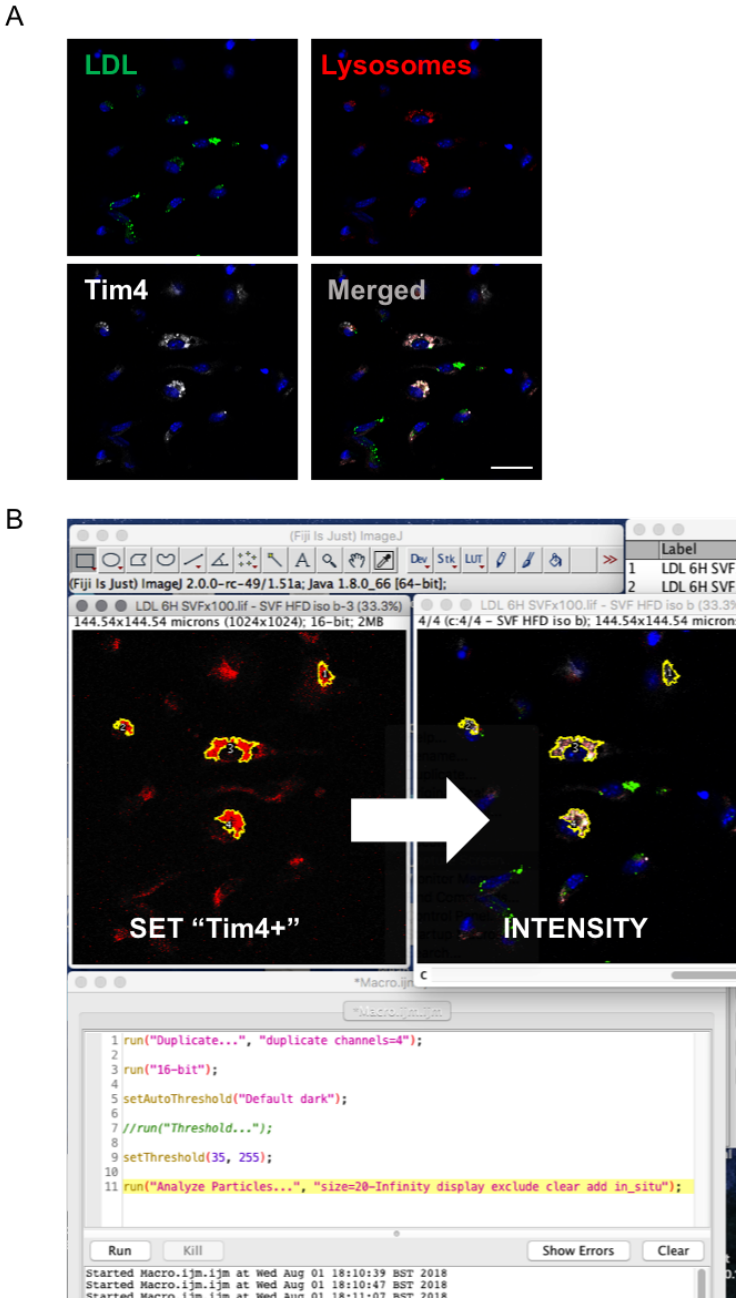

Figure 2.7 Example of automatized measurement of lysotracker and lipid intensity using FIJI

After taking images using the LEICA SP5 microscope (x40) (**A**), images were analysed using FIJI software (**B**). The macro created in FIJI (bottom panel), allowed to select Tim4^{+} cells, according to a set Threshold (upper left panel). The area was stored in the "region of interest" manager. Then the intensity for each channel could be measured within each Tim4^{+} cells (upper right panel).

2.6 Statistics

Statistical analyses were performed using GraphPad Prism 7 software (GraphPad Sotware Inc., La Jolla, CA). Differences between two groups or two cell populations were determined in two steps : D'Agostino-Pearson omnibus normality test was done to rule on the distribution of the data then a nonparametric unpaired Mann-Whitney t tests was done (non-gaussian distribution). One way ANOVA on ranks (Krustal-Wallis H Test) was used to compare two or more groups. Two way ANOVA, with multiple comparisons made using Tukey post-hoc tests, was used for analysis of variables of two factors (for example sex and diet / treatment and diet), and their interaction. Data are shown as mean ± SEM. Full details of analyses are described within each figure legend.

CHAPTER 3 ATM REPLENISHMENT BY BM DERIVED MONOCYTES SHOWS TISSUE HETEROGENEITY

3.1 Introduction

WAT is the primary site of lipid storage in the body, and can represent from 5 to 50% of human body weight. Despite adipocytes being voluminous, immune cells constitute the second major component of the tissue, infiltrated between adipocytes. AT macrophages (ATMs) have been highlighted during obesity, especially in the visceral adipose tissue, as they can expand 10 times in number (Weisberg et al. 2003). Most study have then focused on determining the pro-inflammatory phenotype of ATMs (Catrysse and van Loo 2018). Nonetheless ATMs represent the most abundant immune cells in lean AT, constituting around 5% of the tissue, and their maintenance is essential for AT function as ATMs contribute to AT expansion, tissue remodelling, lipid buffering, removal of apoptotic adipocytes and non–shivering thermogenesis (Ferrante 2013; Thomas and Apovian 2017; Catrysse and van Loo 2018). In lean fat depots, F4/80^{+} ATMs are viewed in the current scientific literature as being anti-inflammatory M2-macrophages, in contrast with macrophages in obese AT which are frequently classified as being inflammatory M1-macrophages (Lumeng *et al.*, 2008). These M2 ATMs can express CD206^{+}, CD301^{+} and encode anti-inflammatory proteins (C. N. Lumeng et al. 2008). Despite this M1/M2 classification, ATMs are often considered as one group of cells instead of acknowledging their inherent heterogeneity of function and/or origin, as seen in other tissues. For instance, the developmental origin of ATMs had still not been elucidated and the existence of any local maintenance mechanisms had not been investigated which was reflected by the lack of ATMs in the biggest reviews on macrophage origin in tissues in the recent years (Hoeffel and Ginhoux 2015; Ginhoux and Guilliams 2016). In tissues, resident macrophages, which support homeostatic functions, are distinguished from newly recruited CCR2^{+} macrophages which are considered as inflammatory macrophages (Davies et al. 2013; Ginhoux and Guilliams 2016). Indeed, inflammation triggers the recruitment of Ly6c^{high} monocytes, which by expressing CCR2, enter the tissues and differentiate into ‘recruited’ macrophages (Komornik 1985; Shi and Pamer 2011). Conversely, resident macrophages can be embryonically derived, and/or proliferate independently from the bone marrow (BM) (Davies and Taylor 2015; Hoeffel and Ginhoux 2015; Epelman, Lavine, and Randolph 2014b). To determine the origin of tissue macrophages in adults, generation of partial bone marrow (BM) chimeric mice

is now widely used (Jenkins et al. 2011; Komornik 1985; Calum C Bain et al. 2014). By injecting donor BM into a host after partial irradiation, where the tissues of interest are shielded, it is possible to follow these cells 8 weeks after reconstitution to evaluate the BM dependency of the macrophage population. Injecting *Ccr2*$^{-/-}$ BM alongside in control mice allow to verify the monocytic origin of macrophage in tissues (Calum C Bain et al. 2014; Serbina and Pamer 2006; Epelman et al. 2014). One study of this kind was done on AT, where authors showed that 85% of ATMs were coming from the BM but the researchers used total irradiation which is known now to artificially increase the number of cells coming from the BM (Weisberg et al. 2003). Thus, it is important to use new technique to investigate ATM BM dependency. In rodent, SAT appears before the GAT, and can be studied from birth (Berry et al. 2013). However, SAT macrophage composition at birth is not known but could be an indicator of macrophage embryonic origin, notably by the study of their F4/80 and MHCII expression (Schulz et al. 2012b).

3.2 Aim of this chapter

- Determine the origin of ATMs in lean adipose depots of adult mice using partial bone marrow chimeras to define resident and recruited macrophages.
- Follow AT development after birth to study the dynamics of macrophage recruitment to the subcutaneous AT (SAT)

3.3 Experimental design

Partial bone marrow chimeras. To study the contribution of monocytes to the development of adipose tissue macrophage (ATMs) populations we used adipose tissue protected BM chimera in collaboration with the laboratory of Dr Stephen Jenkins. Host Ly5.1 female mice ($CD45.1^{+}CD45.2^{+}$) were partially irradiated (either leg irradiation or head irradiation), with a shield covering ¾ of the body and then reconstituted with congenic WT BM ($CD45.2^{+}$) or *Ccr2*$^{-/-}$ BM. After 8 weeks' recovery, GAT, MES AT and SAT were collected to study the non-host chimerism by flow cytometry.

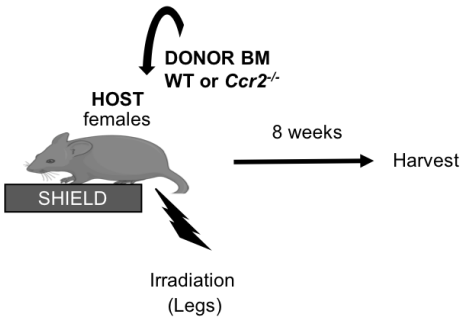

Figure 3.1 Experimental design of partial BM chimera generation

3.4 Results

3.4.1 Novel gating strategy to characterise adipose tissue macrophage subsets

In AT, macrophages were generally described as being "F4/80^{+}CD11b^{+}" cells. However, the gating strategy used by flow cytometry could be refined notably by looking at the levels of F4/80 (high or low) and by using Tim4, a phosphatidylserine receptor generally used to define resident macrophages in the peritoneal cavity (K. Wong et al. 2010). Using F4/80, Tim4 and CD11c, generally used to characterise recruited inflammatory ATMs, (Carey N Lumeng, Bodzin, and Saltiel 2007), four subsets of ATMs could be distinguished (Figure 3.2A):

- F4/80^{+}CD11b^{+}Tim4^{+} CD11c^{-} (named Tim4^{+} subset)
- F4/80^{+}CD11b^{+}Tim4^{+}CD11c^{+} (named CD11c^{+} subset)
- F4/80^{high}CD11b^{+}Tim4^{-}CD11c^{-} (named double negative F4/80^{high} subset)
- F4/80^{low}CD11b^{+}Tim4^{-}CD11c^{-} (named DN F4/80^{low} subset)

As seen in Figure 3.2B-C, DN F4/80^{high} represented 71% of the ATMs, so the vast majority of ATMs. The Tim4^{+} ATMs were also F4/80^{high}, representing 11% of the total ATMs, the CD11c^{+} were majorly F4/80^{low} (6% of the ATMs), with a negligible proportion F4/80^{high}. To finish the DN F4/80^{low} only represented 12% of the ATMs.

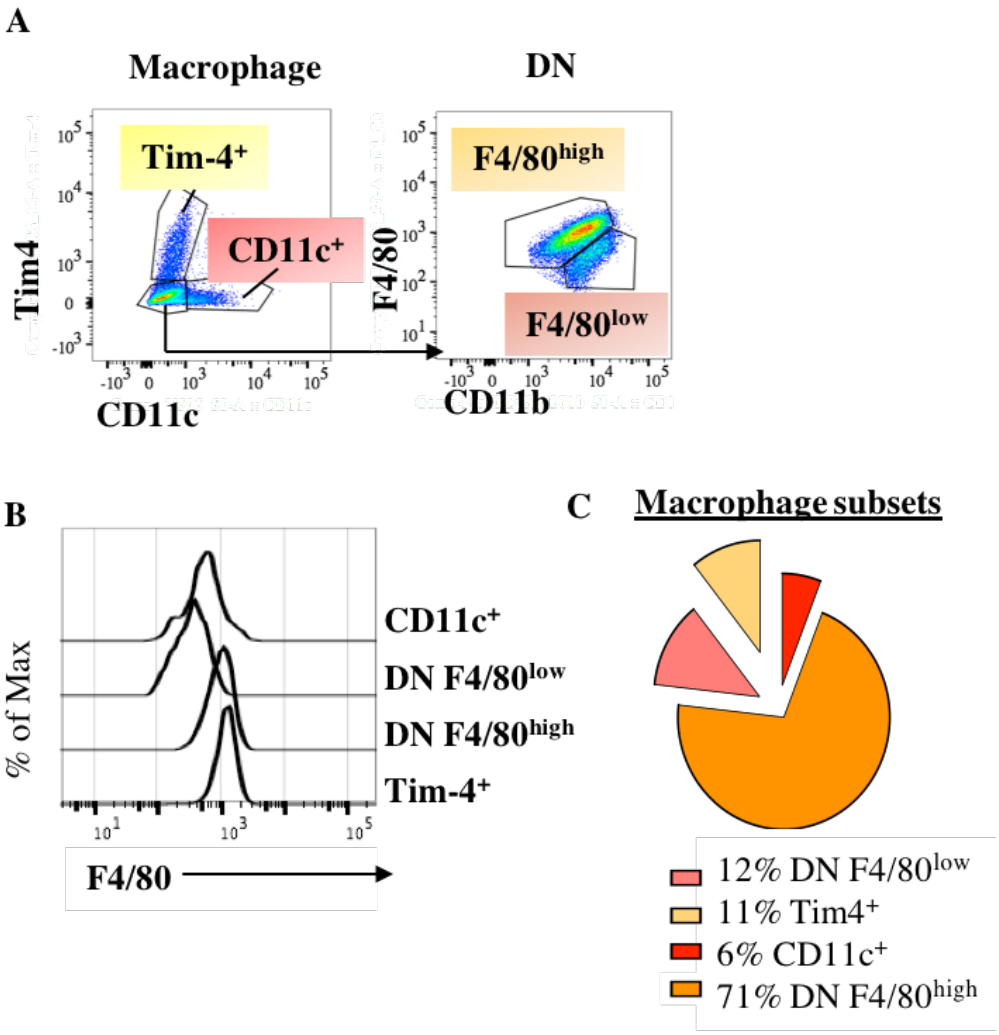

Figure 3.2 Gating strategy used to define ATM subsets and their relative proportion

A. Density plot showing expression of Tim4 and CD11c (left) on F4/80^{+}CD11b^{+} ATMs and the gating used to define Tim4^{+} ATMs, CD11c^{+} ATMs and the expression of F4/80 and CD11b on Tim4^{-} CD11c^{-} ATMs (right) and the gating used to define Tim4^{-} CD11c^{-} F4/80 ^{high} and Tim4^{-} CD11c^{-} F4/80^{low} ATM populations.

B. Histogram showing Mean Fluorescence Intensity of F4/80 on ATM populations as gated in A.

C. Proportion of each subset within ATM.

3.4.2 Tissue non-host chimerism of immune cells in the adipose tissue

The model of protected BM chimeras was used to elucidate the origin of ATMs based upon studies released previously in the peritoneal cavity (Jenkins et al. 2011; Murphy et al. 2008). In brief, after partial irradiation, Ly5.1 recipient mice (expressing CD45.1 and CD45.2) were injected iv with CD45.2 wild type (WT) or *Ccr2*$^{-/-}$ KO donor BM. Chimerism of immune cell populations was studied 8 weeks later in the blood. GAT and mesenteric AT (MES AT) were taken to study the replenishment (non-host chimerism) of the ATM populations. This was performed by analysing the proportion of CD45.2 donor cells for each subset as presented in Figure 3.3. ATMs (F4/80^{+}CD11b^{+}) were further divided according to their CD11c and Tim4 expression as shown in Figure 3.2.

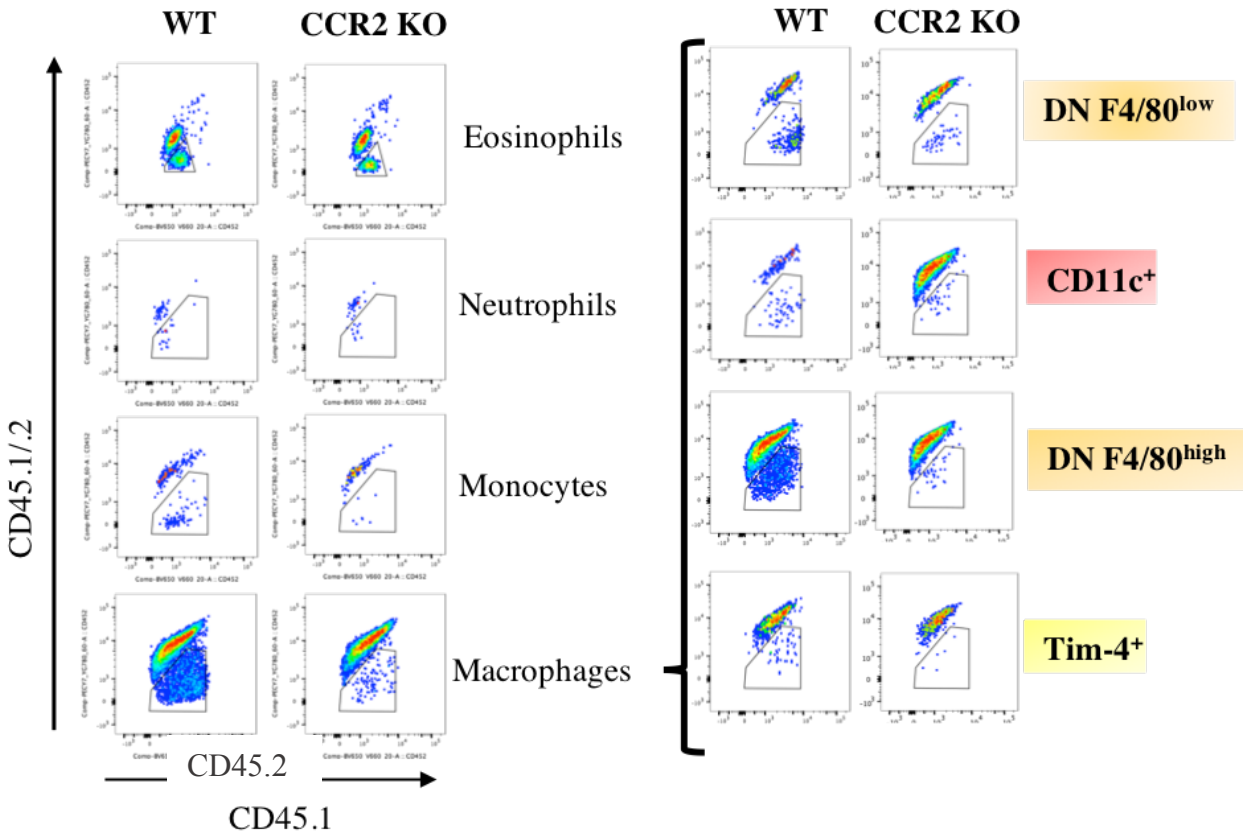

Figure 3.3 Tissue chimerism of immune cells in GAT

After irradiation of the legs, Ly5.1 recipient mice (expressing CD45.1and CD45.2) were injected iv with CD45.2 wild type (WT) or *Ccr2*$^{-/-}$ KO donor BM. Non-host chimerism was studied by flow-cytometry 8 weeks after irradiation. Dot plot analysis showing gating of CD45.1 donor cells in CD45^{+}SiglecF^{+}CD11b^{+}MHCII^{-} eosinophils, Ly6c^{+}CD11b^{+}MHCII^{-} monocytes, CD45^{+}Gr1^{+}CD11b^{+}MHCII^{-} neutrophils and CD45^{+}F4/80^{+}CD11b^{+}MHCII^{+} macrophages (left). Chimerism of ATM subsets were further analysed using gating defined in Figure 3.2 (right).

In this model of partial irradiation, granulocytes and monocytes, short lived immune cell populations entirely replenished in 8 weeks, showed a non-host chimerism of 30%. This percentage was in agreement with the percentage of body surface irradiated. As expected, Ly6c^{hi} monocytes non-host chimerism was dependent on CCR2 as shown by the decrease in non-host chimerism in mice reconstituted with *Ccr2*$^{-/-}$ BM, but the granulocytes were not (Figure 3.4).

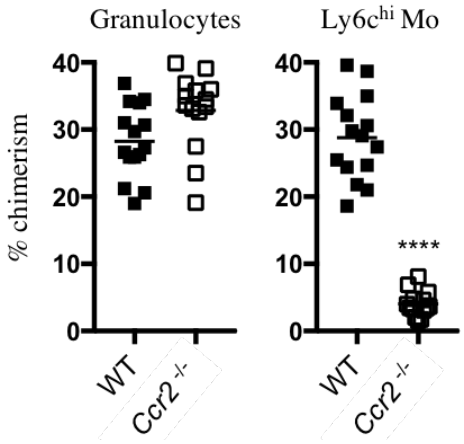

Figure 3.4 Mice reconstituted with *Ccr2* knock-out (*Ccr2*$^{-/-}$) BM had a low monocyte (Ly6C^{hi}) non-host chimerism but CCR2 deficiency did not affect granulocytes.

Partial BM chimeras were set up as described in Figure 3.3. Graph showing non-host chimerism of granulocytes (left) and monocytes (right). Data pooled from 3 independent experiments (n=3-5 mice per experiments) and given by Calum Bain in Steven Jenkins lab. Bar represents the mean. Student t test ****: P<0.0001

In AT, the non-host chimerisms of eosinophils, neutrophils and monocytes were similar to the non-host chimerism of granulocytes and monocytes in the blood (Figure 3.5). As expected only the Ly6C^{high} monocyte compartment non-host chimerism was dependent on CCR2 (Figure 3.5). When looking at F4/80^{+}CD11b^{+} ATMs, independently of their Tim4 or CD11c expression, the ATM non-host chimerism was lower (14%) compared to the granulocytes and monocytes, but CCR2 dependent, confirming their monocytic origin. Non-host chimerism in the GAT and MES AT were comparable, thus indicating that both tissues had similar degrees of BM dependency for these cells (Figure 1.4B).

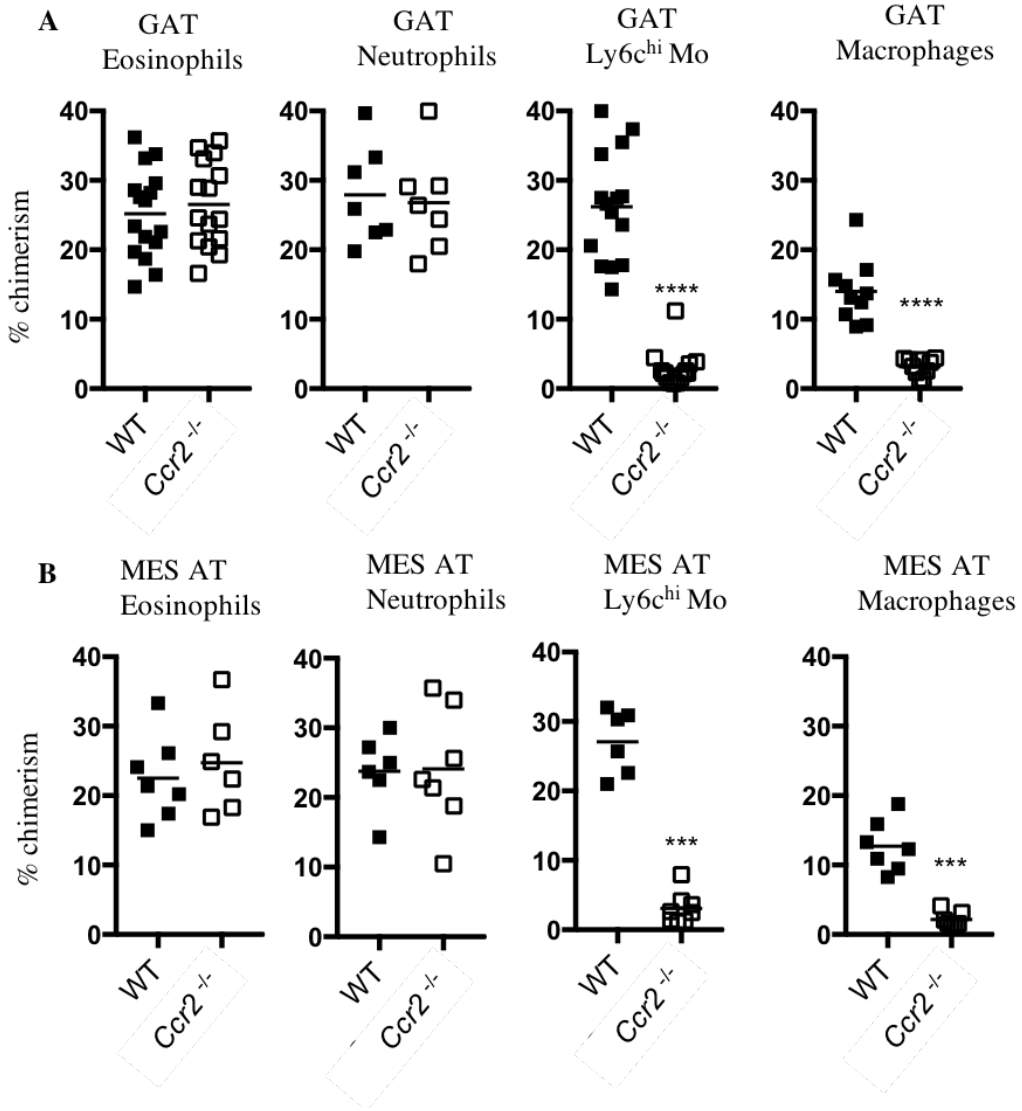

Figure 3.5 Non-host chimerism of eosinophils, neutrophils, monocytes and macrophages in GAT and MES AT.

Partial BM chimeras were set up as described in Figure 3.3. Graph showing non-host chimerism of eosinophils, neutrophils, Ly6c^{high} monocytes and ATMs in the GAT (**A**) and MES AT (**B**). Data pooled from 2 or 3 independent experiments (n=3-5 per group per experiments). Bar represents the mean. Student t test ***: $p<0.001$, ****: $p<0.0001$

3.4.3 Non-host chimerism of ATM subsets was heterogenous

ATMs were further divided according to their F4/80, Tim4 and CD11c expression, as shown in Figure 3.2. Both DN F4/80^{low} and CD11c^{+} ATM subsets showed a non-host chimerism comparable to blood monocyte (29%) (Figure 3.6). In contrast, the DN F4/80^{high} subset showed an intermediate non-host chimerism (10%) and the Tim4^{+} subset a low non-host chimerism (5%). All non-host chimerisms for these ATM subsets were dependent on CCR2 apart from the MES AT where the non-host chimerism in the Tim4^{+} population was too low to allow detection of a defect in replenishment in *Ccr2*$^{-/-}$ reconstituted mice.

To take into account variability in the degree of irradiation that each individual mouse was exposed to, the non-host chimerism of each ATM subsets was normalised to the WT non-host chimerism of blood monocytes. While CD11c^{+} and DN F4/80^{low} showed a replenishment of up to 100% by host derived cells, dependent on CCR2, and the F4/80^{high} subset showed only 40% turnover after 8 weeks which was also dependent on CCR2, the Tim4^{+} ATMs had the slowest turnover of 10% of cells replaced by donor cells after 8 weeks. Once adjusted to blood chimerism, the slow turnover of Tim4^{+} ATMs was not significantly different in mice reconstituted by WT or *Ccr2*$^{-/-}$ BM indicating that replenishment was maybe not dependent on CCR2 expression by monocytes or only very slowly replenished by the BM and could not be detected after 8 weeks (Figure 3.7). F4/80^{low} ATMs (CD11c^{+} of or not) were significantly more BM dependent than F4/80^{high} ATMs. The “waterfall” transition from monocytes to macrophages (F4/80 and MHCII acquisition and loss of Ly6c) can be observed in this gate and is the illustration of their BM dependency (data not shown).

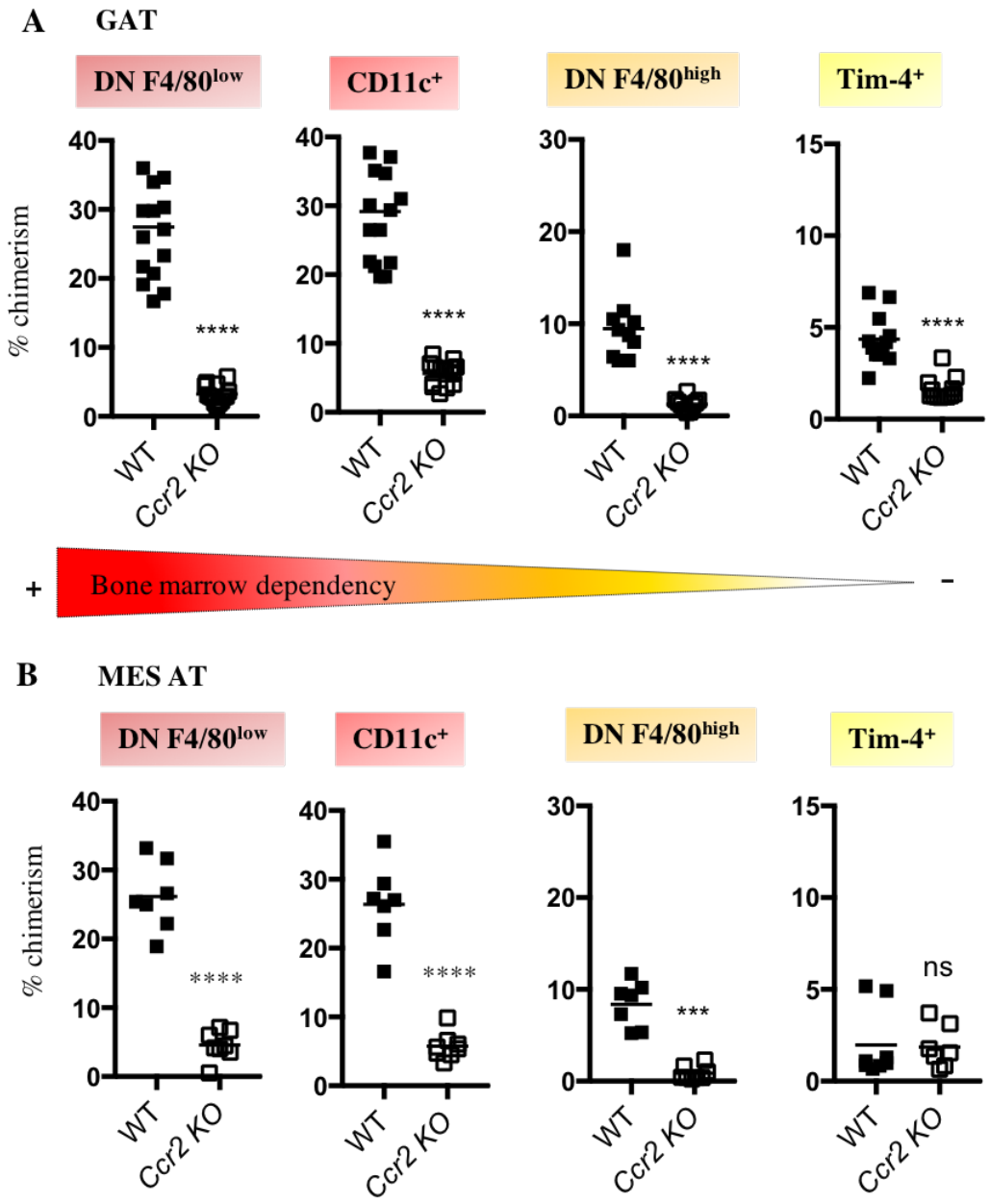

Figure 3.6 ATM subsets in GAT and MES AT showed an heterogeneous non-host chimerism

Partial BM chimeras were set up as described in Figure 3.3. Data reprensent the non-host chimerism for each ATM subsets, described in Figure 3.2. Data pooled from 2 independent experiments (n=3-5 per group per experiment). Bar represents the mean. Student t test ****: $p<0.0001$; *** $p<0.001$

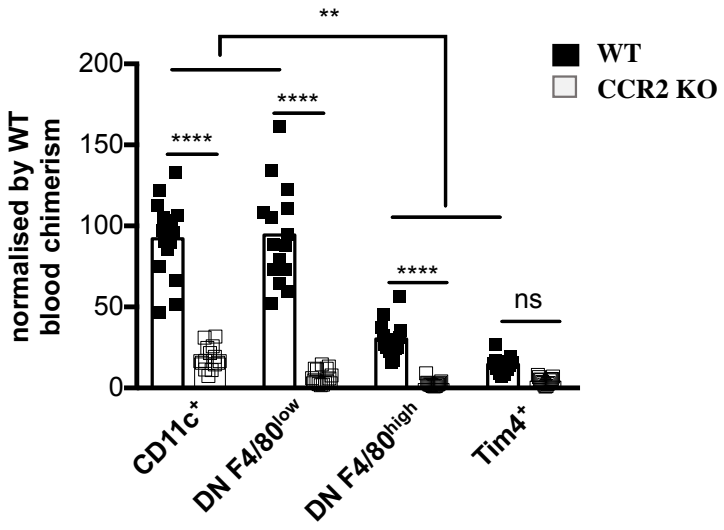

Figure 3.7 Tim4^{+} ATMs had the lowest normalised non-host chimerism which could not be distinguised from the mice injected with CCR2 KO when compared to other ATM subsets.

Partial BM chimeras were set up as described in Figure 3.3. Non-host chimerism of each ATM subsets, gated in Figure 3.2, was normalised by the non-host chimerism of blood monocytes of the WT mice. Data pooled from 3 independent experiments (n=3-5 per group per experiment). Column shows the mean for each group. One-way Anova (non-parametric) ****: $p<0.0001$; ns: non-significant

3.4.4 Head irradiation as a method to study macrophage replenishment in tissues located in the peritoneal cavity

The difference between MES AT and GAT non host chimerism in the resident Tim4$^+$ subset suggested that irradiation of the back legs may have partially exposed the GAT to irradiation, as this depot is located lower than the MES AT. By doing so, it is possible that it displaced the Tim4 ATMs and increased the non-host chimerism artificially. In collaboration with the laboratory of Dr Stephen Jenkins, head irradiations were conducted to verify this hypothesis (Figure 3.8). After normalisation to the chimerism of the blood monocytes for each mouse, the leg irradiation led to a low non-host chimerism for the Tim4$^+$ subset as found previously. However by irradiating the head, the percentage of chimerism in the Tim4$^+$ subset in the GAT was not different from the MES AT (Figure 3.8). Furthermore, during this experiment, the subcutaneous ATMs population was also studied. The Tim4$^+$ ATM subset in the subcutaneous AT (SAT) had a similarly low non-host chimerism compared to the MES and GAT. Thus head irradiation is a safer option to study ATM replenishment.

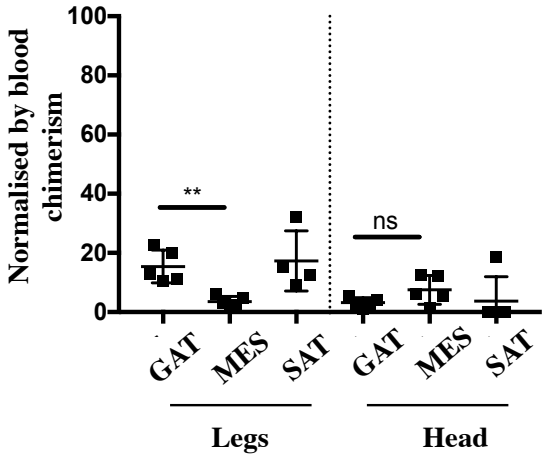

Figure 3.8 Head irradiation decreased differences of Tim4$^+$ non-host chimerism between the GAT and the MES AT, and was a better option to study ATM replenishment using partial BM chimera

Partial BM chimeras were set up as described in Figure 3.3, except that some mice were head irradiated, while some mice were leg irradiated. The non-host chimerism of Tim4$^+$ ATMs, as gated in Figure 3.2, was normalised by the non-host chimerism of blood monocytes for each mouse. Tim4$^+$ macrophages from GAT, MES AT and Subcutaneous AT (SAT) were analysed. Data from 1 experiment (n=5). Student t test *: $p<0.05$

3.4.5 Phenotyping of ATMs in lean GAT

Having established the existence of at least 4 subsets of ATMs with various degrees of dependency on BM monocyte for their replenishment, these subsets were further characterised by using other macrophage markers used broadly in the literature (Figure 3.9). All subsets expressed CD115 or colony stimulating factor-1 receptor (Csf1R), which is expressed by all macrophages in tissues and control their development and differentiation (Jenkins and Hume 2014). Interestingly all ATMs expressed Relma (resistin-like molecule alpha), a marker associated with repair. F4/80^{high} macrophages (Tim4^{+} and Tim4^{-}) expressed CD206 and CD301 (data not shown), markers associated with endocytosis, phagocytosis, repair and alternative activation (Haase et al. 2014b). CD64, a Fc-gamma receptor, is used to differentiate ATMs from dendritic cells (DCs) in AT (Cho et al. 2016). F4/80^{high} ATMs expressed CD64 in greater proportion than F4/80^{low} ATMs, indicating than the latest could be freshly differentiating from monocytes in the tissue.

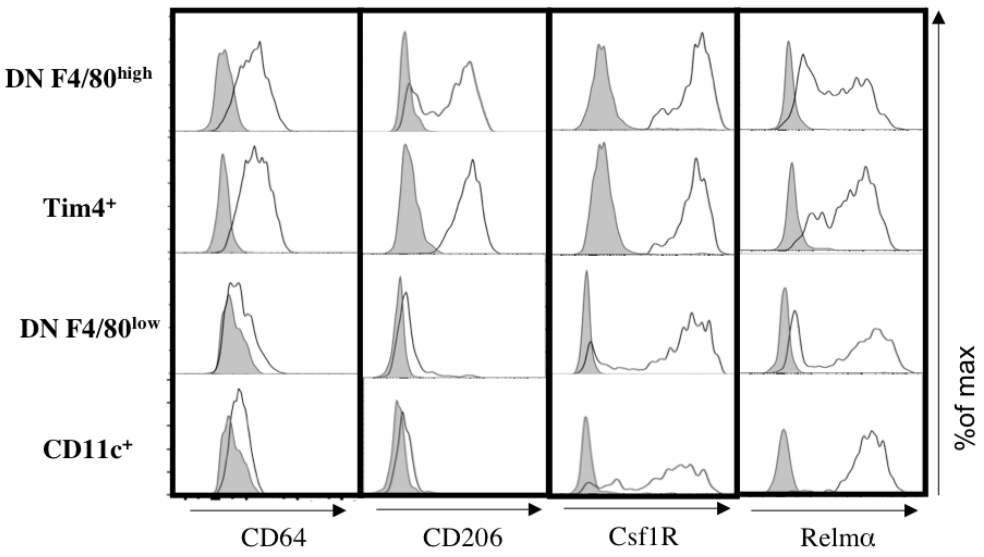

Figure 3.9 Histograms showing CD64, CD206, Csf1R and Relmα expression on ATMs macrophages

ATMs from GAT were stained for CD64, CD206, CD115 and Relma. The negative control (fluorescence minus one) is represented in plain grey for each subset.

3.4.6 Tim4^{+} ATMs were resident in subcutaneous AT and present at birth at a very low proportion

SAT macrophage description is still limited and, as for the visceral AT, their origin is not known. SAT is present at birth, contrary to the GAT (Wang et al. 2013). Therefore combining both chimeras (in adults) and time course in new born could be a simple method to follow macrophages dynamic during development, when other methods are not available. It was not always possible to distinguish a clear F4/80^{high} and F4/80^{low} population in adult SAT. This was possibly due to the lower number of ATMs recovered from the SAT compared to GAT and MES AT. Therefore ATMs in the SAT were divided in 3 subsets, disregarding their F4/80 expression, as shown in Figure 3.10 : Tim4^{+}, CD11c^{+} and Tim4^{-}CD11c^{-} (double negative: DN). After head irradiation, the three subsets of ATMs showed the same pattern of non-host chimerism as ATMs in the GAT. CD11c^{+} cells showed a high non-host chimerism comparable to blood monocyte and Tim4^{+} cells showed a low non-host chimerism.

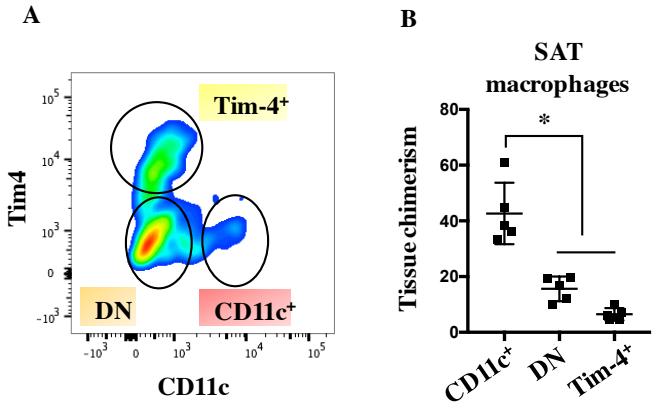

Figure 3.10 SAT macrophages were heterogeneous and Tim4^{+} ATMs had a low BM dependency.

After head radiation, wild type CD45.1 bone marrow was injected intraveneously to CD45.1/.2 mice, and followed after 8 weeks of replenishment. The non-host chimerism is the percentage of CD45.1 cells within each subsets.

A. Cells were gated on live CD45^{+}SiglecF^{-}Ly6c^{-}MHCII^{+}F4/80^{+}CD11b^{+} and divided on their Tim4 and CD11c expression. **(B)**. Tissue non-host chimerism. Data from 1 experiment (n=5) ± SD. One way anova *: $p<0.05$.

To study the origin of the resident Tim4^{+} ATMs, SAT was taken from pups and analysed by flow cytometry over a time course from birth to adulthood. Typically, yolk sac derived macrophages present a F4/80^{bright} phenotype, contrary to F4/80^{low} cells, derived from HSC, thus this could be an indicator of ATM origin (Schulz et al. 2012b). At birth, SAT was void of lipids (data not shown) and weighing aroung 5 mg (Figure 3.11). Quickly, the size of the fat pads expanded (ten-fold heavier after 1 week) and reached around 230 mg at 4 weeks and remained stable up to adulthood. At birth all macrophages were F4/80^{high} , suggesting a YS origin. Shortly after, during SAT expansion, a F4/80^{low} population was distinguished up until 4 weeks, then the frontier between the F4/80^{low} and F4/80^{high} ATMs was less clear (Figure 3.12A). Moreover, as shown in Figure 3.12B, shortly after birth (postnatal day 1: P1) the F4/80^{high} macrophages present were MHC-II^{low} (population IV), again resembling what have been described in the literature as being YS derived macrophages (Ginhoux and Guilliams 2016). At the first week of life (P7), MHC-II^{high} cells appeared (population I) and this pool kept growing to finally become the majority of adult SAT macrophages (population I and II). The resident Tim4^{+} ATMs appeared between P1 and P7 (population III) and they acquired MHC-II (population II) after weaning (P21). In terms of relative proportion, Tim4^{+} ATMs in the SAT reached a peak around weaning (P21) and then their proportion remained stable (pop II + III), with a mix of MHC-II^{high} and MHC-II^{low} cells (Figure 3.12C). There might be a mix origin of macrophage in the SAT, with YS derived cells at first and then participation of BM derived cells (F4/80^{low}) that acquired MHCII. However without lineage tracing it would be difficult to confirm these findings.

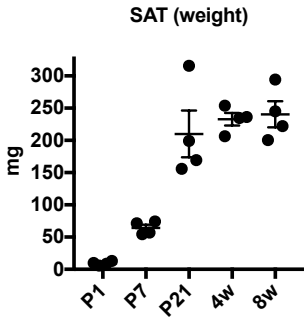

Figure 3.11 Evolution of SAT weight during mouse development

SAT was taken from mice and weighed to follow fat mass evolution from P1 (post-natal day 1) to adulthood (8w = 8 weeks). Data representative of 2 independent experiment (n=4).

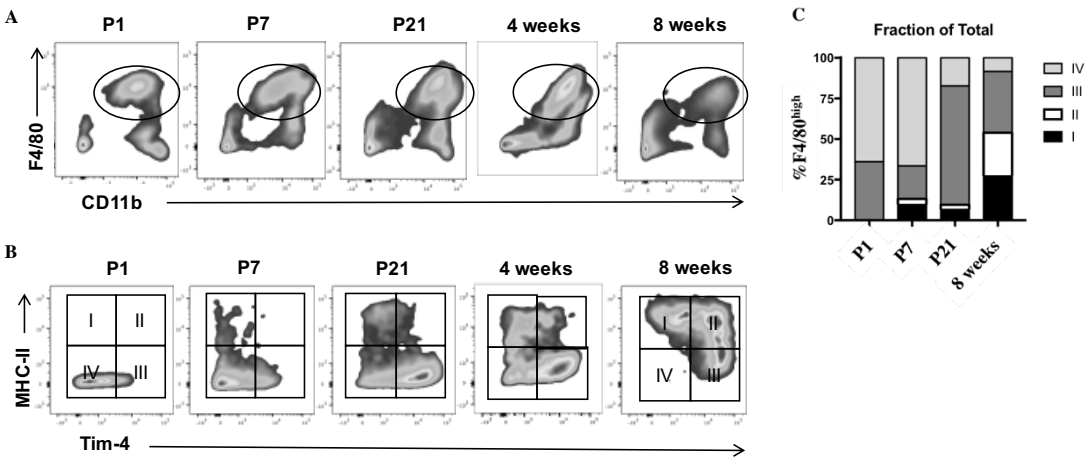

Figure 3.12 SAT contains yolk sac derived F4/80^{high}MHCII^{low} macrophages at birth

A Density plot showing SAT ATMs (CD45^{+}F4/80^{+}CD11b^{+} cells; circled) during a time course: P1 (post-natal day 1), P7 (post-natal day 7), P21 (post-natal day 21), and at 4 weeks and 8 weeks after birth **B.** Density plot showing the evolution of MHCII and Tim4 expression in the F4/80^{high} macrophage population during SAT development. **C.** Relative proportion of each subsets represented in **B**. Data representative of 2 independent experiment (n=3-4).

I : MHCII^{high}Tim4^{-} ; II : MHCII^{high}Tim4^{+} ; III: MHCII^{low}Tim4^{+} ; IV: MHCII^{low}Tim4^{-}

.

3.5 Discussion

The main results of this chapter are summarised in the Table 3-1.

Table 3-1 Summary of findings from chapter 3

Subsets	CCR2 dependency	Non-host chimerism after 8 weeks	Replenishment by monocyte after 8 weeks	Proportion in the tissue
Tim4+	low	Low	Very slow	11% of ATMs
CD11c+	Yes	High	Quick	6% of ATMs
F4/80^{high}	Yes	Intermediate	Slow	71% of ATMs
F4/80^{low}	Yes	High	Quick	12% of ATMs

Importance of partial body irradiation and gating strategy to study ATMs

In previous studies, partial body irradiation (legs irradiation) used to study macrophages in the peritoneal cavity, showed the same blood non-host chimerism to the one in the set of experiment realised for this chapter (of about 30%) (Jenkins et al. 2011). This reflects a good reproducibility of the technique. However, unintentional irradiation of some tissue can lead to an artificial increase in non-host chimerism. This can be explained by the niche competition between recruited and resident macrophages (Guilliams and Scott 2017). Indeed, irradiating the tissue can deplete resident ATMs thus, the "niche" being free, these macrophages could be replaced by recruited monocytes in order to restore their number (Guilliams and Scott 2017). However, resident macrophages can repopulate a tissue by proliferation, in a M-CSF dependent manner (Hashimoto et al. 2013). Head irradiation seemed to be a good alternative to the irradiation of the legs, so the tissues are untouched and studies of residency can be performed.

By only defining ATMs as being F4/80^{+}CD11b^{+} cells, the non-host chimerism 8 weeks post-legs irradiation was of 12% in GAT and MES (around 41% once

normalised). It was only by dividing F4/80^{+}CD11b^{+} ATMs into subsets that the diversity in BM dependency appeared which emphasis the need of characterising better ATMs to understand their origin. Recently, an another group used partial BM chimera with head irradiation to study ATMs in the GAT, and found a ATM non-host chimerism of 3.57% 15 weeks post-irradiation, then 14% 19 weeks post irradiation (Zheng et al. 2016a). In their study, ATMs were defined as Siglec-F^{-}F4/80^{+} cells. Differences between their groups (3.57% vs 14% in only few weeks apart), but also with results presented in this chapter could be due to two things: first, their gating strategy based on Siglec-F^{-}F4/80^{+} seemed limited. Secondly, the consistency of the operators to performed irradiation could be questioned. As shown by the legs versus head irradiation, how irradiations are performed can artificially increase non-host chimerism. Normalisation by blood chimerism could potentially decrease differences between independent experiments, assuming that tissues of interest are not irradiated.

Macrophages were recruited at homeostasis in lean AT

The current dogma is that ATMs recruitment occurs mainly during obesity (Weisberg et al. 2003; Reilly and Saltiel 2014; Patsouris et al. 2008a). However, our results suggested that, in lean AT, at least 18% of ATMs (CD11c^{+} and DN F4/80^{low}) were highly dependent on the BM and 71% (DN F4/80^{high}) were partially dependent. If only looking at the literature, recruited ATMs are characterised as M1 macrophages, pro-inflammatory, thus their presence in lean healthy tissue could be a paradox (C. N. Lumeng et al. 2007). The M1/M2 classification has to be challenged as, even though it could work *in vitro* after supervised stimulations with LPS or IL4, the *in vivo* reality is different. These recruited M1 macrophages did express what the literature classifies as M2 markers (Martinez and Gordon 2014). Indeed, by adding more markers to the panel, it was to notice that macrophages with higher chimerism, also expressed Relm-α, a M2 marker according to the literature (Zheng et al. 2016b). Actually, Relm-α was uniformly expressed by the CD11c^{+} subset, while this marker showed some heterogeneity in expression in the resident subset. In the murine serous cavity, Relm-α defines macrophages with a high non-host chimerism, CCR2 dependent, thus monocyte derived (Calum C Bain et al. 2016). Interestingly, the authors suggest that the fraction of F4/80^{high} macrophages expressing Relm-α derive from F4/80^{low}

macrophages. This could indicate that Relm-α could also delimit other subtypes of ATMs within the DN F4/80^{high} and Tim4 subsets with different BM dependency. More markers would be needed to dissociate them or, ideally, techniques such as single cell RNA sequencing.

Tim4^{+} were resident macrophages which may not require CCR2 to enter the tissue in adults GAT and MES AT

Tim4^{+} is a PS receptor that recognise apoptotic cells, which typically express PS at their surface as a "eat me" signal to be recognised and engulfed by macrophages (Miyanishi et al. 2007; Nishi et al. 2014). Tim4 is expressed on resident peritoneal macrophages, spleen macrophages, gut macrophages and Kupffer cells (Davies et al. 2013; Shaw et al. 2018). Eight weeks post irradiation, Tim4^{+} ATMs showed a very low non-host chimerism. If compared with mice injected with CCR2 KO BM, the difference in normalised chimerism between WT and CCR2 KO donor groups was non-significant, which could mean that CCR2 is dispensable for their entry to the tissue. CCR2 is the receptor for monocyte chemoattractant protein 1(MCP1 / also known as CCL2) produced by tissues. CCR2 is usually expressed by monocytes and recruited macrophages (C. N. Lumeng et al. 2007). In *Ccr2*$^{-/-}$ mice, fewer monocytes are present in the bloodstream, as they fail to exit the BM and be recruited to tissues upon MCP-1 release (Tsou et al. 2007). However, *Ccr2*$^{-/-}$ mice still contain ATMs (C. N. Lumeng et al. 2007). Either the remaining ATMs rely on other recruitment signals to enter the tissue or, resident macrophages are evolving independently from the BM, by proliferation. For example, in the small intestine, Tim4^{+} macrophages were dominant in *Ccr2*$^{-/-}$ mice (Shaw et al. 2018). They were present at birth in high proportion, and the authors hypothesised these to be FL derived or from an early BM influx of monocytes. These cells were also found to be maintained independently from the BM (Shaw et al. 2018). Similarly, Kupffer cells are also maintained independently from the BM, however, monocytes contribute to their pool during liver development as well as embryonically derived macrophages (Scott et al. 2016). Looking at these data together, Tim4^{+} ATMs could potentially be a self-replenishing population that might find their origins in early monocyte recruitment to the GAT.

Tim4^{+} ATMs could be yolk sac derived in the SAT at birth

Macrophage origins have been thoroughly described in the literature, with the exception of ATMs. GAT is absent in the murine embryo, however the subcutaneous AT develops *in utero* (Wang et al. 2013) which allowed the study of possible embryonic macrophages seeding this tissue and persisting with age. SAT was populated by F4/80^{high} macrophages at P1, which were mainly Tim4^{-}MHCII^{low}. F4/80^{high} (also called "bright") macrophages are characteristic of yolk sac (YS) derived macrophages in tissues thus indicating that macrophages present at birth in the SAT might also be of YS origin (Schulz et al. 2012b; Hoeffel et al. 2012). F4/80^{low} macrophages entered the tissue around P7, certainly coming from the BM. These macrophages could be monocyte derived and indicate that SAT has a mix population of macrophages during the first week(s) of life.

A small proportion of Tim4 ATMs was present at birth and grew in number during SAT development. Either these Tim4^{+} ATMs are recruited from the BM or derived from the F4/80^{high} macrophages present at birth. In the heart, MHC-II^{high} macrophages are derived from embryonic MHC-II^{low} macrophages (Epelman et al. 2014), which indicated that embryonic macrophages can acquire more markers with time which could also be the case for the Tim4^{+} SAT macrophages. F4/80^{high} YS macrophages might acquire Tim4^{+} and MHCII over time and persist in the tissue by self-renewal which would explain the low chimerism in adult. Nonetheless, F4/80^{low}MHC-II^{high} ATMs could replace the YS derived cell over time, acquire Tim4 and proliferate in the tissue. For example, in the peritoneal cavity, newly recruited cells from the BM acquire *in fine* the same phenotype as the previous F4/80^{bright} embryonic macrophages but first they undergo a F4/80^{low}MHCII^{+} stage (Calum C Bain et al. 2016). Lineage tracing such as injection of tamoxifen at E.8 in Csf1r-mer-iCre-mer crossed with Rosa26-LSL-YFP reporter mice pregnant female would label embryos YS derived macrophages with YFP and the follow up of these cells by flow cytometry could give more definite informations about macrophage origin in the SAT (Schulz et al. 2012b). Interestingly Tim4^{+} ATM population seem to expand at a time where lipids started to fill adipocytes in the SAT (around P4) certainly inducing an important tissue remodelling and cell death which require Tim4^{+} ATMs to clear the tissue.

Conclusion

We identified 4 populations of ATMs in adipose tissue showing different degree of dependency on the BM for their maintenance in adult GAT and SAT. In the next chapter we will analyse how HFD affects the turnover of these populations

CHAPTER 4 ATMS INCREASE BOTH BY PROLIFERATION AND RECRUITMENT IN OBESE AT

4.1 Introduction

Obesity has become a worldwide epidemic affecting around 650 million individuals ("WHO | Obesity and Overweight" 2018). Obesity causes a low grade inflammation, related to the excessive AT expansion (Ye 2013). Visceral AT accumulation is associated with an increased risk of developing insulin resistance and type 2 diabetes. In contrast, accumulation of AT below the waist, in the subcutaneous AT, appears to be less detrimental (Pereira and Alvarez-Leite 2014; Fu, Hofker, and Wijmenga 2015). Interestingly females accumulate less VAT than males during HFD, which is also associated with less macrophage infiltration and less inflammation (Fuente-Martín et al. 2013). The link between AT inflammation during obesity and macrophages recruitment was established in the early 2000s. Weisberg *et al.* revealed that macrophage numbers were multiplied by 5 in obese mice and were linked with pro-inflammatory cytokine release (Carey N Lumeng, Bodzin, and Saltiel 2007). By creating chimeras with full body irradiation, they showed that most ATMs were recruited from the BM during obesity (Weisberg et al. 2003). However a later study showed that after 7 weeks of HFD, local macrophage proliferation occurred and contributed to ATM number increase (Amano et al. 2014). These two conflicting results show the necessity to further study ATMs to understand their origins in the tissue. Moreover, these studies mainly considered macrophages as a whole instead of defining functional subsets, with the novel exception of CD11c expressing macrophages (Patsouris et al. 2008a; Li et al. 2010; Carey N Lumeng, Bodzin, and Saltiel 2007). Indeed $CD11c^+$ ATMs have been linked with insulin resistance, AT inflammation and whole body low-grade inflammation during obesity (Patsouris et al. 2008b; Carey N Lumeng, Bodzin, and Saltiel 2007; J. M. Wentworth et al. 2010). The discovery of a novel resident $Tim4^+$ macrophage population that was discussed in chapter 3, plus the fact that ATM recruitment is very heterogeneous, raises the question of how each subset would change during HFD feeding. As females and males do not seem to have the same AT expansion and macrophage recruitment dynamic, sex differences in ATM phenotype will also be considered.

4.2 Aim

In the previous chapter, four ATM subsets were found in the GAT, including a Tim4^{+} population with a very low BM dependency, DN F4/80^{high} subset with an intermediate BM dependency and two subsets (CD11c^{+} and DN F4/80^{low}) with a high BM dependency. In the SAT, due to lower cell number, it was more difficult to find a clear distinction between DN F4/80^{high} and DN F4/80^{low} so these subsets were considered as one population defined as DN.

The aims of this chapter are:

- To follow the changes in ATM recruitment after 8 weeks of HFD using partial BM chimeras (head irradiation), in SAT and GAT.
- To compare macrophage recruitment dynamics within male and female adipose depots during HFD feeding.
- To investigate the impact of HFD on the novel resident Tim4^{+} ATM population

4.3 Experimental design

Partial BM chimeras coupled with HFD. To study the contribution of monocytes to the development of ATM populations we used adipose tissue protected BM chimera in collaboration with the laboratory of Dr Stephen Jenkins. Host mice (males and females) ($CD45.1^+CD45.2^+$) were partially irradiated (head irradiation), with a shield covering ¾ of the body and then reconstituted with congenic WT BM ($CD45.2^+$). After 4 weeks of recovery, a control diet (CD) or a HFD (HFD; 60% fat) was provided ad libitum for 8 weeks. GAT and SAT were collected to study the non-host chimerism by flow cytometry.

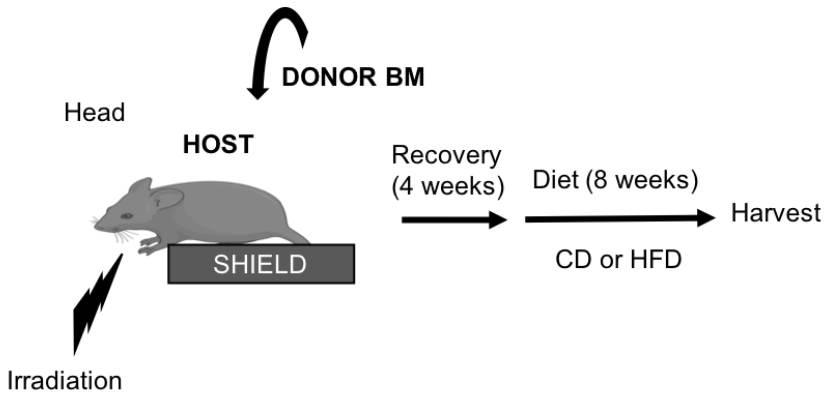

Figure 4.1 Experimental design of partial BM chimeras coupled with diet to study macrophage turn-over during HFD.

After irradiation of the head, Ly5.1 host mice (expressing CD45.1 and CD45.2), both males and females, were injected i.v. with $CD45.2^+$ donor BM. After recovery, mice were then put on a control diet or a HFD (60% fat) for 8 weeks. Non-host chimerism was studied at the cull in the blood, GAT and SAT.

4.4 Results

4.4.1 Heterogeneity in weight gain and macrophage number between adipose depots

Males accumulated similar amount of GAT than females when compared to body weight

After generation of BM chimeras (as shown in Figure 2.2), and 8 weeks of either a control diet or HFD, mice (males and females) were sacrificed. As anticipated, after 8 weeks of HFD, both males and females put on weight significantly compared to the control groups (Figure 4.2A). Both the subcutaneous and gonadal adipose depots were heavier in mice fed on a HFD compared to the control mice in both male and female mice (Figure 4.2). Nonetheless, female adipose depots were smaller when compared with their male counterparts (Figure 4.2 A). However, if normalised by body weight (BW), there was no more sex differences (Figure 4.2 B). Therefore, the GAT expansion was proportional to the weight gain in males and females, even if males contained more GAT than females.

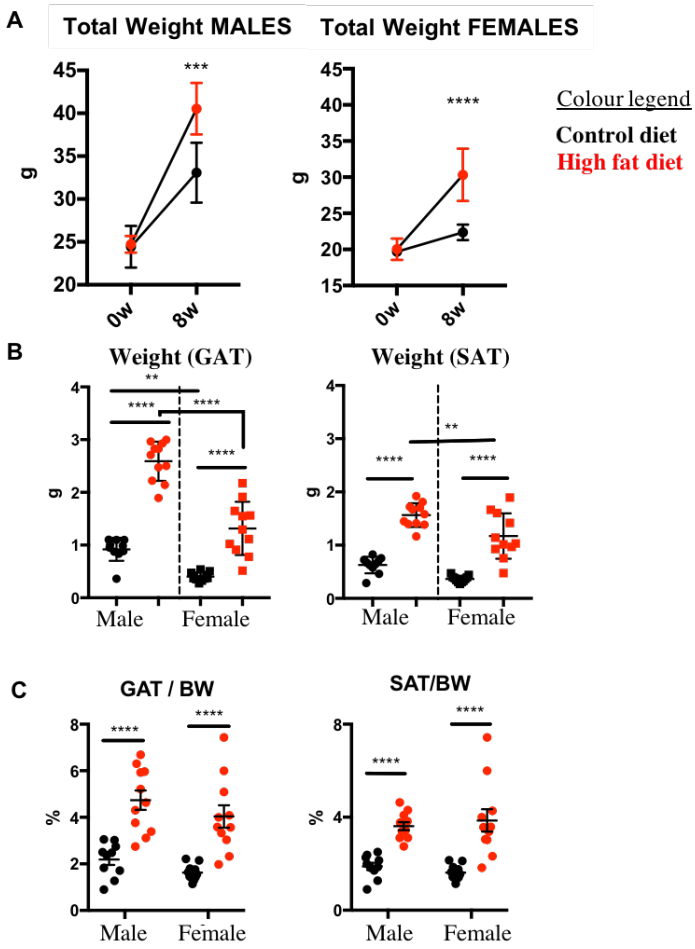

Figure 4.2 Males accumulated more GAT and SAT than females after 8 weeks of HFD but when compared to body weight, the differences were null.

Partial BM chimeras were set up as described in Figure 2.2. **A.** Weights of mice before and after 8 weeks of HFD **C.** GAT (left) and the SAT (right) were weighed (grams) after 8 weeks of control diet or HFD. **C.** GAT and SAT weights reported to the body weights (BW).Data pooled from 2 independent experiments (n=4-6 per group per experiment). The bar represent the SEM. Two-way Anova was performed to determine the p-value. ****: $p<0.0001$; **: $p<0.01$

Males had more macrophages in the GAT than females

The total number of GAT macrophages ($F4/80^{+}CD11b^{+}$ cells) showed a nearly 3 fold increase in the male mice. In female mice, GAT ATM number only increased slightly (Figure 4.3, left). In the SAT, the total number of ATMs remained constant for both sexes and diets (Figure 4.3, right).

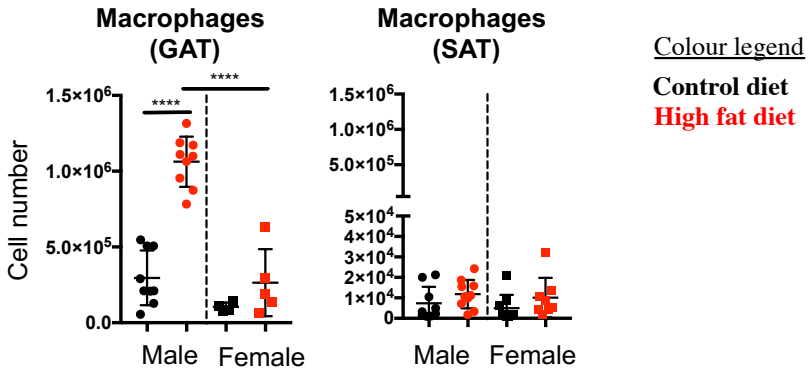

Figure 4.3 The total number of macrophages in the GAT increased in male but not in female mice nor the SAT after 8 weeks of HFD.

Partial BM chimeras were set up as described in Figure 2.2. The total number of ATMs per fat pad was assessed in the GAT (left) and the SAT (right) using live cell count of the stromal vascular fraction and flow cytometry.
Data pooled from 2 independent experiments (n=4-6 per group per experiment) for SAT and male GAT, 1 experiment for female GAT (n=5). Two-way Anova was performed to determine the p-value. ****: $p<0.0001$

4.4.2 Heterogeneity of recruitment during HFD is sex and depot specific

First, male and female ATM turnover were compared by analysis of the non-host chimerism. In the GAT, there was no significant differences in non-host chimerism between males and females independently of the diet for the $CD11c^+$ and DN $F4/80^{low}$ subsets (Figure 4.4). However changes occurred within the subsets with lower chimerism. The DN $F4/80^{high}$ and $Tim4^+$ macrophages had a higher chimerism in lean male compared to lean female. With HFD, DN $F4/80^{high}$ non host chimerism increased in males, but not in females, implying a higher turnover of these cells during obesity in males but not females. Even though the chimerism of $Tim4^+$ macrophages did not increase with HFD in both sex, male $Tim4^+$ macrophages had a higher non-chimerism after HFD compared to the females fed with the same diet. This suggested than $Tim4^+$ macrophages in females were more slowly replaced.

In the SAT (Figure 4.4B), the DN subset non-host chimerism increased in obese males and was significantly higher than in the obese females. Although the $Tim4^+$ non-host chimerism was slightly increased in males after HFD (non-

significant), the obese females showed a significant increase in chimerism. Implying that the Tim4^{+} population in the SAT relied more on the BM for its replenishment.

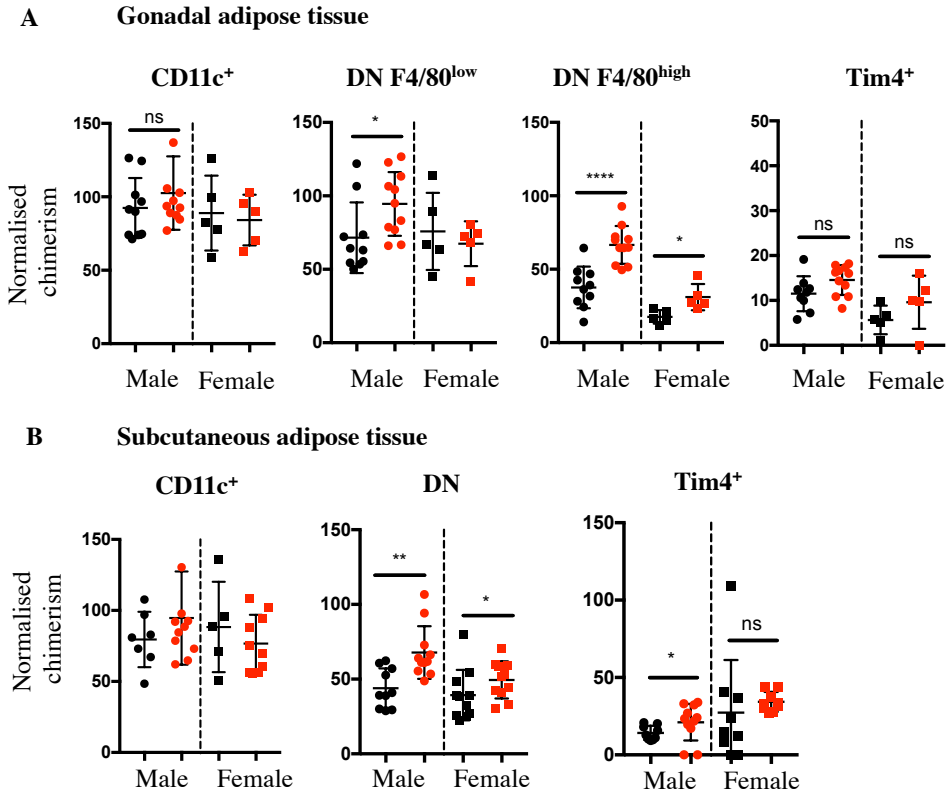

Figure 4.4 DN F4/80^{high} and Tim4^{+} non-host chimerism showed the highest sex specificity, in the GAT (A) and SAT (B), after 8 weeks of HFD (red)

Partial BM chimeras were set up as described in Figure 2.2. The percentage of chimerism was normalised by the Ly6c^{high} chimerism in the blood for each mouse. Data pooled from 2 independent experiments (n=4-6 per group per experiment) for SAT and male GAT, 1 experiment for female GAT (n=5). In black : control diet; in red : HFD. Bars represent mean v. Two-way Anova was performed to determine the p-value **** : p<0.0001; **: p<0.01; *: p<0.05

4.4.3 Heterogeneity of ATM recruitment during HFD

Non-host chimerism of Tim4^{+} ATMs did not increase with HFD

To better compare the impact of HFD on non-host chimerism, male mice were utilised as they gained more weight and had the most striking increase in macrophage number. Their non-host chimerism was normalised by the Ly6c^{high} monocyte non-host chimerism in the blood for each mouse and the control group was compared to the

HFD group. When considering ATMs ($F4/80^+CD11b^+$ cells) as one population, the normalised chimerism was 39.5% (± 6.3) in mice fed a control diet, and 71.5% (± 9.5) in mice fed a HFD (Figure 4.5).

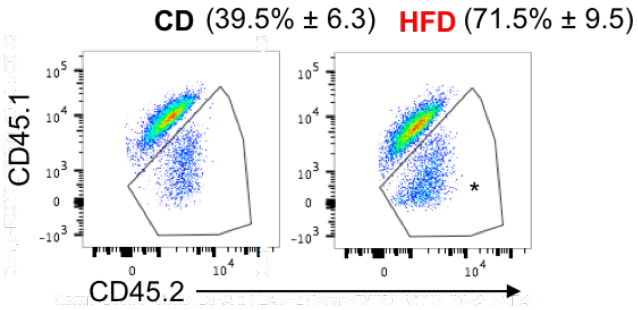

Figure 4.5 ATM non-host chimerism was increased during HFD in the GAT of male mice.

Partial BM chimeras were set up as described in Figure 2.2. Non-host chimerism was measured as showed on the FACS plot, by gating on CD45.2 cells within the $F4/80^+CD11b^+$ gate (after exclusion of eosinophils, neutrophils, monocytes). The percentage of chimerism was normalised by the $Ly6c^{high}$ chimerism in the blood for each mouse and is represented in the between bracket as mean ± SEM . Representative data from 1 of 2 independent experiments (n=4-5 per group per experiment).

As seen in chapter 3, it was only when the ATM population was considered as defined subsets delineated using surface expression of CD11c, CD11b, F4/80 and Tim4 that the heterogeneous ATM recruitment dynamics could be unveiled. The DN $F4/80^{high}$ subset had the highest non-host chimerism increase due to HFD. Although $CD11c^+$ and DN $F4/80^{low}$ ATMs also increased due to input from the donor BM., the changes were not statistically significant. However, both subsets were already nearing maximum turnover of 100% in the lean state. As for the $Tim4^+$ ATMs, they conserved their low BM chimerism, irrespective of the diet that the mice were fed (Figure 4.6A).

The number of recruited macrophages increased in the GAT during HFD

The number of cells within each subset raised during HFD : $F4/80^{low}$ had a 13.6 fold increase, $CD11c^+$ a 12.9 fold increase, DN $F4/80^{high}$ a 6.4 fold increase and $Tim4^+$ a 5 fold increase. For each subset, when comparing the total number of ATMs in the tissue with the number of cells coming from the BM, $Tim4^+$ macrophages showed the lowest number of cells coming from the BM. While the $Tim4^+$ macrophage numbers in the tissue increased, the input of BM derived cells was very minimal, suggesting

that this population was increasing via proliferation expansion (Figure 4.6B), which was confirmed by a later experiment. In contrast, the total number of $CD11c^+$ cells in the AT was equivalent to the number of CD11c coming from the BM indicating that this population was entirely dependent on BM derived cells for its increase during HFD. ATM recruitment during HFD seemed to outnumber $Tim4^+$ ATMs, as their relative proportion went from 24% in lean mice to only 16% of ATMs in obese mice (Figure 4.6C). $CD11c^+$ macrophages, who were linked with inflammation in previous studies, had an increase of 64% (from representing 14% in control mice to 23% in obese mice). This increase was the highest increase in proportion in the tissue.

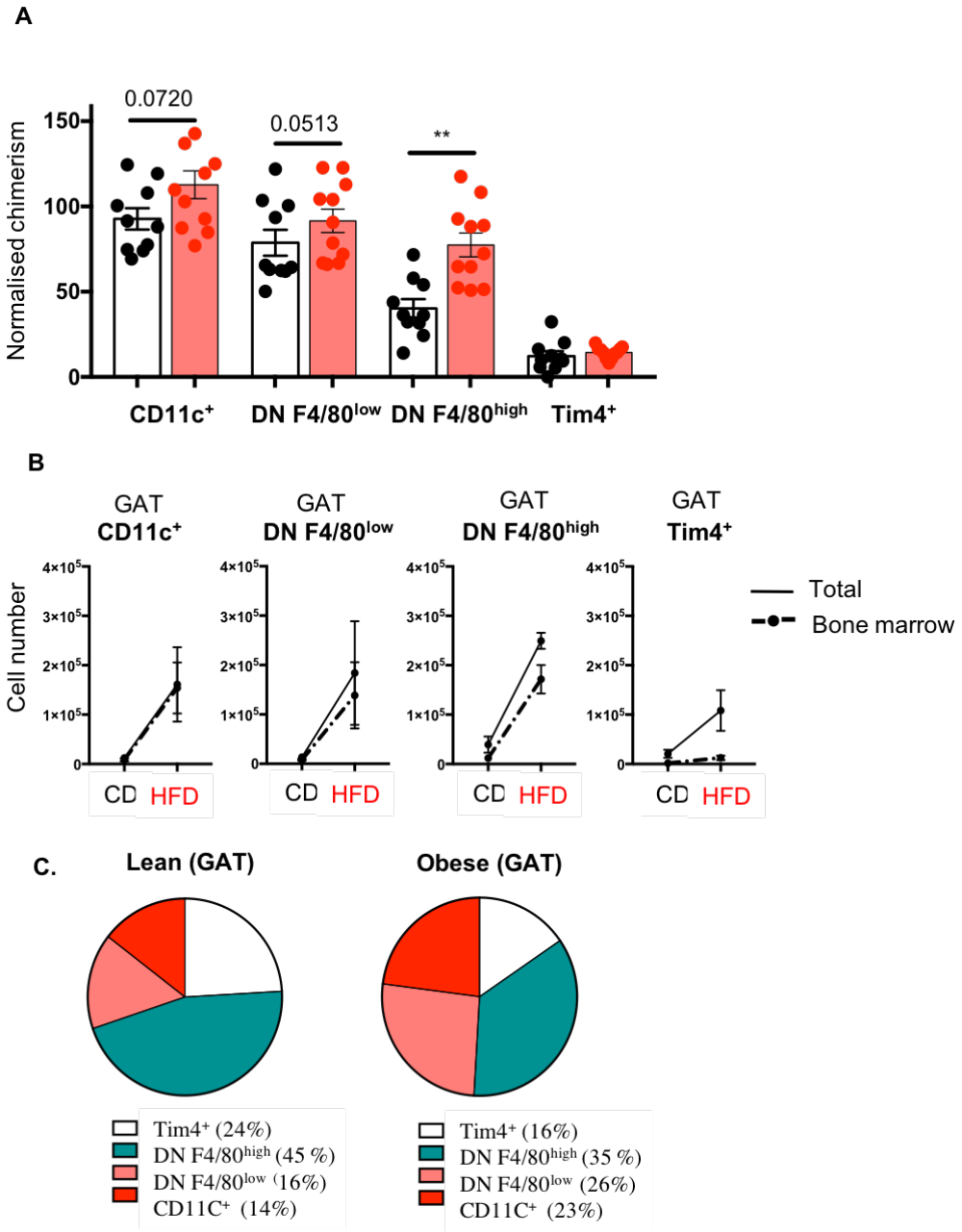

Figure 4.6 Tim4$^+$ ATMs did not rely on the BM to increase in number during HFD but their overall proportion decreases due to the arrival of BM derived ATMs in the GAT after 8 weeks of HFD (males).

Partial BM chimeras were set up as described in Figure 2.2. Non-host chimerism was assessed in GAT from male mice (**A**) after a control diet (black dots) or HFD (red dots) (data pooled from 2 independent experiments, n= 4-6 per group per experiment ; student t test ** $p<0.001$) **B.** The number of macrophages for each subset in the tissue compared to the number of cells coming from the BM in mice fed a CD or a HFD **C.** Proportion of each subset in lean or obese mice (Data representative of 1 from 2 independent experiments).

Tim4^{+} macrophages proliferated during HFD

To measure proliferation, macrophages were stained with Ki67, a protein absent from quiescent cells, and the percentage of Ki67 positive ATMs was measure by flow cytometry. As expected, Tim4^{+} ATMs had a higher proliferation level during HFD (14%) and although not significant, higher than the other ATM populations confirming that their maintenance was dependent on self - renewal by proliferation than by input from the BM during HFD.

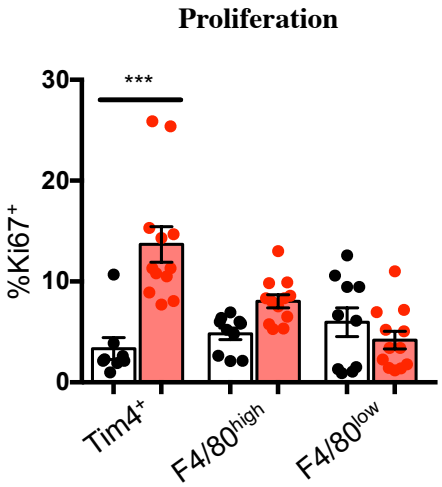

Figure 4.7 Tim4 macrophages proliferated in the GAT during HFD, as measured by Ki67.

Mice were fed a HFD for 14 weeks (red) or a control diet (black). ATMs were stained using Ki67, a marker of proliferation, and analysed by flow cytometry. The percentage of Ki67^{+} cells for each subsets is represented in the histogram. Data pooled from 2 independent experiments. Bar represent the mean ± SEM. Student t test *** $p<0.0001$.

4.4.4 ATMs had dynamic changes in MHCII expression and lipid content during the course of HFD

ATMs have previously been described as becoming lipid-laden during HFD feeding, notably the CD11c^{+} ATMs (Grijalva et al. 2016; X. Xu et al. 2013). To study the impact of HFD on ATM lipid content, mice were put on a HFD for 8 weeks, and after ATM isolation from the GAT, cells were analysed by flow cytometry.

After 8 weeks of HFD, new subsets of macrophage with a lower expression of MHC class II appeared in the tissue. The analysis of MHCII surface expression (gMFI and histogram) showed that the Tim4^{+} population shifted toward being mainly

MHCII^{low} in obese mice (Figure 4.8). The non-host BM chimerism of these subsets was unchanged compared to the MHCII^{high} cells within the same subset (data not shown).

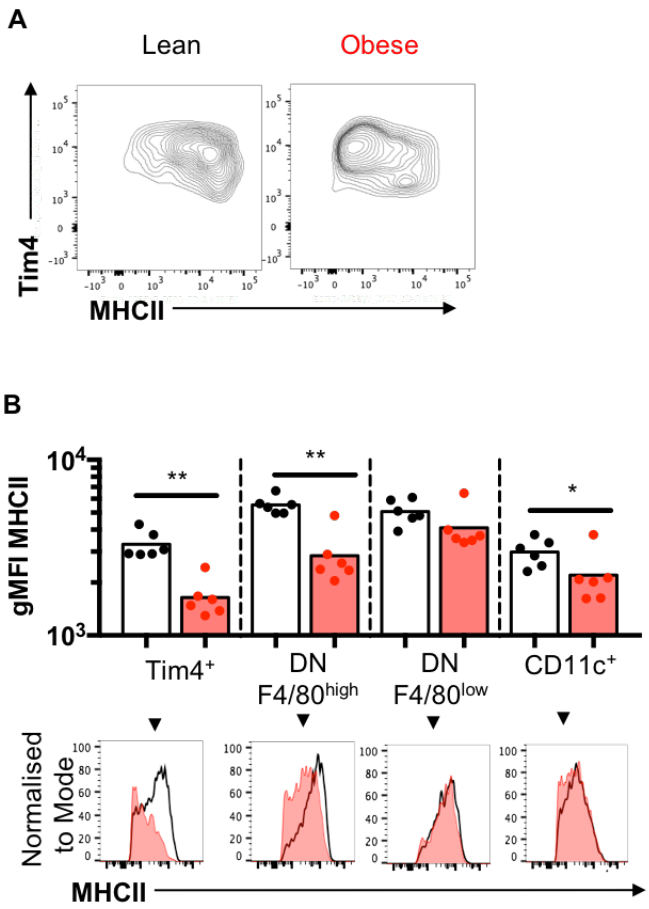

Figure 4.8 Tim4^{+} ATM MHCII expression decreased after 8 weeks of HFD

After 8 weeks of HFD, GAT macrophages were analysed after staining by flow cytometry. **A.** FACS plot of MHCII expression on Tim4 macrophages in lean and obese mice and **(B)** geometric mean fluorescence intensity and histograms of MHCII expression on ATM subsets during control diet (black) or HFD (red). Student's t test : *:p<0.05; **p<0.01

Macrophage granularity was also assessed by looking at the side scatter area (SSC-A), a higher SSC-A correlating with a higher granularity or internal complexity. ATMs (F4/80$^+$CD11b$^+$) from obese GAT had a higher percentage of cells with an SSC-A^{high} phenotype, notably within the CD11c$^+$ and Tim4$^+$ subset (Figure 4.9A-B). The analysis of the geometric mean fluorescence intensity (gMFI), a measure of per-cell fluorescence levels, of Lipidtox, a dye for neutral lipid content, showed that the higher the SSC-A, the higher the neutral lipid content of these macrophages was (Figure 4.9C). Moreover, analysis of lipid content within each ATM subset, as opposed to the whole population, showed that in lean and obese AT, Tim4$^+$ macrophages, tended to contain more lipids than the 3 other subsets, in both lean and obese mice (Figure 4.10).

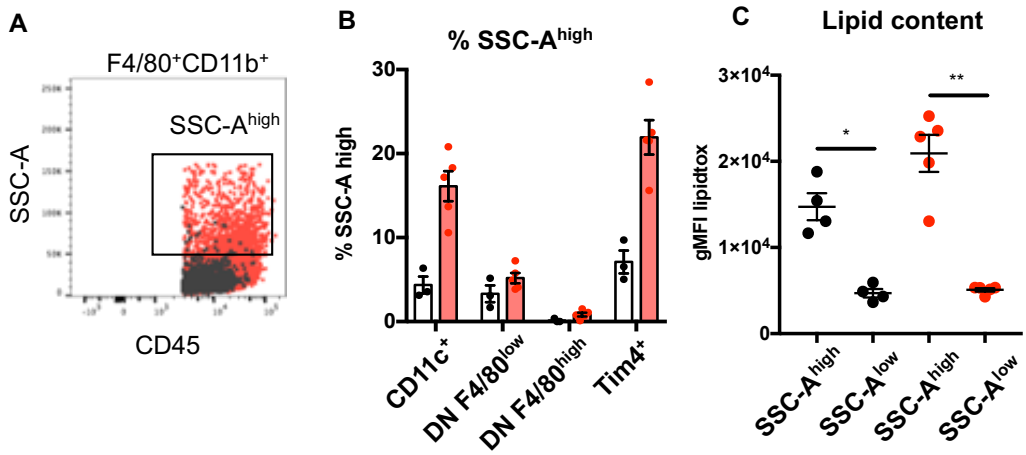

Figure 4.9 SSC-A^{high} macrophages are more abundant during HFD and contain more neutral lipids

After 8 weeks of HFD, ATMs from GAT were analysed by flow cytometry to measure their lipid content after LipidTox staining. SSC-A^{high} ATMs (F4/80$^+$CD11b$^+$) were distinguished from SSC-A^{low} (**A**) and were quantified (**B**) as a percentage of SSC-A^{high} cell within the subset. **C.** ATM lipid content analysed using LipidTox staining by flow cytometry (geometric mean fluorescence intensity: gMFI). In black: ATMs from control diet mice; in red: macrophages from HFD mice. Data representative of 2 experiments (n=4-5 mouse per group). Student t test : *:$p<0.05$; **$p<0.01$

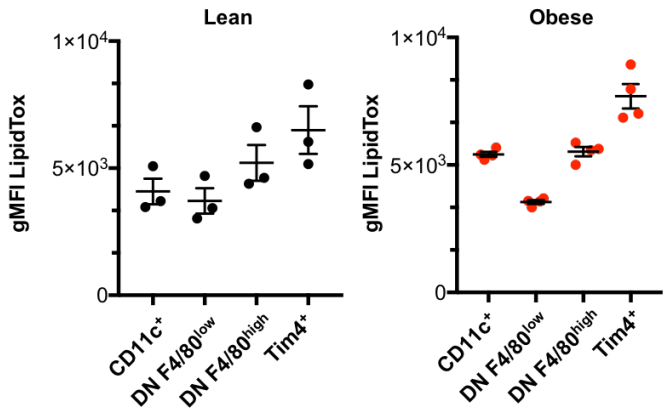

Figure 4.10 Tim4$^+$ ATMs from lean and obese mice tended to have the highest lipid content.

After 8 weeks of HFD or control diet, ATMs from GAT were analysed by flow cytometry to measure their lipid content after LipidTox staining. The gMFI (geometric mean of intensity) was used to compare the 4 different ATM subsets (n=3 to 4 mice per diet). Data representative of 1 from 2 independent experiments.

After 14 weeks of HFD, all ATMs significantly increased their proportion of lipid filled SSC-A^{high} cells (Figure 4.11A). CD11c$^+$ macrophages had the highest proportion of SSC-A^{high} cells, followed by the Tim4$^+$ macrophages. By sub-dividing subsets according to their MHCII expression (high and low), it was interesting to see that Tim4$^+$ SSC-A^{high} macrophages were mainly MHCII^{low} meanwhile the CD11c$^+$ SSC-A^{high} were MHCII^{high} (Figure 4.11B and C). As a whole, the Tim4$^+$ MHCII^{low} macrophages had a higher SSC-A than their counterpart MHCII^{high} (data not shown) cells, indicating that this subset would be a good lipid scavenger without increasing antigen presentation.

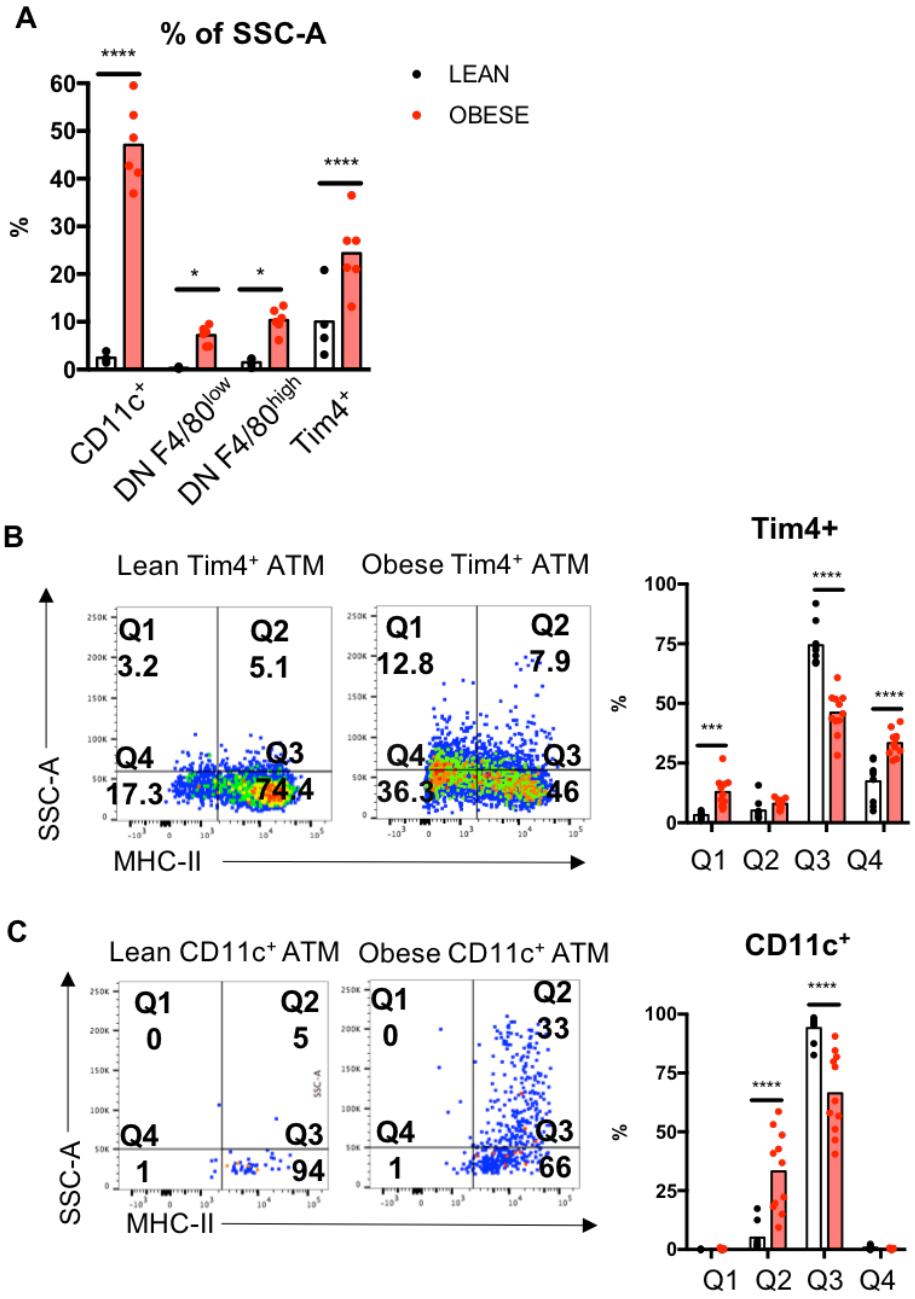

Figure 4.11 SSC-A and MHC-II expression on adipose tissue macrophages

After 14 weeks of control diet or HFD, ATMs were analysed by flow cytometry.
A. Quantification of the percentage of SSC-A^{high} ATMs within each population.
B. MHC-II expression and SSC-A allowed the subdivision of ATMs Tim4^{+} and CD11c^{+} (**C**) of lean mice and obese mice.
Q1: MHCII^{low}SSC^{high} Q2 MHCII^{high} SSC^{high} Q3: MHCII^{high} SSC^{low} Q4: MHCII^{low} SSC^{low}. The graph shows the percentage that represent Q1-Q4 within the subset.
Representative of 2-3 independent experiments of n=4 to 6 mice per group per experiment. Student t test : *p<0.05 ***p<0.001;****p<0.0001

4.4.5 Tim4^{+} ATMs were filled with lipids and lysosomes at homeostasis and during obesity

As shown previously (Figure 4.10), Tim4^{+} macrophages were filled with lipid during HFD, but also on control diet. Morphologically, after fluorescence activated cell sorting and H&E staining, they appeared to contain vesicles, reflecting their higher internal complexity. Utilising whole mount staining of GAT, the internal vesicles of Tim4^{+} ATMs were confirmed to contain lipids (lipidtox staining), these droplets could be distinguished within ATMs, in both lean (Figure 4.12B) and obese mice (Figure 4.12C), supporting the data acquired by flow cytometry and presented in Figure 4.9 and Figure 4.10.

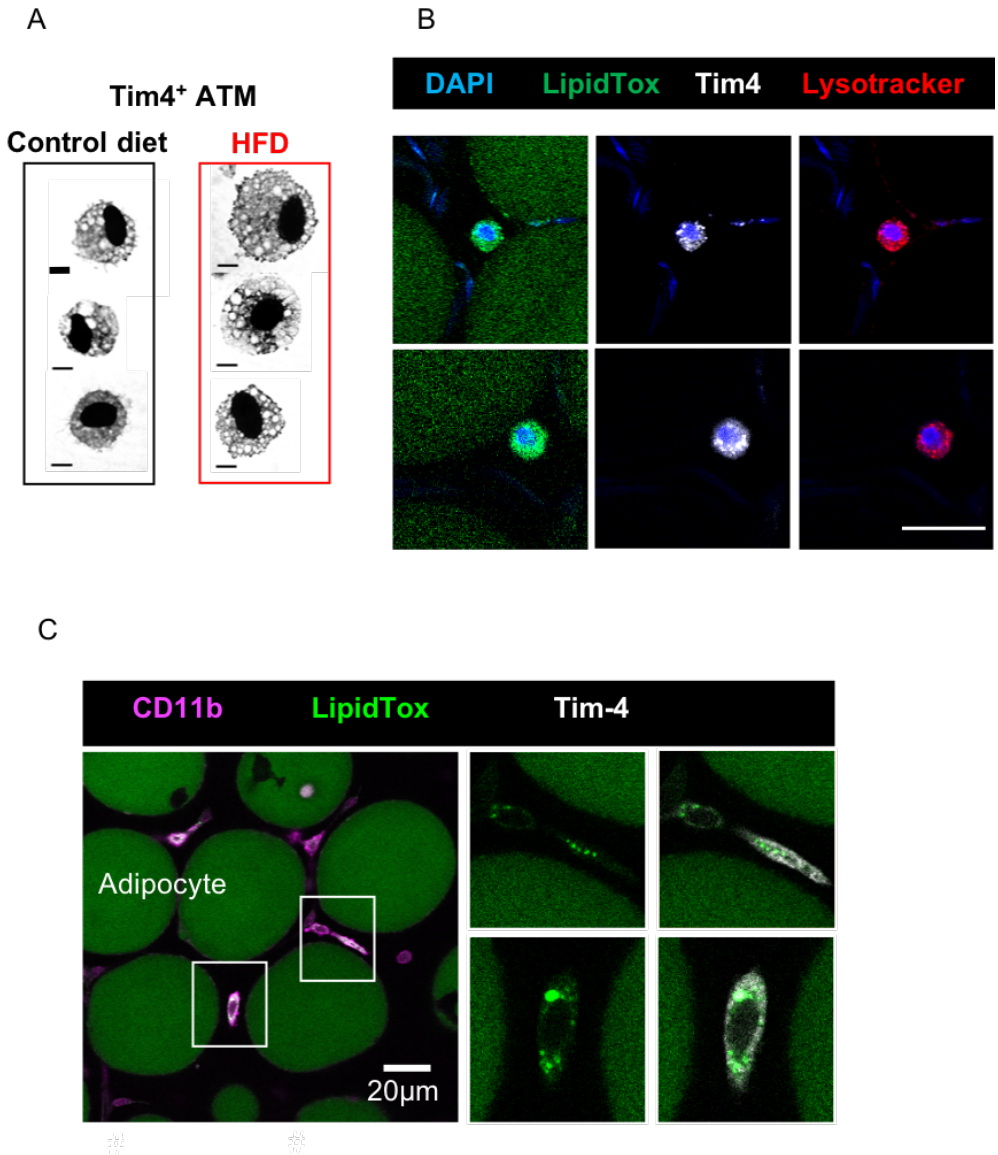

Figure 4.12 Tim4$^+$ ATM morphology in lean and obese GAT

A. H&E staining after FACS sort of Tim4$^+$ macrophages from digested GAT (scale bar: 5µm)

B. Whole mount staining (objective x40) of lean GAT and obese adipose tissue (**C**), showing neutral lipids (Lipidtox (green)), CD11b (magenta) and Tim4 (grey). Scale bar: 20 µm

The high granularity could also be explained by the presence of lysosomes within the cells. Tim4^{+} ATMs contained numerous active lysosomes, as shown by lysotracker staining (Figure 4.12B). To confirm these results, ATMs were also stained with Lamp1, a protein found at the lysosome's surface and commonly used for flow cytometry. Analysis showed that similarly to lysotracker, Tim4^{+} ATMs contained more Lamp1 fluorescence (Figure 4.13). Due to the absence of CD11c staining during the experiment, ATMs were divided in F4/80^{high} and F4/80^{low}. Most of the CD11c^{+} macrophages are F4/80^{low} as seen previously in chapter 3. F4/80^{low} macrophages had the lowest Lamp1 gMFI, the F4/80^{high}Tim4^{-} ATMs had an intermediate Lamp 1 content (Figure 4.13). There was no difference in Lamp 1 gMFI between the lean and obese GAT.

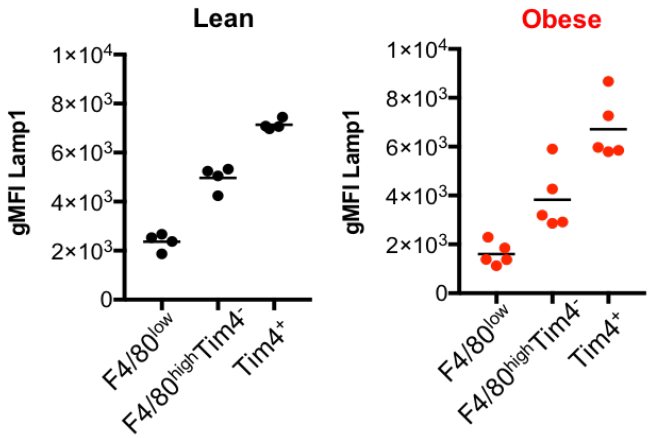

Figure 4.13 Tim4 ATMs tended to have more lysosomes, as shown by Lamp1 expression, compared to other macrophage populations in lean and obese GAT

Male mice were put on HFD or control diet for 14 weeks. Cells were stained and analysed by flow cytometry. Lysosomal-associated membrane protein 1 (Lamp1) geometric mean fluorescence intensity (gMFI) was used to measure lysosomal content within F4/80^{high}, F4/80^{low} and Tim4^{+} macrophages. Data representative of 2 independent experiments

4.4.6 Tim4+ ATMs were better at LDL uptake

As Tim4 ATMs contained more lipids and more lysosomes, their capacity to uptake lipids was tested in comparison to other ATMs. LDL, a low density lipoprotein, was added to wells containing ATMs. LDL was coupled with a fluorescent dye, BODIPY, so it was possible to quantify its uptake by macrophages using flow cytometry. It is known that CD36 is a class B scavenger receptor, expressed by macrophages and involved in lipid uptake (Kunjathoor et al. 2002; Aouadi et al. 2014). In lean AT, CD36 had a similar expression on all the macrophage subsets (data not shown). CD36 expression was also analysed after LDL addition. After 2 hours, Tim4$^+$ ATMs contained more LDL than other ATMs, and this difference increased over time. CD36 expression peaked at 4h but surprisingly was decreased at 6h post LDL feeding. CD36 tended to be higher on Tim4$^+$ macrophages which could be linked to the higher LDL uptake by those macrophages.

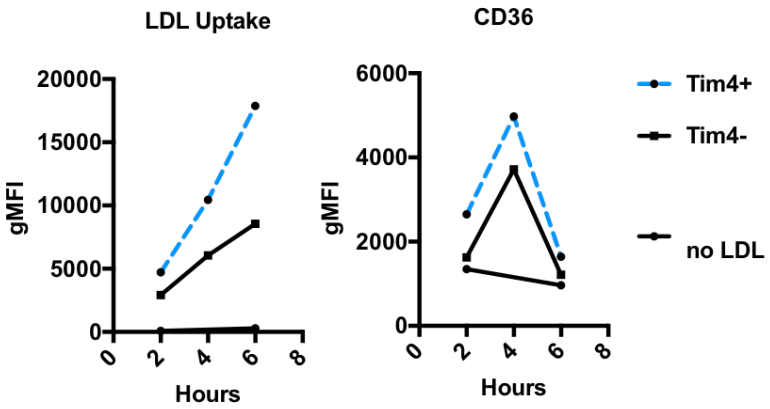

Figure 4.14 Tim4$^+$ ATMs uptaked more LDL and expressed more CD36 compared to Tim4$^-$ ATMs.

After immune cell isolation from GAT, ATMs were fed with LDL-BODIPY for 2h, 4h and 6h. ATMs content (left) and CD36 expression (right) were then analysed by flow cytometry. A control well was left with no LDL addition. Results represent 1 experiment with triplicates.

4.5 Discussion

The main results of this chapter are summarised in the table below.

Table 4-1 Summary of findings from chapter 4

	Impact of 8w HFD		**Lipid uptake**	
ATM Subsets	**On non-host chimerism**	**On cell numbers (fold increase)**	**8w HFD**	**14w HFD**
$Tim4^{+}$	No impact	+5	+++	+++
DN $F4/80^{high}$	Increased (significant)	+6.4	++	+
DN $F4/80^{low}$	already maximal at CD	+12.9	+	+
$CD11c^{+}$	already maximal at CD	+13.6	++	++++

In this chapter, macrophage heterogeneity in recruitment, sex specificity and differences between depots during HFD were highlighted. Males were more susceptible to macrophage recruitment than females (Figure 4.3). Macrophage number increase during HFD occurred via different mechanisms, with subsets highly dependent upon BM derived cells for their expansion and one particular subset, the resident population $Tim4^{+}$, which was increasing in number without any input from the BM (Figure 4.6-7). These "true" resident ATMs were notably distinguishable from the other cells by their ability to pick up lipids, their high lysosomal content, and their MHCII downregulation during HFD (Figure 4.12-13).

Differences in weight increase between depots

In this chapter, the comparison of weight and macrophage content between GAT and SAT after 8 weeks of HFD showed that GAT was subject to a greater mass

increase than SAT, as well as an increase in ATM number, which remained stable between lean and obese SAT. These results were similar from those previously described in studies including both human and mouse adipose depots (Altintas et al. 2011; Murano et al. 2008). A lower number of macrophages were found in lean and obese SAT, compared to visceral depots (Harman-Boehm et al. 2007). MCP1 (also known as CCL2), a potent chemokine regulating monocyte infiltration, increases in human omental fat proportionally to weight gain, however, no association has been found with the SAT (Harman-Boehm et al. 2007). In mouse, the same relationships were observed (Kanda et al. 2006b; Amano et al. 2014). Thus, the current literature would suggest that the SAT does not increase MCP1 expression during obesity, explaining the minimal macrophage recruitment to this tissue.

Sex differences in non-host chimerism

In the GAT, female non-host chimerism within the DN F4/80 ^{high} and Tim4^{+} ATM was lower compared to the same subset in the male GAT, in both obese and lean mice (Figure 4.4). Gender also influences F4/80^{high} resident macrophage recruitment within the peritoneal cavity and kidney (Calum C Bain et al. 2016). In male mice, after partial BM chimera, where the peritoneal cavity was protected, the peritoneal macrophages normalised non-host chimerism after 9-11 weeks reconstitution was of 70% whereas in females it was only around 11%. This lower macrophage turnover does not have any clear explanation but could be linked with the reproductive organs. Indeed, ovaries play a role in macrophage phenotype and number in the peritoneal cavity by their hormonal production (notably the 17β-estradiol) (Scotland et al. 2011). Surprisingly, in the SAT, female Tim4^{+}ATM non-host chimerism was increased by HFD and was even higher than the same population within obese males (Figure 4.4). The number of cells for analysis in the SAT was very low compared to the GAT. Cells could have been lost, as the SAT was more difficult to digest and seemed to contain more "undigested" deposition, maybe reflecting matrix deposition or entities that could not be digested by collagenase D. However, Tim4^{+} macrophages are important for apoptotic cell uptake (Miyanishi et al. 2007; Nishi et al. 2014). Female SAT could have increased BM derived macrophages that acquire Tim4 *in situ* to control AT inflammation. Thus it could be interesting to measure IL6, IL10 and other cytokines

in SAT to compare female and male inflammation status. Moreover, a study showed that after 9 weeks of HFD, GAT creates new adipocytes (hyperplasia growth) after a hypertrophy phase, while SAT remains with the same number of adipocytes, only growing by hypertrophy (Wang et al. 2013). It is possible that in the SAT of females, $Tim4^{+}$ ATMs are necessary to inhibit adipocyte proliferation, as seen with $CD206^{+}$ ATMs in a recent study which shows that these macrophages play a role in the modulation of adipocyte progenitors proliferation (Nawaz et al. 2017).

Tim4+ resident macrophages are outnumbered by BM derived cells during obesity.

This chapter showed that recruited and resident macrophages both coexist in the AT tissue of lean and obese mice. If considering the ATM population as a whole, during partial BM chimera, lean males had a normalised non-host chimerism in the GAT of 39.5%, obese males 71.5%, lean females 22.5% and obese females 34.5% suggesting that the contribution of the bone marrow to ATMs increased during obesity (Figure 4.5). $Tim4^{+}$ ATMs were the exception, as this subset showed no significant increase in BM input and was proliferating (14%). Amano and colleagues showed that 4.5% of ATMs in the GAT of obese mice were proliferating vs 1% in the lean GAT (Amano et al. 2014). This was shown using a pulse of 5-ethynyl-2′-deoxyuridine (EdU), which is incorporated into DNA only exclusively if a cell is in S phase (proliferating cells). Previously, a team showed that BrDu incorporation, an alternative to Edu, corresponds to $Ki67^{high}$ cells (Jenkins et al. 2013b). In my experiment, I could not distinguished high from low $Ki67^{+}$ ATMs and using Edu or BrDU might be more specific. IL6, IL4 and IL13 drives ATM proliferation in AT explants, and could be a driver for Tim4 proliferation *in vivo* (Braune et al. 2017).

Another group recently used partial BM chimera to study impact of HFD on macrophages, but did not see any non-host chimerism increase in GAT macrophages after 8 weeks of HFD (1.87%) but rather later. By 12 weeks, an increase in chimerism of 21.66% was found (Zheng et al. 2016b). Their gating was very different of mine as they considered macrophages as an homogenous population ($F4/80^{+}$). Their control group also largely increased their non-host chimerism at 12 weeks (14.2% at 12 weeks vs 2% at 8 weeks). Moreover the non-host chimerism of blood monocytes seems to

vary between groups, as such, normalisation should have been used. As no statistic were showed and it seems that there was no replication of these experiments, it uplifts the question of their reproducibility or the trust to have in these results (Zheng et al. 2016b). However, they did show proliferation (on a group of 3-4 mice) of ATMs during HFD.

Lipid buffering properties of macrophages

After 8 or 14 weeks of HFD, although all macrophages were able to uptake lipids, $Tim4^+$ ATMs were able to internalise more lipids per cell as shown by their higher lipid content in both lean and obese AT (Figure 4.10). Furthermore, $Tim4^+$ macrophages had increased lysosomal activity, suggesting that these macrophages may preferentially degrade the phagocytosed lipids. As they are long lived cells, it is possible that $Tim4^+$ ATMs metabolise fatty acids to assure functionality, as shown for M2 macrophages (O'Neill, Kishton, and Rathmell 2016). Indeed, M2 macrophages preferentially use fatty acid to fuel mitochondrial oxidative phosphorylation which leads to ATP production in large quantity (Van Den Bossche, Neill, and Menon 2017; O'Neill, Kishton, and Rathmell 2016; Gaber, Strehl, and Buttgereit 2017).

Lipid buffering by macrophages has also been shown in mice prone to obesity (ob/ob mice) after 6 weeks of HFD (Aouadi et al. 2014). Aouadi and colleagues showed that expression of lipoprotein lipase (LpL) by macrophages mediated their ability to uptake lipids; silencing LpL reversed lipid accumulation. Other studies using also obese ob/ob mice, showed that $CD11c^+$ ATMs have the highest lipid content when compared to $CD11c^-$ ATMs (Grijalva, Xu, and Ferrante 2016), and that ATMs accumulates free cholesterol and saturated triglycerides (Prieur et al. 2011). However, in both studies, a global gating on $CD11c^-$ might have hidden the importance of $Tim4^+$ATMs in lipid uptake. Our results suggested that the longer the mice were on HFD the more $CD11c^+$ ATMs increases their lipid content. This might be due to the fact that $Tim4^+$ ATMs were overloaded and not able to increase in number proportionally with the increase of lipids to buffer in the tissue. It would be interesting to study if Tim4 ATMs produce cytokines dictating recruitment of monocytes in the tissue.

Tim4^{+} ATMs seemed able to uptake more LDL than other macrophages in vitro and expressed more CD36 (Figure 4.14). A study from 2009 showed that F4/80^{high} ATMs express the peroxisome proliferator-activated receptor γ (PPAR γ) and CD36 in large quantity, combined with a higher number of SSC-A^{high} cells (Bassaganya-Riera et al. 2009). These data and the data presented in this chapter suggest that F4/80^{high}, which includes the F4/80^{high}Tim4^{+} ATMs, have a greater capacity to uptake and metabolise lipids. Indeed, PPAR γ is a transcription factor which induce CD36 and increases oxidized low density lipoproteins (oxLDL) uptake by macrophages (Tontonoz et al. 1998). A specific deletion of PPARγ in macrophages, thus a decrease in CD36 expression, increases weight gain and insulin resistance in mice (Odegaard et al. 2007). Therefore macrophage ability to uptake lipids is important to maintain body lipid and glucose homeostasis during HFD. Tim4 ATMs could be a central actor in these processes.

Tim4, inflammation silencer ?

CD11c^{+} ATMs have been linked to AT inflammation (Patsouris et al. 2008a; Carey N Lumeng, Bodzin, and Saltiel 2007; M. T. A. Nguyen et al. 2007). HFD markedly increases their number in the tissue within crown like structures around dying adipocytes, and has been linked with pro inflammatory gene expression (John M Wentworth et al. 2010; Patsouris et al. 2008b; Carey N Lumeng, Bodzin, and Saltiel 2007). In this study, the CD11c^{+} ATMs which were uptaking lipids expressed high levels of MHCII, whereas the Tim4^{+} ATMs which were uptaking lipids expressed low levels of MHCII. CD11c^{+} ATMs might be associated with antigen presentation, after lipid engulfment, to T cells and thus could promote their proliferation. ATMs, and notably CD11c^{+}, have been linked with interferon-γ-producing CD4 T cell proliferation during HFD (Morris et al. 2013). In contrast, Tim4^{+}, which seem to partially downregulate MHCII might act as inflammation silencer. In the context of cancer, tumor associated macrophages expressing Tim4 are able to phagocytes dying cells and decrease antigen presentation following Tim4 uptake of dead tumor cells (Baghdadi et al. 2013). Indeed they showed that Tim4 induces autophagic vesicles that "over-digest" any left particles which has for effect to reduce antigen presentation (Baghdadi et al. 2013). Tim4 intervention in removing apoptotic cells appears to be

finely controlled. Indeed, directed apoptotic cells clearance through Tim4 expressing cells rather than recruited inflammatory monocytes controls inflammation (Uderhardt et al. 2012). They showed that if Tim4 macrophages in the peritoneal cavity sequester MFG-E8 (milk fat globule E8), which is a molecule "adapter" between PS and macrophages that do not express Tim4. By sequestering MFG-E8, $Tim4^+$ macrophages rend impossible for inflammatory macrophages to uptake dying cells which in turn reduce inflammation (Uderhardt et al. 2012). A recent study showed that a new class of ATM BM derived $CD9^+$ are lipid laden but have a pro-inflammatory phenotype (D. A. Hill et al. 2018). In contrast, Tim4 might have an anti-inflammatory phenotype.

Conclusion

Tim4 is a new subset of ATMs, which increase in number by proliferation rather than recruitment. However BM derived ATMs outnumber them during obesity. Since this subset had a higher amount of lipids and lysotracker compared to other macrophages, and seemed better at uptaking LDL, I then choose to study how Tim4 macrophages handle lipids during obesity.

CHAPTER 5 TIM4 BLOCKADE REDUCES LIPID UPTAKE AND LYSOSOMAL ACTIVITY OF TIM4^{+} ATMS

5.1 Introduction

The ATMs micro-environment is quite singular due to their lipid rich neighbours: the adipocytes. During fasting periods, adipocyte lipolysis is activated in order to release energy (free fatty acids) to other tissues by lysis of their triglyceride (Stern, Rutkowski, and Scherer 2016). Local lipid influxes are then increased and lipid laden macrophages are found in the AT (Kosteli et al. 2010a). During obesity, there is an increase in basal rates of lipolysis, as the tissue become insulin resistant and dysfunctional, which increases the number of lipid laden macrophages in the tissue (Duncan et al. 2007). Notably, the pro-inflammatory CD11c$^+$ ATMs were found to have a higher lipid content compared to CD11c$^-$ cells (Carey N Lumeng, Bodzin, and Saltiel 2007). Fast and obesity are opposite states but in both cases macrophages seem to be able to respond to lipid availability in the tissue. In addition to simply containing lipids, ATMs have the ability to activate a lysosomal program which can cause lipid catabolism (X. Xu et al. 2013). Blocking lysosomal activity, using chloroquine, a drug which penetrates the lysosomes and inhibits their acidification, resulted in an increase in ATM lipid content and a decrease in net free fatty acid release by the AT *in vitro* (X. Xu et al. 2013). However, chloroquine targets all macrophages, so it is unclear if all macrophages are able to release FFA or if it is subset specific. Excessive release of FFA by AT to the liver and elevated triglyceride and LDL cholesterol are key features of obesity, and concomitantly increase the risk of cardiovascular disease (Klop, Elte, and Cabezas 2013). Lowering plasma LDL, using commercially available drugs, or reducing FFA levels in the plasma is sufficient to improve insulin resistance (Boden 2008). The fact that ATMs are involved in FFA release could potentially lead to the development of new drugs to lower the lipid content of the plasma (X. Xu et al. 2013). In the previous chapter, Tim4 ATMs were found to have the highest lipid content, the highest lysosomal content and also a greater ability to pick up LDL compared to other ATMs. This indicates that Tim4$^+$ ATMs are well equipped to perform lysosomal lipolysis and predicts the involvement of these cells in FFA release during HFD challenge. Importantly, several genome wide association studies (GWAS) have shown an association between *timd4,* the gene encoding TIM4, with blood lipid content (cholesterol, LDL, TG) (Kathiresan et al. 2009b; Teslovich et al. 2010; Do et al. 2013; Surakka et al. 2015). Nonetheless, the role of Tim4 has never been discussed in the

setting of HFD and obesity. Thus, I hypothesised that, out of all ATMs, Tim4+ ATMs are the subset of macrophages controlling FFA in the plasma during HFD challenge.

5.2 Aim

In the previous chapters of this thesis, a resident population Tim4+ was characterised which seemed to contain more lipids and lysosomes than the other macrophages, notably in lean and at the early onset of obesity. Since ATMs were shown to be involved in lipid metabolism, due to lipid degradation via their lysosomes, the aim of this chapter is to test the hypothesis that Tim4+ macrophages are the subset of ATMs that specifically control lipid metabolism and participate in FFA release into the bloodstream. To do this, experiments were performed as follow :

In vivo blockade of Tim4 to study its impact on FFA in the blood and other metabolic parameters such as glucose tolerance.

In vitro blockade of Tim4 to study the role of Tim4 in lipid uptake and lysosomal activation.

5.3 Experimental design

To study the impact of the phosphatidylserine receptor Tim4**,** *in vivo* blockade of Tim4 was carried out as shown in Figure 2.3. Eight week-old C57BL/6 males were placed on either HFD or control diet (CD) for 8 weeks. After 4 weeks of diet, mice from both groups were i.p. injected twice a week for the rest of the experiment with 100µl of PBS containing either 200ng of blocking anti-Tim4 IgG2a or 200ng of isotype IgG2a control. During the last week of the diet, an oral glucose tolerance test was performed and the mice were culled 2 days later. For short term HFD challenge, mice were only injected once with either anti-Tim4 IgG2a or isotype IgG2a control the day before the start of the diet (D0), then placed on either CD or HFD for an additional 3 days (Figure 1.1B).

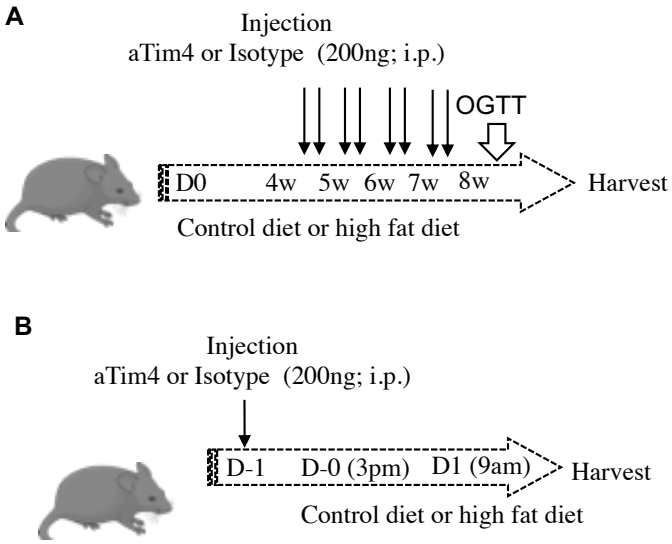

Figure 5.1 Experimental design of Tim4 blockade during long (A) and short HFD (B)

Male mice were given a HFD for 8 weeks (w: weeks) or for a shorter period of time (D: day). **A** After 4 weeks of diet, mice from both groups were i.p. injected twice a week for the rest of the experiment with 100µl of PBS containing either 200ng of blocking anti-Tim4 IgG2a or 200ng of isotype IgG2a control (plain arrow). An oral glucose tolerance test (OGTT) was performed 2 to 3 days before the cull. **B** Short HFD with injection of 100µl of PBS containing either 200ng of blocking anti-Tim4 IgG2a or 200ng of isotype IgG2a control (plain arrow)

5.4 Results

5.4.1 Impact of *in vivo* Tim4 blockade with monoclonal antibodies on macrophages

To study the impact of Tim4$^+$ macrophages on lipid homeostasis, mice were injected (i.p.) twice a week, from week 4 to the cull, with a monoclonal IgG2a antibody against Tim4 (aTim4). Control mice were injected with IgG control antibodies (Isotype) (Figure 2.3). Flow cytometry analysis of CD45$^+$F480$^+$ cells in the GAT and the peritoneal exudate cells (PEC) showed that injection of anti Tim4 antibody totally blocked its recognition by flow cytometry in the GAT (Figure 5.2, upper graph) but not totally in the PEC (Figure 5.2, lower graph) where some cells were still presenting Tim 4 at their surface, even if the intensity was decreased. Few F4/80$^-$CD11b$^-$ cells expressing Tim4 and MHC-II, probably dendritic cells, were also blocked in this process. But their number in AT was very low (data not shown).

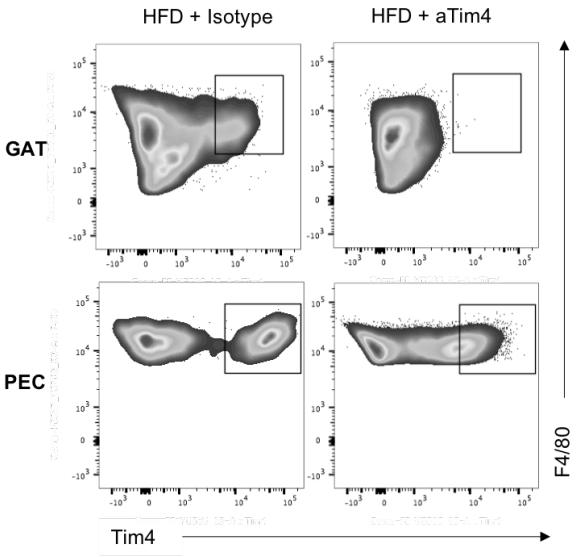

Figure 5.2 Tim4 blockade twice a week for 4 weeks during a long HFD blocked Tim4 in ATMs but only partially in the PEC

Mice were fed ad libitum either control diet or a HFD for 8 weeks and injected (200 ng i.p) with an isotype control or an anti-Tim4 (aTim4) blocking antibody as shown in Figure 2.3A. Flow cytometry analysis on GAT and peritoneal exudate cells showed Tim4 expression on CD45$^+$Lin$^-$F4/80$^+$ cells at the time of the cull. Images representative of 1 experiment (n=5 per group).

5.4.2 Impact of *in vivo* Tim4 blockade coupled to long term HFD

Tim4 blockade had no effect on body and GAT weight

To study the impact of Tim4+ macrophages on lipid homeostasis during obesity, mice were given HFD composed of 60% fat (Reseach Diet) and were injected (i.p.) twice a week, from week 4 to the cull, with a monoclonal IgG2a antibody against Tim4 (aTim4). Control mice were injected with IgG control antibodies (Isotype) (Figure 2.3). After 8 week of HFD, mice gained a significant amount of body weight and had a higher GAT fat mass compared to controls. The aTim4 treatment had no impact on weight gain.

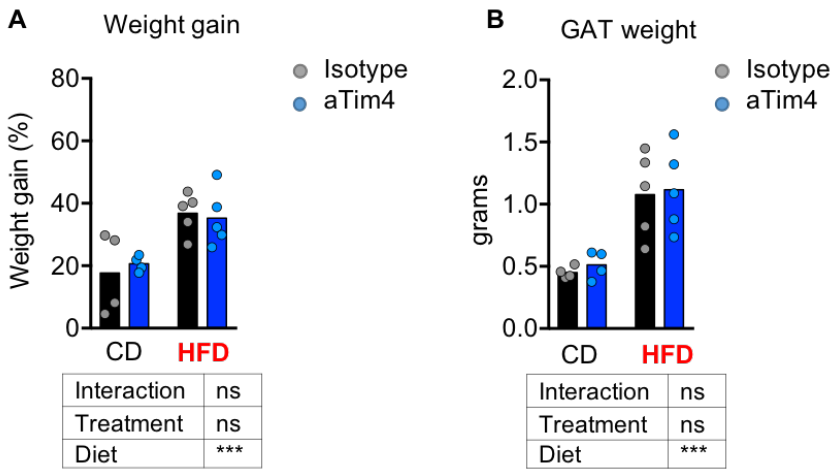

Figure 5.3 Weight gain and GAT weight of C57BL/6 male mice fed a control diet or a HFD for 8 weeks, with or without Tim4 blockade.

Mice were fed ad libitum either control diet or a HFD for 8 weeks and injected (200 ng i.p) with an isotype control or an anti-Tim4 (aTim4) blocking antibody as shown in Figure 2.3A.

Percentage of weight gain is shown in (A) and weight of the GAT is shown in (B) Data are representative of 2 experiments. Each data point represents a mouse and the column the mean. Two-way-Anova was performed ***: $p<0.001$.

Tim4 blockade had no impact on glucose tolerance

After 8 weeks of diet, an oral glucose tolerance test (OGTT) was performed. A bolus of glucose (2mg/mg of body weight) was given by gavage to each mouse. Before the glucose gavage (T_0) and after 15, 30, 60, and 120 minutes, a sample of blood was taken from the tail to measure glucose levels. The glucose levels at T_0 were not significantly different between diets and treatments. However, levels of plasma glucose at T_{15} were higher in HFD fed mice compared to the controls. Moreover, the overall plasma glucose levels measured by area under the curve was increased during HFD compare to controls. However, Tim4 blockade had no impact on glucose intolerance.

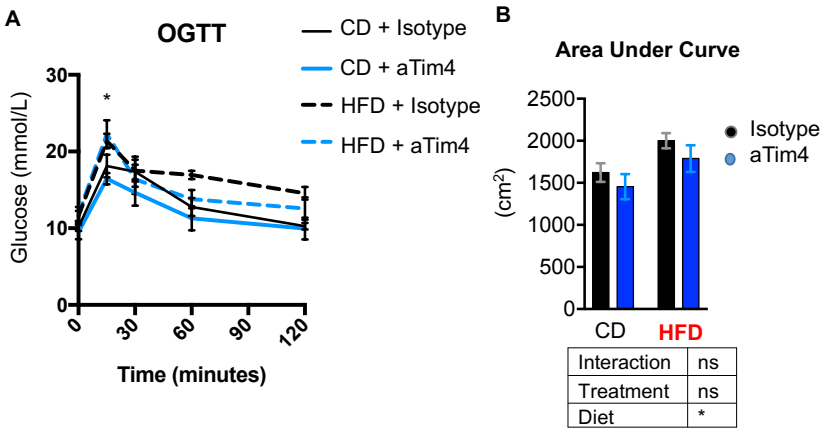

Figure 5.4 Plasma glucose level after administration of a glucose bolus to mice fed a control diet or a HFD for 8 weeks, with or without Tim4 blockade.

Mice were given a control diet or a HFD for 8 weeks and injected (200 ng i.p.) with a isotype control or an anti-Tim4 (aTim4) antibody as shown in Figure 2.3A. At the 8th week of diet, a bolus of glucose was given by gavage to the mice (2mg/gram of body weight) to perform an oral glucose tolerance test (OGTT). **(A)** Plasma glucose levels (mmol/L) measured in plasma 15, 30, 60, 90 and 120 minutes after gavage(**B)** Area under the curve of glucose levels during OGTT was measured (0 being the baseline). Data are represented as mean ± SEM (2 independent experiments, n=5 per group per experiment). Two-way-Anova was performed *: $p<0.05$.

In vivo Tim4 blockade decreased free fatty acid in the plasma of obese mice after 8 weeks of HFD

FFA in the plasma was measured on blood withdrawn from mice just before cull (non-fasted mice). Eight weeks of HFD significantly increased FFA in the plasma compared to control mice, however mice treated with aTim4 antibodies had lower FFA levels than control mice (Figure 5.5), thus indicating that Tim4 was involved in lipid metabolism during HFD challenge.

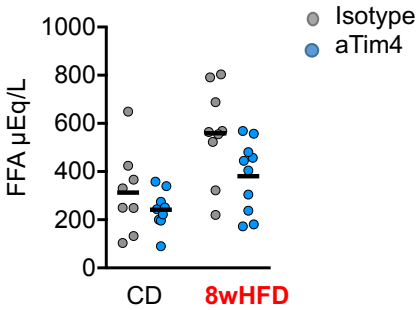

Interaction	ns
Treatment	*
Diet	***

Figure 5.5 FFA levels in plasma of mice fed a HFD for 8 weeks was decreased by aTim4 treatment.

Mice were given a control diet or a HFD for 8 weeks and injected (200 ng i.p.) with a isotype control or an anti-Tim4 (aTim4) as shown in Figure 2.3A. FFA was measured in the plasma. Data pooled from 2 independent experiments (n=4-5 per group per experiment). Each dot represents a mouse and the mean is represented by the black bar for each group. Two-way-Anova was performed.

HFD led to increased lysosomal activity in Tim4+ ATMs and blocking Tim4 abrogated lysosomal activity

In a previous study by Xu et. al, a macrophage lysosomal program was observed to be activated after HFD feeding, which the authors concluded was responsible for the release of FFA by macrophages, following lipid degradation within the lysosomes (X. Xu et al. 2013). As blocking Tim4 reduced FFA level in the serum (Figure 5.5), I next assessed the lysosomal activity of Tim4$^+$ macrophages. Injection of anti-Tim4 antibodies was not targeting adipose macrophages specifically, and other Tim4$^+$ macrophages could be targeted (Figure 5.2). Indeed, Tim4$^+$ is expressed by resident peritoneal cavity macrophages, resident Kuppfer cells in the liver. Since Kupffer cells, are the largest resident population in the body (Miyanishi et al. 2007; Zigmond et al. 2014; Nishi et al. 2014), it was critical to assess if the diet and/or Tim4 blockade could impact lysosomal activation in this important macrophage population. To look at lysosomal activity and assess the impact of Tim4 blockade, macrophages from GAT, peritoneal lavage and liver were taken after 12-14 weeks of HFD. After purification of macrophages by adhesion method, cells were stained with lysotracker to quantify lysosomal activity within Tim4$^+$ cells after 6h in culture. HFD led to an increase of lysosomal MFI in Tim4$^+$ ATMs (Figure 5.6). This increase was unique to ATMs as no changes were observed in Tim4$^+$ macrophages from the liver or the PEC due to HFD. However, Tim4 blockade decreased lysotracker MFI in both control and high fat fed mice, and this occured independently from macrophage tissue origin (Figure 5.6). Therefore the main effect of Tim4 was to decrease lysosomal activity in all tim4 expressing macrophage populations assessed.

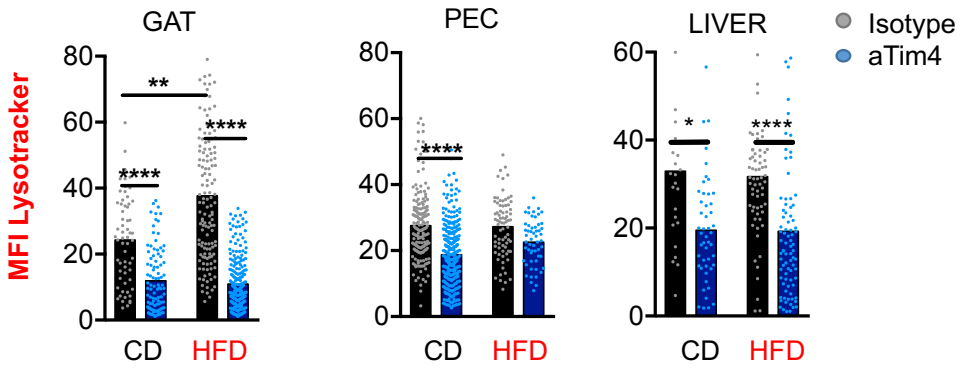

Figure 5.6 Tim4 blockade decreased lysotracker MFI in Tim4+ macrophages from the GAT, PEC and liver, in both lean and obese mice (8 weeks HFD).

Tim4 blockade was achieved as shown in Figure 2.3A. After adhesion-purification, macrophages were stained with lysotracker (500nM). Images were acquired using a Leica SP5 confocal microscope and the mean fluorescence intensity was quantified for each Tim4+ macrophage population, either blocked with aTim4 or not. The bar represent the mean intensity. Each dot represent one Tim4+ macrophage. One Way Anova was performed. *: $p<0.05$; **: $p<0.01$; ****: $p<0.0001$.

Tim4 blockade decreased LDL uptake by adipose, PEC and liver Tim4+ macrophages

As Tim4 blockade reduced lysosomal activity in macrophages extracted from both lean and obese mice, I then compared the ability of Tim4+ macrophages from AT, liver and PEC to uptake lipids, specifically low densitiy lipoproteins (LDL). LDL are lipoproteins composed mainly of cholesterol. LDL, coupled with Bodipy (a fluorescent dye), was added for 6h to wells containing adhesion purified macrophages isolated from the GAT, PEC and liver of either lean or obese mice (12-14 weeks of HFD), and blocked or not with aTim4 *in vitro*. Images were taken by confocal microscopy (Figure 5.7) and LDL and lysotracker fluorescence intensities were quantify for each cells (Figure 5.8 and Figure 5.9). By adding LDL in the wells, macrophages increased their lysosomal activity as seen by the increase in lysotracker intensity in the control and HFD groups. However, this was not observed in the wells blocked with aTim4 antibodies (Figure 5.8).

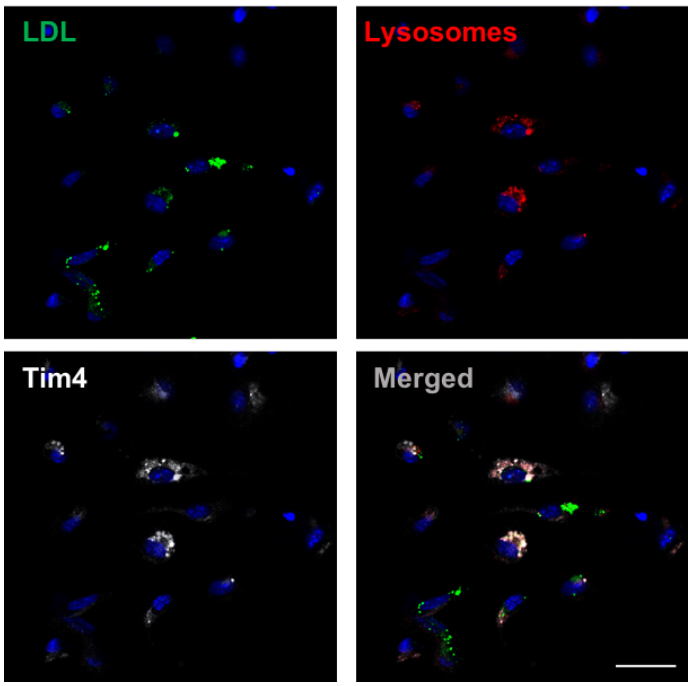

Figure 5.7 LDL uptake by ATMS seen by confocal microscopy (x100)

LDL- Bodipy was added for 6h to wells containing plate purified macrophages isolated from the GAT then stained with Lysotracker (lysosomes) and Tim4. This is a representation of ATMS from obese mice (12-14 weeks of HFD). Scale bar 10µm.

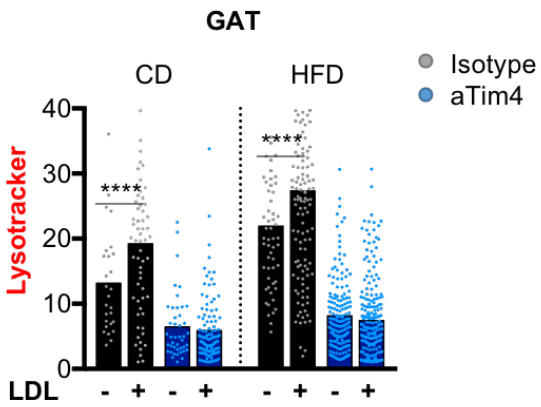

Figure 5.8 Lysotracker was increased in Tim4+ ATMS by addition of LDL only when the receptor was not blocked

Tim4 blockade was performed as shown in Figure 2.3A. After adhesion-purification, macrophages were cultured with LDL-Bodipy for 6h (50µg/ml) and stained with lysotracker (500nM). Images were acquired using a Leica SP5 confocal microscope and the MFI was quantified for individual Tim4+ macrophages, either blocked with aTim4 or not. Bars represent the mean intensity. Each dot represents one Tim4+ macrophage. Reprensentative of 1 experiment. Student t test ****: $p<0.0001$.

The ability of Tim4$^+$ macrophages to uptake LDL was increased in ATMS of obese mice compared to lean mice (Figure 5.9 A, left). In contrast, there was a significant deficit in the ability of liver macrophages purified from obese animals to acquire LDL *in vitro* compared to liver macrophages isolated from the livers of lean mice. However, there was a striking increase in lysotracker activity within macrophages isolated from both GAT and liver of obese mice compared to lean controls (Figure 5.9 B). Tim4$^+$ macrophages from the PEC did not increase their ability to uptake lipid nor to activate their lysosomes following HFD feeding (Figure 5.9 A-B). Remarkably, Tim4 blockade consistently decreased LDL uptake and lysotracker intensity in all tissues selected, independently of the diet (Figure 5.9 A-B).

Since I found that a short *in vitro* blockade impacted lipid uptake and lysosomal activity, I then assessed the impact of a short *in vivo* blockade associated with a short HFD to mimic an excessive lipid rich meal.

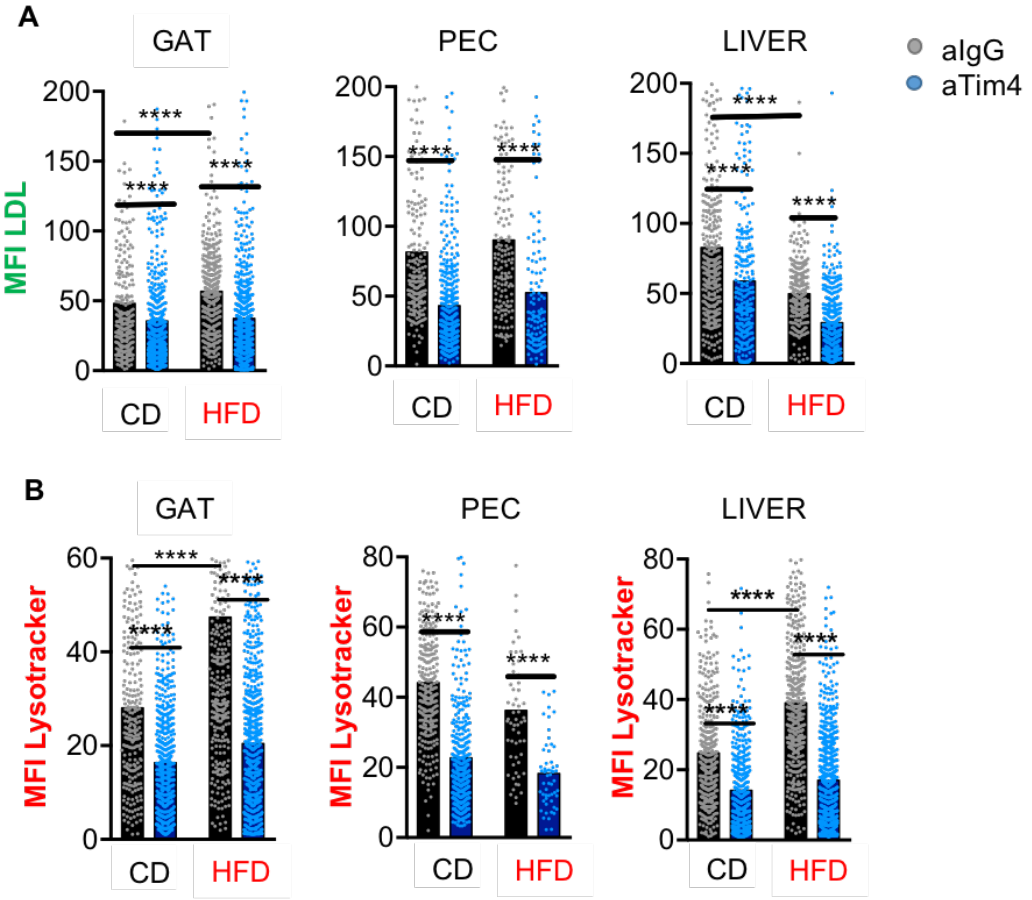

Figure 5.9 Tim4 blockade reduced LDL uptake (A) and lysotracker MFI (B) in Tim4+ macrophages from the GAT, PEC and LIVER, both in lean and obese mice fed a HFD for 12-14 weeks.

Tim4 blockade was performed as shown in Figure 2.3A. After adhesion-purification, macrophages were cultured with LDL-Bodipy for 6h (50µg/ml) and stained with lysotracker (500nM). Images were acquired using a Leica SP5 confocal microscope and the MFI was quantified for individual Tim4+ macrophages, either blocked with aTim4 or not. Bars represent the mean intensity. Each dot represents one Tim4+ macrophage. One Way Anova was performed for statistical analysis. *: $p<0.05$; **: $p<0.01$; ****: $p<0.0001$.

5.4.3 Impact of *in vivo* Tim4 blockade coupled to short term HFD

Interestingly, short term HFD, as little as 3 days, can increase the number of macrophages in the visceral AT and increase glucose intolerance, which could be easily reproduced by human by a large lipid rich meal or couple of days of lipid rich food (Lee et al. 2011). As 8 weeks of HFD only influenced the levels of plasma FFA and did not alter glucose tolerance, it was interesting to determine if this impact was dependent of the length of diet or simply the presence of a high fat meal. Mice were given HFD for 3 days or 1 day, with 1 injection of aTim4 at D0 or D-1 respectively.

Blocking Tim4 decreased FFA in the plasma after a short HFD

After 3 days of HFD, mice showed increased level of FFA in the plasma compared to the control mice. Tim4 blockade led to a noticeable decrease in FFA levels in HFD fed mice but this failed to reach significance (p=0.056) (Figure 5.10 A).

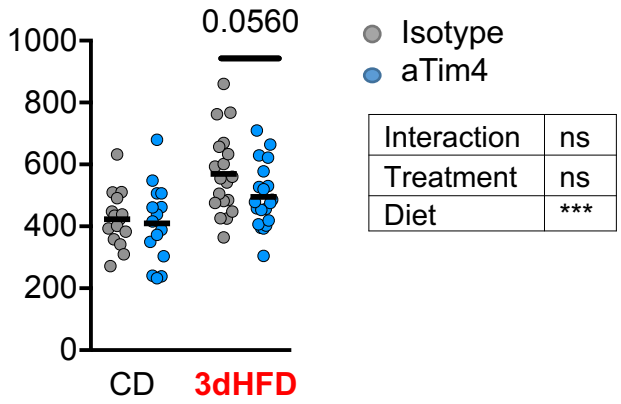

Figure 5.10 Tim4 blockade decreased FFA in the plasma of mice fed a HFD for 3 days compared to mice injected with isotype

Mice were given a control diet or a HFD for 3 days with or without Tim4 blockade, as shown in Figure 2.3. The free fatty acid in the plasma was measured in non-fasted mice using WAKO kit (µEq/L). Data grouped from 3-4 independent experiments (n=5 per group per experiment). Two-way-Anova was performed for statistical analysis : ***: $p<0.001$

As the Tim4 treatment tended towards a decrease in FFA in the blood of HFD mice compared to untreated controls, independently of the length of the diet (8 weeks and 3 days), I then hypothesised that the blocking impact might be due to the meal itself and not the length of the diet.

One day of HFD was sufficient to increase FFA in the blood and was blocked by Tim4 blockade.

Mice were given a single day of HFD; mice were given access to HFD ad libitum at 3pm and culled the next day at 9am prior to assessment of FFA in terminal blood. One day of HFD was sufficient to increase FFA in the blood, however Tim4 treatment lowered this effect neatly (Figure 5.11).

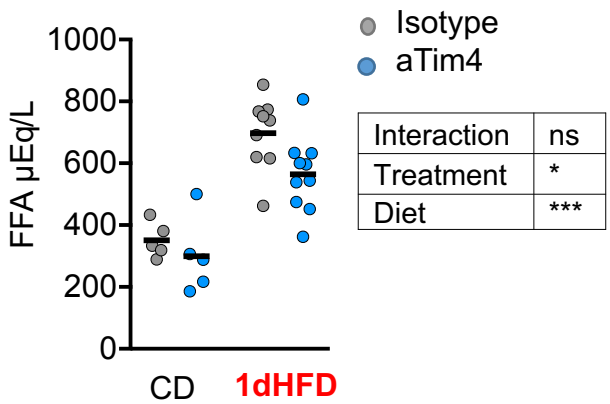

Figure 5.11 Tim4 blockade decreased FFA in the plasma of mice fed 1 day of HFD compared to mice injected with isotype control

Mice were given a control diet or a HFD for 3 days with or without Tim4 blockade, as shown in Figure 2.3. The free fatty acid in the plasma was measured in non-fasted mice using WAKO kit (µEq/L). Data grouped from 2 independent experiments for the HFD group (n=5 per group per experiment) and 1 experiment for the control group. Two-way-Anova was performed for statistical analysis : *: $p<0.5$; ***: $p<0.001$

As FFA was decreased, macrophages taken from these mice were analysed to verify their lysosomal activity., as seen with macrophages for the long HFD (Figure 5.6)

One day of HFD increased lipid content in Tim4+ ATMs and was sufficient to increase FFA in the blood; this increase was inhibited by Tim4 blockade.

As 1 day of HFD significantly reduced FFA in the plasma, lipid content and lysosomal activity of macrophages from these mice were also analysed after adhesion mediated purification. One day HFD increased neutral lipid content in GAT, PEC but not liver Tim4+ macrophages (Figure 5.12A). This increase was blocked by Tim4 blockade. Surprisingly, I found that 1 day HFD decreased lysosomal activity in GAT and liver (Figure 5.12B). Tim4 blockade decreased lysosomal activity in all tissues and for each diet.

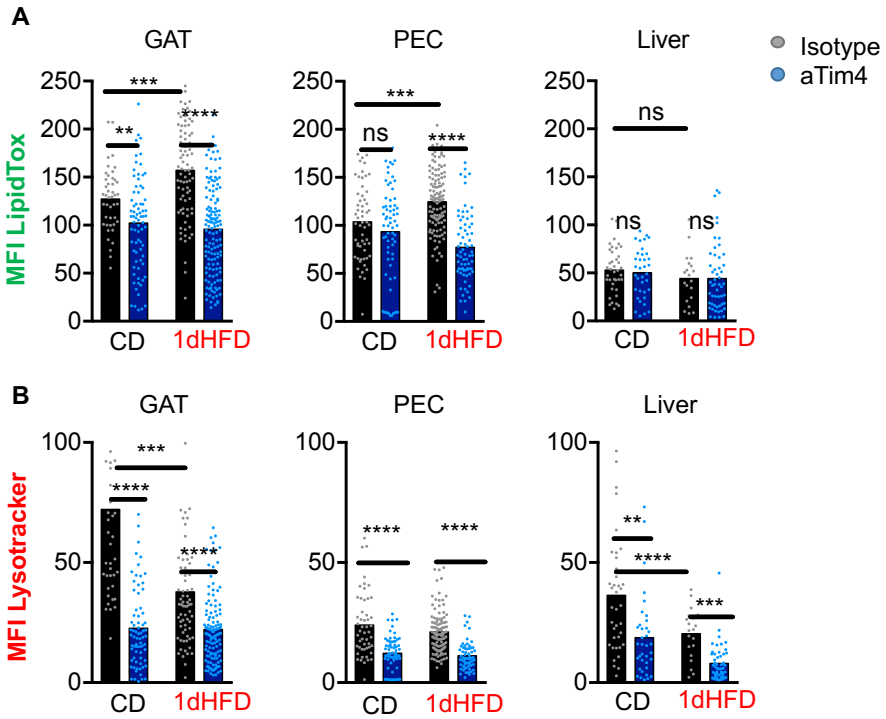

Figure 5.12 Tim4 blockade on Tim4+ macrophages from GAT, PEC, and Liver decreased lysotracker MFI in all groups independently of the diet and decreased lipid content in the GAT (control and HFD), and the PEC (HFD only).

Tim4 blockade was realised as shown in Figure 2.3. After adhesion-purification, macrophages were stained with lysotracker (500nM) and lipidtox. Images were acquired using a Leica SP5 confocal microscope and the MFI was quantified for each Tim4+ macrophage, either blocked with aTim4 or not. Bars represent the mean intensity. Each dot represents one Tim4+ macrophage. One Way Anova was performed for statistical analysis. *: p<0.05; **: p<0.01; ***: p<0.001 ****: p<0.0001

5.4.4 Lysotracker intensity and lipid uptake was correlated with Tim4 intensity on ATMs after being fed with chylomicrons

To test the ability of macrophages to uptake lipids other than LDL, macrophages from the GAT and PEC were exposed to chylomicrons (CM) after, or not, *in vitro* Tim4 blockade. The media used was serum free so the only fatty acids found or lipids would be coming from the CM and intracellular lipids. CM composition is very different from LDL, as they contain triglycerides at a high level and only a few molecule of cholesterol. As the CM used were not coupled with a dye, LipidTox Neutral lipid staining was added to stain lipids contained within the cells following fixation. Therefore, this staining was not specific to CM and included endogenous lipids already present within the cells. Adding CM increased the lipid content of Tim4$^+$ ATMs as seen by the increase of LipidTox MFI (+42) when compared to control macrophages that were not exposed to CM (Figure 5.13A). Nonetheless, CM had no impact on Tim4$^+$ PEC lipid content. Therefore, CM uptake was more specific to Tim4$^+$ ATMs. CM uptake by ATMs was accompanied by an increase in lysosomal activity (+15) (Figure 5.13B). Tim4 blockade decreased lipid content within ATMs and reversed the lysosomal activity increase caused by addition of CM (Figure 5.13A-B).

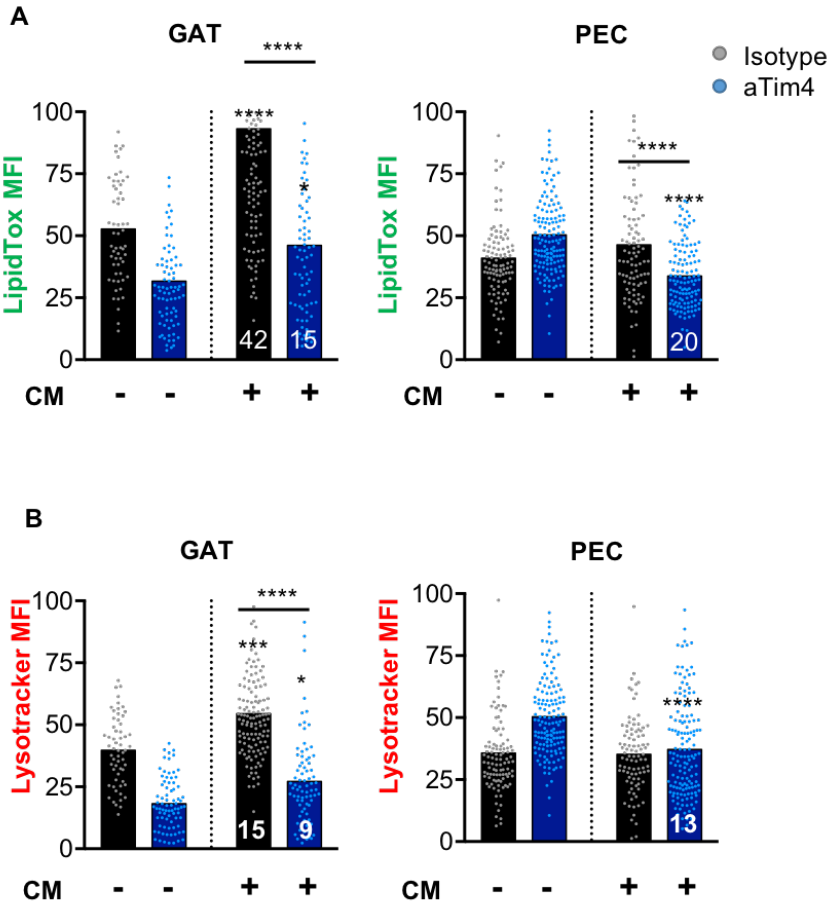

Figure 5.13 Tim4 blockade decreased lipid uptake and lysosomal activity in the GAT but not in the PEC macrophages

After purification of macrophages by adhesion method on a coverslip, macrophages from the GAT or the PEC were blocked or not with anti-Tim4 antibodies. Then they were given chylomicrons (83µg/ml) for 3h at 37°C. The cells were stained with Lipidtox (**A**) and lysotracker (**B**). The white number in columns represents the absolute difference between the control column with no CM, only if the difference reached significance (indicated above the column). One way anova was performed for statistical analysis. *: $p<0.05$; ***: $p<0.001$ ****: $p<0.0001$.

Moreover, statistical linear regression showed that the amount of lipids and lysotracker was positively correlated to Tim4 MFI after CM challenge. A weak positive correlation (R^2 = 0.28) existed between the amount of lipids inside macrophages and the presence of Tim4 (Figure 5.14A). This relationship was almost cancelled by Tim4 blockade (R^2 = 0.07) (Figure 5.14B). A moderate correlation existed between lysotracker MFI and Tim4 MFI (r^2>0.50) which became weaker with Tim4 blockade (r^2=0.14) (Figure 5.14 A-B). To conclude, Tim4 seemed to be moderately linked with lipid uptake and more strongly with lysosomal activity.

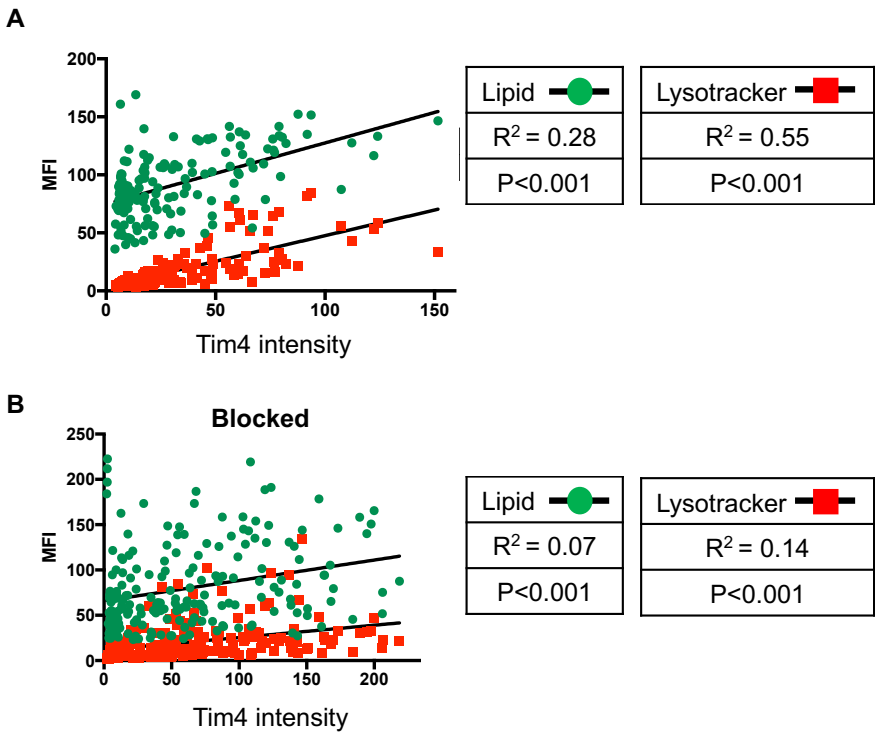

Figure 5.14 Tim4 correlates positively with lysotracker and lipidtox content after chylomicron challenge.

After purification of macrophages by adhesion method on a coverslip, macrophages were blocked or not with anti-Tim4 antibodies. Then they were given chylomicrons (83µg/ml) for 3h at 37°C. The cells were stained with lysotracker (lysosomes) and lipidtox (Lipid). Lipid content and lysotracker was measured in each F4/80$^+$ macrophage (MFI) and correlated to Tim4 intensity non-blocked (A) and blocked (B) conditions. Pearson product-moment correlation (R^2) and the P value were calculated and presented in the table.

5.5 DISCUSSION

In this chapter, I analysed the impact of Tim4 blockade on lipid handling. The main results are presented in the table below (Table 5-1).

Table 5-1 Summary of findings from chapter 5

		Tim 4 blockade (compare to control)		
		After long HFD	**After short HFD**	***In vitro* blockade**
Glucose tolerance		Unchanged	N/A	N/A
FFA (blood)		Decreased	Decreased	N/A
Lipid content	**GAT**	N/A	Decreased	Decreased
	PEC	N/A	Decreased	Decreased
	LIVER	N/A	Decreased	Decreased
Lysotracker (lysosomal acidification)	**GAT**	Decreased	Decreased	Decreased
	PEC	Decreased	Decreased	Decreased
	LIVER	Decreased	Decreased	Decreased
LDL uptake	**GAT**	Decreased+ Lyso. decreased	N/A	N/A
	PEC	Decreased+ Lyso. decreased	N/A	N/A
	LIVER	Decreased+ Lyso. decreased	N/A	N/A
CM uptake	**GAT**	N/A	N/A	Decreased+ lyso. decreased
	PEC	N/A	N/A	No effect

Lysosomal activity during HFD

In the present study, following 14 weeks of HFD, lysosomal activity in Tim4+ ATMs was increased (Figure 5.6). A previous study demonstrated that HFD increased lysosomal activity in ATMs and its inhibition (using chloroquine) increased lipid content in ATMs (X. Xu et al. 2013). To add, they also showed that blocking lysosomal activity decreased the release of FFA from fat tissue *in vitro*. In this chapter, long and short term Tim4 blockade reduced the amount of lysosomal activity and was accompanied by a decrease of FFA levels in the plasma of mice. This decrease was not accompanied by an improvement of glucose tolerance (OGTT) (Figure 5.4). Insulin levels were not measure in these experiments but could be a further indication of the general metabolic states of mice, notably if the mice developed insulin resistance (Boden 2008). Moreover, more lipids could be measured in the blood, notably levels of LDL and cholesterol, which were correlated with timd4 SNP in genome wide association studies in human (Kathiresan et al. 2009a).

ATMs accumulate lipids after 1 day of HFD however, I did not find any sign of lysosomal activation (Figure 5.12), which could mean that increase of lysosomal activity in ATMs might take several days or weeks to take place. However, caution must be used in the interpretation of the data as I encountered some technical challenges in the design of this experiment. The first technical challenge to overcome would be to control the timing of the last meal eaten by the mice prior to harvest. For all experiments, mice were culled at the same period of time (between 9 am and 10am), and the mice were not fasted beforehand as fasting can also increase lipolysis and lipid uptake by macrophages (Kosteli et al. 2010b). However, depending on mice, it is possible that some differences between the last meal and the time of the cull occurred. The use of metabolic cages would be interesting to follow the overall mice activity per hour and track the food and water intake, the physical activity, O_2 consumed and CO_2 produced. Secondly, Tim4 macrophages are charged with lipids. This can potentially make them less dense and result in floatation during the cell preparation as observed in other studies for F4/80+ macrophages (Weisberg et al. 2003; X. Xu et al. 2013). A preliminary experiment showed that indeed, Tim4+ macrophages and F4/80high macrophages were found in the floating fraction of adipose digest and both represented around 40% of CD45+. The floating fraction could not be analysed during long HFD

due to the amount of lipids present in the fraction that rendered impossible flow cytometry analysis.

Tim4 and lipid uptake

Blocking Tim4 blocked LDL (Figure 5.9) and CM uptake (Figure 5.13). This explains the decrease in lysotracker staining as macrophages were not able to pick up more lipids. The source of lipids present in Tim4$^+$ ATMs could be various. Firstly, Tim4 could participate in the engulfment of apoptotic adipocytes through the recognition of PS on dead cells (Miyanishi et al. 2007; Kobayashi et al. 2007; K. Wong et al. 2010). Secondly, PS are found on the surface of lipid particles. Indeed phospholipids are hydrophilic and are at the surface of the lipoprotein to encapsulate hydrophobic lipids, allowing transport in the circulation (Feingold and Grunfeld 2000). Tim4 could participate in the recognition and uptake of excess PS$^+$ lipid particles coming from the bloodstream and that can't be picked up by adipocytes after a fat rich meal. In this chapter, it was demonstrated that compared to the PEC, Tim4+ ATMs had a higher affinity for CM (Figure 5.13) which could suggest that Tim4$^+$ ATMs are specialised in the uptake of CM when the AT is saturated as happens after a HFD meal. Shin et al. showed that very low density lipoprotein receptor (VLDLR) mRNA expression is increased in ATMs with HFD, but no increase in LDLR is observed (Shin et al. 2017). VLDLR is involved in CM metabolism and would explain the affinity of ATMs with CM but further analysis would be required (Goudriaan et al. 2004).

It is possible that after Tim4 recognises phospholipids , it allows its uptake to the lysosome and its degradation. Analysis of images taken with confocal microscope, such as in Figure 5.7, suggesting that Tim4 colocalised with lysosomes. The same observation was done in a study where the authors showed that Tim4 colocalised with Lamp1$^+$ phagosomes after apoptotic tumour engulfment (Baghdadi et al. 2013). They further showed that Tim4 phagocytic activity was linked to an AMPK pathway. More images need to be analysed with higher resolution to confirm these results, but Tim4 seem to carry lipids to the lysosomes via translocation. The mechanisms linked with Tim4 are still not fully understood. Tim4 could act as a tethering receptor, with no direct signalling to the cell, and might rely on other surface receptor to assure its

phagocytic role (Park, Hochreiter-Hufford, and Ravichandran 2009). However Baghdadi et al. suggested that Tim4 mediates an AMP-activated protein kinase (AMPK) activation (Baghdadi et al. 2013). AMPK is a known activator of transcription factor regulating lysosomal and autophagic genes (Hipolito, Ospina-Escobar, and Botelho 2018). Therefore, Tim4 might upregulate indirectly lysosomal synthesis.

Tim4+ macrophages from different tissues don't show the same affinity to lipids

Here, I demonstrated that ATMs, PEC and Liver have various affinity to lipids (LDL or CM) and various associated lysosomal activities and particularly that . Tim4+ ATMs had a higher lysotracker intensity compared to PEC and liver, in lean mice (data not shown). This stresses the importance on analysing "real life" tissue macrophage populations and highlights the limitations of the use of PEC or bone marrow derived macrophages to illustrate mechanisms relating to a specific organ as environment can prime microphages to express certain receptors more than others. For example in the study of Shin *et. al* in 2017 about VLDLR, they characterised the receptor on ATMs but they used PEC and BMDM to study the impact of VLDL on cytokines production and inflammation (Shin et al. 2017). Some authors highlighted the difference between PEC and ATMs by looking at gene expression and linked obesity with a metabolic activation in ATMs but not in PEC (Boutens et al. 2018). This could explain the differences in lysotracker activity (Figure 5.6) and LDL uptake (Figure 5.9) during long term HFD. At homeostasis, Tim4+ ATMs are naturally dealing with lipid spill-over and lipid influxes from adipocytes, which is increased by HFD or fasting (Kosteli et al. 2010a; C. N. Lumeng et al. 2007). In the same way, Kupffer cells are also in contact with lipids as the liver synthesises VLDL, but also have receptors for molecule rich in cholesterol such as LDL and HDL (Krenkel and Tacke 2017; Remmerie and Scott 2018). Kupffer cells are indeed enriched in genes involved in cholesterol metabolism (Scott and Guilliams 2018). In the liver, recruited macrophages accumulate lipids coming from oxLDL within their lysosomes. These macrophages generate hepatic inflammation and fibrosis which are linked with the promotion of non-alcoholic liver diseases (Houben et al. 2017). The role of Tim4+ macrophages in

this context needs to be explored as they might have higher lysosomal capacity of degradation and do not accumulate lipids. Acute HFD is sufficient for liver to accumulate lipids, to induce hepatic insulin resistance (Samuel et al. 2004) and AT inflammation (Lee et al. 2011) so it could be an easy and good model to study Tim4 blockade. The intestines also contains Tim4 resident macrophages (Shaw et al. 2018). This organ is particularly involved with lipid handling and release FFA to the portal circulation as well as liposaccharides from its microbiota. The gut microbiota is heavily influenced by diet (Konrad and Wueest 2014) and only few days after a change of diet, the microbiome can be changed (David et al. 2014). The impact of Tim4 blockade on this organ could be useful to understand inflammation but also how lipid availability can be altered if Tim4 is blocked and how it could impact bacteria.

Conclusion

Tim4 capacity to engulf apoptotic cells have been largely explored. However, Tim4 signalling is not very clear. Here, I found a novel role for this PS receptor, notably in lipid handling. Tim4 is involved in lipid and lysosomal degradation of lipids, and the release of FFA in the bloodstream *in vivo*. This leads to more questions about the mode of action and the exact nature of the lipids that Tim4 is up taking. As Tim4 is also present in the gut, which is a hub for dietary lipid absorption and chylomicrons synthesis, it would be interesting to study the impact of Tim4 blockade in this organ.

CHAPTER 6 TIM4^{+} MACROPHAGES ARE PRESENT IN HUMAN ADIPOSE DEPOTS

6.1 Introduction

The World Health Organisation recognised that in 2016, 650 millions of adults were obese ("WHO | Obesity and Overweight" 2018). A body mass index (BMI) superior to 30 kg/m^2 is an indicator of obesity, however fat distribution is also an important factor, as measured by the waist to hip ratio (WHR). The "pear shape" characterises people with WAT accumulation around the hips, in the subcutaneous depot, while the "apple shape" is a central accumulation, in the visceral AT. After being adjusted to the BMI, central WAT accumulation, otherwise said VAT accumulation in the abdomen, is more often associated with chronic diseases such as type 2 diabetes and cardiovascular diseases (Matsuzawa et al. 1995; Fu, Hofker, and Wijmenga 2015). A ratio above 0.85 in woman and 0.90 in man defined obesity according to the World Health organisation ("WHO | Waist Circumference and Waist–Hip Ratio" 2018). Accumulation of macrophages in the visceral depot, the main depot being called omentum in human, is a feature of obesity (Weisberg et al. 2003; H. Xu et al. 2003). The accumulation of ATMs in the omentum and subcutaneous AT is positively associated with insulin resistance and AT inflammation (Koppaka et al. 2013; Cinti et al. 2005; John M Wentworth et al. 2010). Early study described the presence of lipid laden CD14$^+$CD64$^+$ ATMs around apoptotic adipocytes, in "crown like structures" (CLS) (Cinti et al. 2005). Later, CD14$^+$CD11c$^+$ proinflammatory ATMs were also found in human AT and were particularly expressed by ATMs within CLS (John M Wentworth et al. 2010). The quest to understand ATM biology during obesity led to the discovery of macrophages alternatively activated in high numbers in obese AT, such as CD163$^+$ ATMs (scavenging receptor), but also CD206$^+$ ATMs (mannose receptor) (Kristiansen et al. 2001; John M Wentworth et al. 2010; Fjeldborg et al. 2014). The presence of subsets that can have different functions in human AT has to be investigated further. My study of mouse AT revealed the existence of a lipid laden Tim4$^+$ ATM population with a have a high lysosomal activity (chapter 3&4). Up to this date, there is no study showing the presence of Tim4$^+$ ATMs in human. Interestingly, *timd4*, the gene coding for Tim4, has been highlighted to be associated with dyslipidaemia in genome wide association studies (Kathiresan et al. 2009a; Weissglas-Volkov et al. 2013; Teslovich et al. 2010). In mouse, ATMs seem to

influence the level of FFA in the blood, thus it is important to determine if Tim4^{+} ATMs are also present in human and could influence lipid homeostasis.

6.2 Aim

The aim of this chapter is to gather preliminary evidences that Tim4^{+} macrophages are also present in human adipose tissue and if they are to verify that human Tim4^{+} ATMs present with the same high lipid content and lysosomal activity characteristic of mouse Tim4^{+} ATMs.

6.3 Experimental design

In collaboration with Mr Damian Mole (University of Edinburgh, CIR), I obtained omental adipose tissue samples from patients who were undergoing laparoscopic surgery for laparoscopic cholecystectomy for biliary colic (surgery for gallstones without active inflammation). In collaboration with Dr Roland Stimson (University of Edinburgh, CVS), I obtained subcutaneous and omental adipose tissue from patients undergoing hernia repair or laparoscopic gastric bypass. This was done under Research Ethics Committee approval and after gaining informed consent in collaboration with the Clinical Research Facility (CRF). All cell numbers coming from this study were given after analysis by Dr Lucy Jackson-Jones (University of Edinburgh, CVS / now in Lancaster). All subjects were considered as non-inflamed patients.

6.4 Results

6.4.1 Tim4 is expressed by the majority of CD14^{+} cells in the omentum and SAT

To better study ATM population, flow cytometry analysis of omentum and subcutaneous AT was done using markers defining monocytes and macrophages. I used the markers CD14 and CD16 which define in the blood three distinct populations: CD16^{+}CD14^{-} non-classical monocytes (P1), CD16^{+}CD14^{+} intermediate monocytes (P2) and CD16^{-}CD14^{+} classical monocytes (P3) (K. L. Wong et al. 2011; Patel et al. 2017). All three populations could be found in human VAT and SAT (Figure 6.1A). P2 and P3 expressed Tim4 (Figure 6.1B) and had other macrophage characteristics such as the expression of HLA-DR, CD206, CD163, CD64 and CD62L (Figure 6.1C). CD16^{+}CD14^{-} cells expressed none of these macrophage markers thus appeared to be different from the population found in the blood (K. L. Wong et al. 2011; Patel et al. 2017). CD16^{+}CD14^{+} cells had intermediate expression of these markers and CD16^{-}CD14^{+} had the highest expression of these markers. Hence, this indicated that Tim4 is expressed on CD16^{-}CD14^{+} ATMs and that potentially its expression is induced on "intermediate monocytes" as they differentiate into ATMs *in situ.*

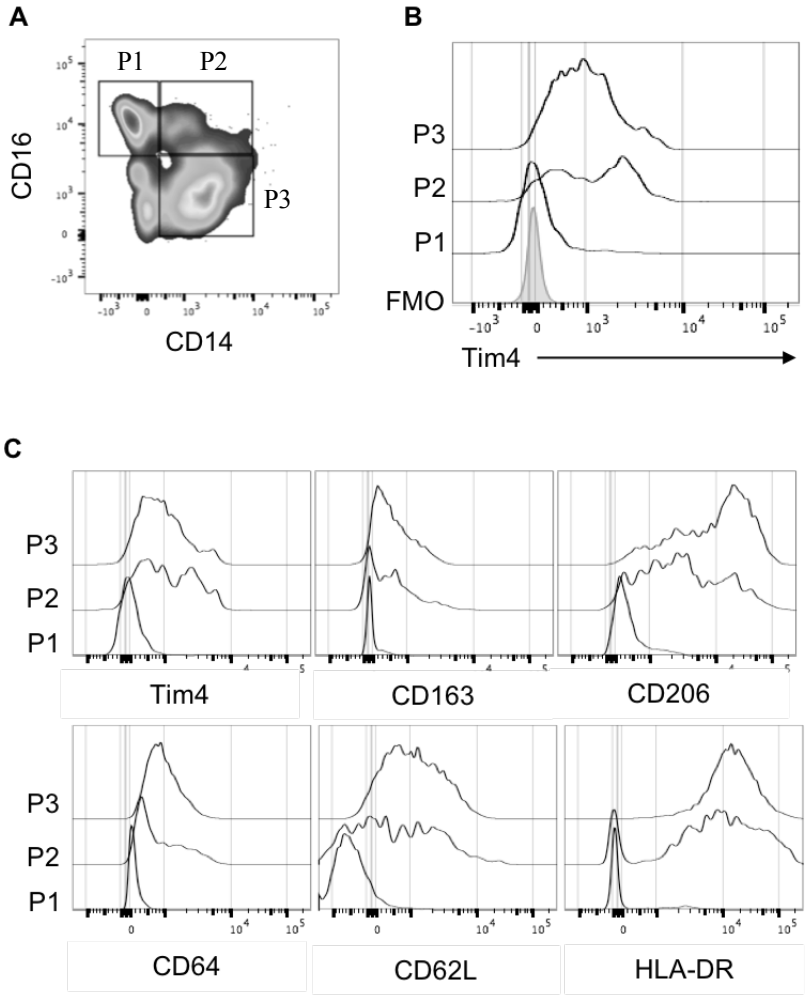

Figure 6.1 Tim4 is expressed on CD14+ ATMs alongside with other macrophage markers.

A Density plot representative of $CD45^+Lin^-CD11b^+$ cells in omentum of obese male (BMI 34) showing 3 populations of macrophages in the tissue : $CD16^+$ $CD14^-$ (P1), $CD16^+CD14^+$ (P2) and $CD16^-$ $CD14^+$ (P3). **B** Histograms showing Tim4 expression on these subsets and the fluorescence minus one (FMO) as a negative control. **C** Histograms showing the expression of other macrophage markers on these subsets. The histograms y axis represent the percentage of maximum intensity.

ATMs could be further separated by subsets according to CD163 and CD206 expression. Four subsets of ATMs were found: CD163^{+}CD206^{+}, CD163^{+}CD206^{-} , CD163^{-}CD206^{+} , CD163^{-}CD206^{-} . Overall, Tim4 was more highly expressed in the CD163^{+} subsets, independently of CD206 expression and was only lowly expressed in CD163^{-}CD206^{+} (Figure 6.2). Thus CD163 could be used as a marker for Tim4 ATMs.

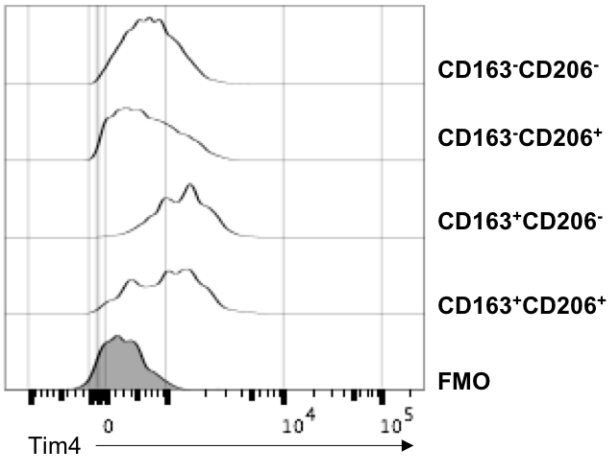

Figure 6.2 CD163^{+} ATMs had a higher Tim4 fluorescence intensity
Density plot representative of CD45^{+}Lin^{-}CD11b^{+}CD14^{+} cells in omentum of obese male showing Tim4 expression on different subsets and the fluorescence minus one (FMO) as a negative control. The histograms y axis represent the percentage of maximum intensity

6.4.2 Not all ATM populations show a positive correlation between their number and hips to waist ratio

Visceral adipose tissue expansion during obesity is associated with macrophage recruitment in human (Weisberg et al. 2003). Notably CD11c^{+}CD163^{+} ATMs and CD11c^{+}CD206^{+} ATMs were found positively associated with the BMI (Nakajima et al. 2016; J. M. Wentworth et al. 2010). ATM number can be related to BMI, but the WHR is a better indicator of risks to develop metabolic disease (Smith 2015). Hence, the ATM subsets were reported to the WHR.

Study of ATM cell number according to subsets revealed heterogeneity in number increase with waist to hips ratio (Figure 6.3). Tim4 was not on the panel during this study but as mentioned in 6.4.1, CD163^{+} ATMs are Tim4^{+}. As reported, we found that the total number of CD163^{+} ATMs was highest in obese individuals (waist to hips

ratio >0.9 (Obese individuals) (cell number given by Lucy Jackson-Jones). However, a sub-population of CD163^{+}CD206^{-} ATMs tended to stay stable. All CD206^{+} ATMs were increased with obesity, independently of their expression of CD163 (Figure 6.3).

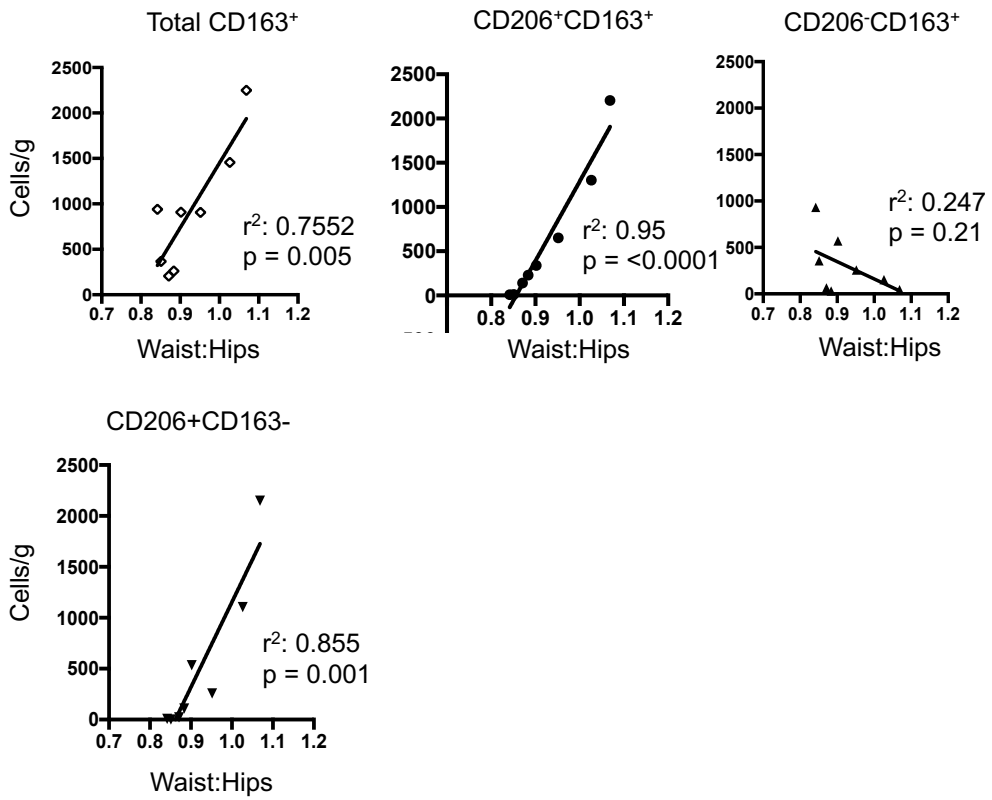

Figure 6.3 Not all ATM populations show a positive correlation between their number and hips to waist ratio.

Human omentum were digested and cells were analysed by flow cytometry (n= 7). The number of cells was correlated to the waist to hips ratio for each subject. Correlations were assessed with the Pearson correlation coefficient with p value>0.05 considered as significant.

6.4.3 Human omentum contained Tim4+ cells disposed in crown like structures

To assess the spatial localisation of Tim4+ ATMs, wholemount staining with lysotracker, LipidTox and Tim4 showed that the omentum (male, BMI = 32 (obese)) contained Tim4+ cells disposed around adipocytes in a crown like shape in the omentum (Figure 6.4). Other cells (Tim4-) were also present in the CLS. In addition, Tim4+ cells contained distinct lysosomes and neutral lipid vesicles which appeared to colocalise with Tim4 staining (Figure 6.4B).

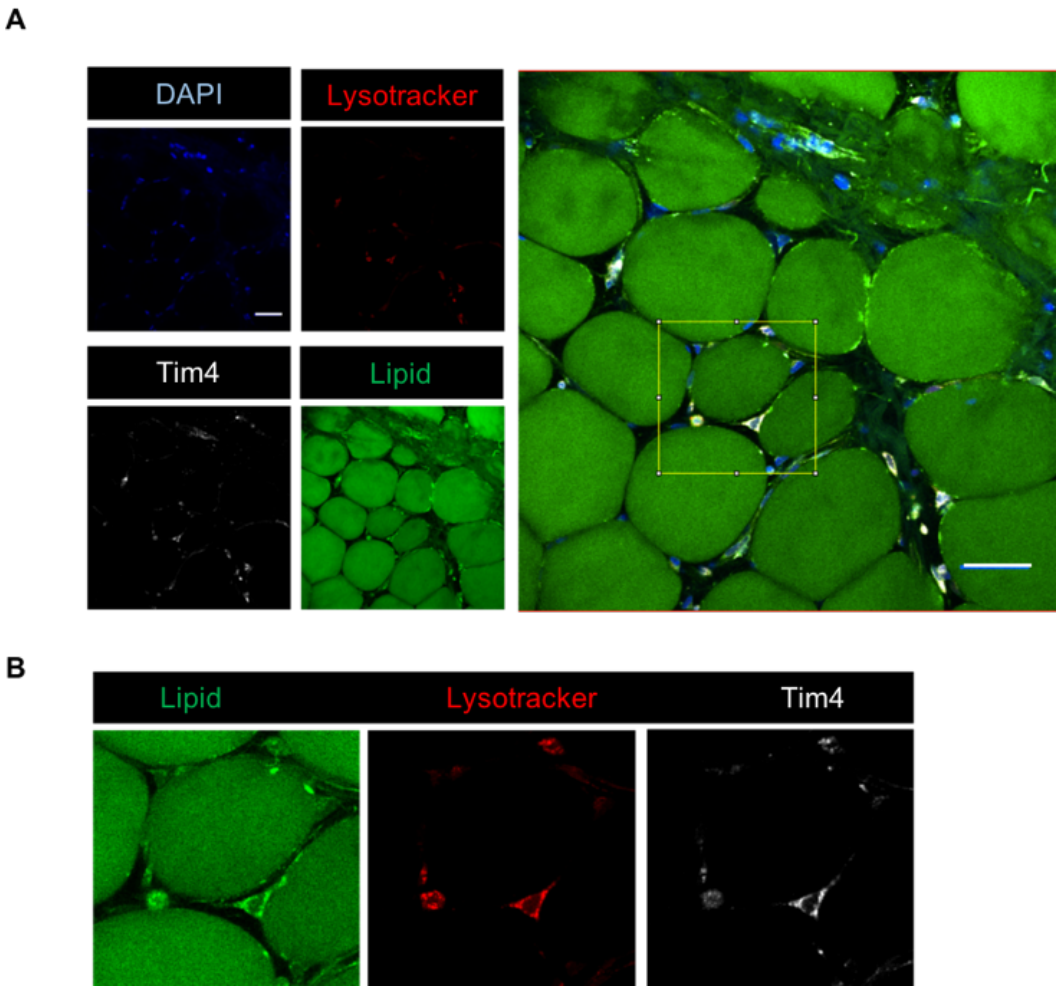

Figure 6.4 Human omentum had Tim4+ ATMs that contained lysosomes and were lipid laden.

A Wholemount immunofluorescence staining and confocal imaging showing lysosomes stained with Lysotracker (red), neutral lipids stained with Lipidtox (green) and Tim4 (grey) (Leica SP5 x40). **B** Zoom in of selected area (yellow) in the figure A. Scale bar represents 50µm.

The SAT also contained lipid laden Tim4^{+} cells with very active lysosomes (Figure 6.5 and Figure 6.6). Some Tim4^{+} ATMs appeared to contains lysosomes (Figure 6.6B, number 1 and 2), but some did not (Figure 6.6B, number 3), suggesting that lysosomes might by inducible or that subsets of macrophages exist within the Tim4 population, some being more active than others.

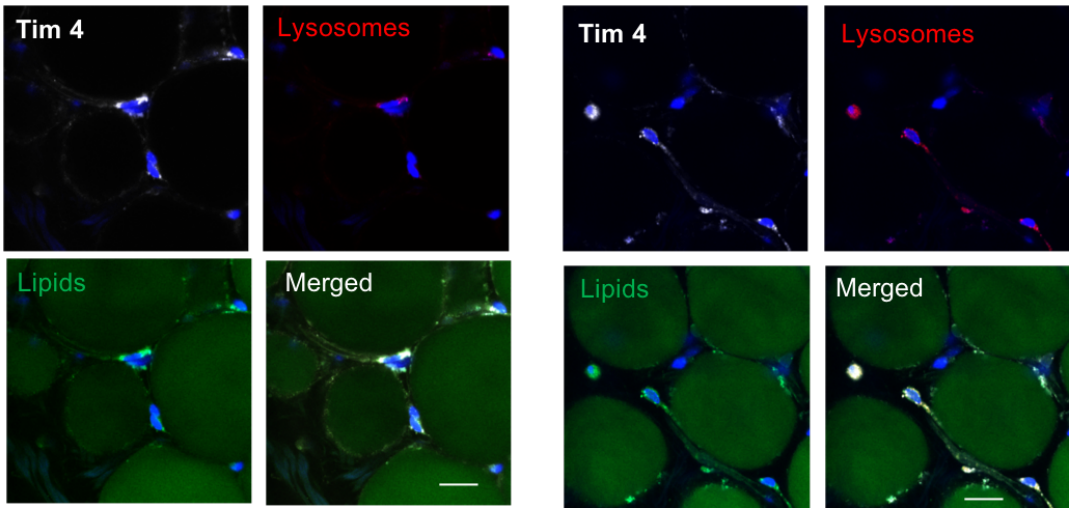

Figure 6.5 Human SAT had lipid laden Tim4^{+} ATMs that contained lysosomes
Wholemount immunofluorescence staining and confocal imaging showing lysosomes stained with Lysotracker (red), neutral lipids stained with Lipidtox (green) and Tim4 (grey) (Leica SP5 x40). Scale bar represents 25µm. Images from SAT taken from 2 obese (BMI>32) subjects.

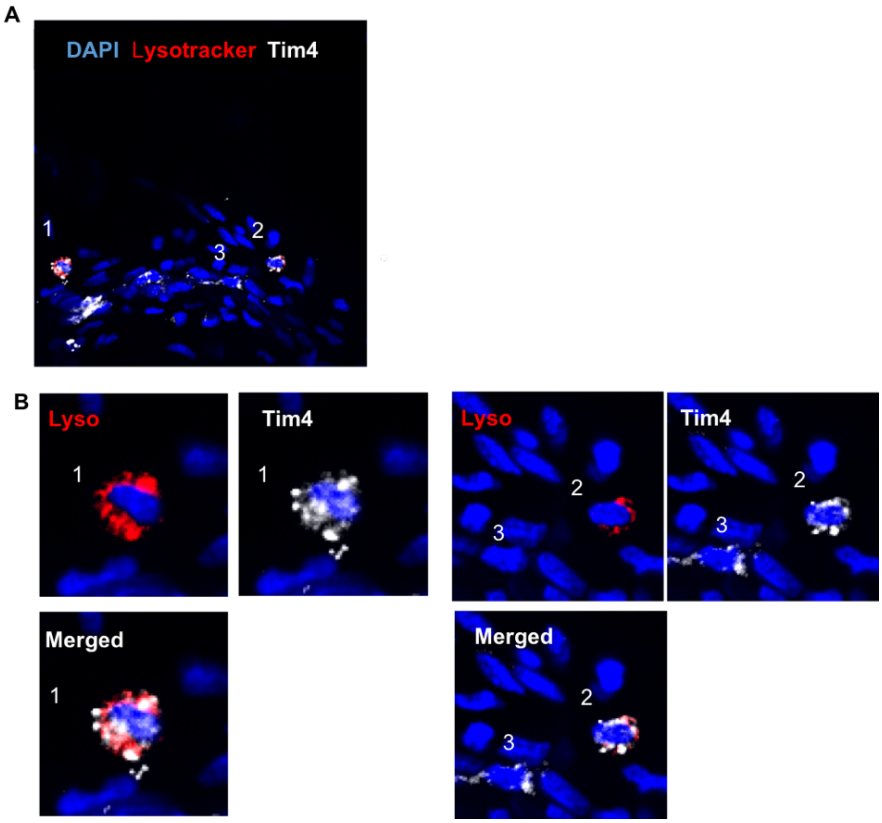

Figure 6.6 Obese human SAT contained Tim4+ ATMs, which some were filled with lysosomes

A Wholemount immunofluorescence staining and confocal imaging showing lysosomes stained with Lysotracker (red) and Tim4 (grey) (Spin disk x40). **B** Zoom in of selected macrophage in the figure A.

In all pictures analysed from omentum and SAT, the staining for Tim4 did not seem to be restricted to the cell surface and had a punctuated appearance partially overlaying with the lysosomal staining (Figure 6.4-6.6)

To test the ability of ATMs to uptake lipids, after purification of macrophages by adhesion method of omental SVF, ATMs were fed with LDL-Bodipy (50µg/ml) for 4h. Only few macrophages could be found on the plate, which could be improved in the future. Tim4+ ATMs were charged in LDL and lysosomes (Figure 6.7, ATM number 2-4). However some Tim4- ATMs presented lysosomes but no LDL (number 1). Hence, lysosomal activity might not be restricted to Tim4+ ATMs, but it seems

these macrophages had an affinity for LDL uptake. Moreover, lipids lysosomes and Tim4 colocalised in some ATMs (number 2).

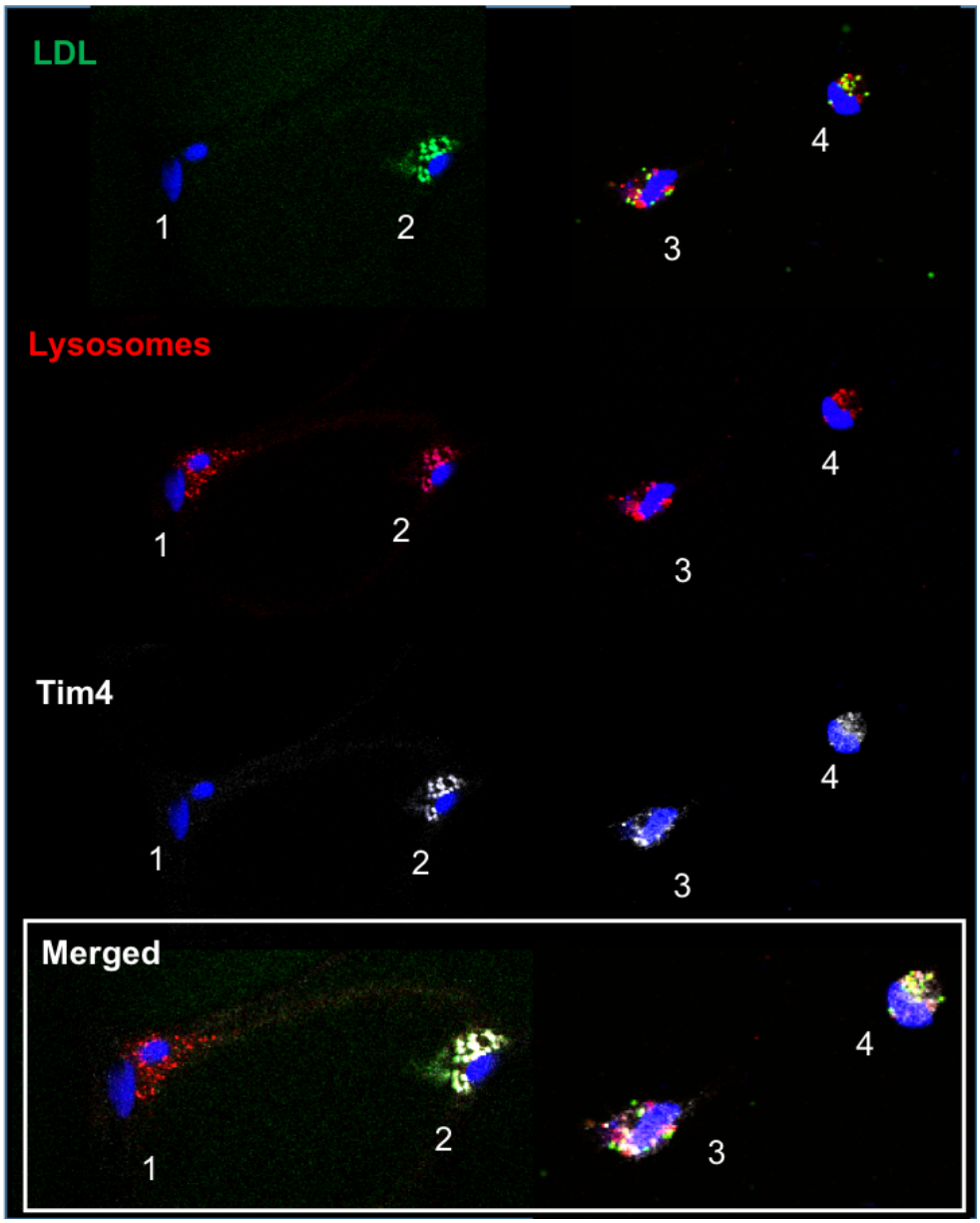

Figure 6.7 Tim4+ ATMs (omentum) were able to pick up LDL *in vitro*

Adhesion purified ATMs from omentum sample from an obese patient were incubated with LDL-Bodipy (green) for 4 hours previous to immunofluorescence staining and confocal analysis showing nuclei stained with Dapi (blue), lysosomes stained with Lysotracker (red), Tim4 (grey), LDL-Bodipy (green) (Leica SP5).

6.5 Discussion

I confirmed using microscopy and flow cytometry that human omentum and SAT contained Tim4^{+} ATMs (Figure 6.1). Tim4 was expressed heterogeneously across macrophages however CD163^{+} ATMs expressed it the most, independently of CD206 expression (Figure 6.2). Moreover, Tim4^{+} ATMs were lipid laden, contained lysosomes and take up LDL, similarly to what was described in mice in previous chapters (4 and 5) (Figure 6.6 - Figure 6.7).

Contrary to murine Tim4^{+} ATMs that were resident, humans Tim4^{+} ATMs seem to come from the CD16^{+}CD14^{+} (P2) population, which are intermediate monocytes, and thus might have a monocytic origin (Figure 6.1). Some macrophages in human are known to be self-replenishing. Indeed, following macrophages at different time points after human organ transplant showed that Langerhans cells, alveolar macrophages and Kupffer cells from donors could be still present in the recipients years after transplant (Schlitzer and Schultze 2017; Davies et al. 2013). Knowing macrophage origin in human's tissues is challenging as there is no specific methods or markers allocated to this purpose. Even if ATMs in human contained resident self-replenishing cells, the inflammatory status of the patients might skewed the results. The samples collected from the analysis of Tim4 ATMs were coming from obese patients (BMI > 30). As shown in mouse in chapter 4, obesity increases the amount of cells coming from the BM so much that resident cells decrease in proportion in the tissue.

Multiple studies showed that ATM content correlates with the amount of fat in human and their BMI (Curat et al. 2006; Weisberg et al. 2003; Nakajima et al. 2016). Here, I showed that even though the cell number of most subsets increased in parallel with the WHR, the CD163^{+}CD206^{-} ATM subset did not (Figure 6.3). The WHR, compared to the BMI, acknowledges the fact that not only fat accumulation is a risk factor to develop diseases but AT distribution is important too (Smith 2015). Indeed, waist accumulation leads to higher risks of cardiovascular diseases and diabetes (Smith 2015).

Macrophages accumulate specifically in CLS with obesity in mouse and human (Murano et al. 2008). Tim4^{+} ATMs could be found in what could qualify as CLS in

the omentum (Figure 6.4), however they seemed quite sparse in the SAT (Figure 6.6). It is reported that other subsets expressing CD11c (CD11c^{+}CD206^{+}) are spatially restricted to CLS, while CD11c^{-}CD206^{+} are found with no defined spatial arrangement (John M Wentworth et al. 2010). CD11c^{+} ATMs can also express CD163 (Nakajima et al. 2016). While both CD206 and CD163 are considered as M2-like macrophage markers, they have both been shown to be expressed on inflammatory CD11c^{+} ATMs (Martinez and Gordon 2014) which secretes large amount of TNF, MCP1 and IL 6, cytokines inducing AT inflammation during obesity (Zeyda et al. 2007). Therefore, at this stage of the study, I can't exclude that Tim4 could also be expressed by CD11c^{+} ATMs, as it was present on both CD206^{+} and CD163^{+} ATMs (Figure 6.2).

The intense Lipidtox staining found in Tim4+ ATMs is reminiscent of the foamy CD14^{+}CD64^{+} ATMs described in the omentum of obese human (Shapiro et al. 2013) and of the lipid laden CD11c^{+} ATMs described in human omentum (J. M. Wentworth et al. 2010). This raises the question of the exact nature of the lipid staining found in Tim4^{+} ATMs: Is it an accumulation of lipid droplets characteristics of foamy ATMs or is it lipid vesicles transiting to the lysosomes for their catabolism as described by Xu et al? The frequent association of Tim4, lipid neutral staining and lysosomal staining in Tim4 ATMs would indicate that Tim4 is associated with the second type of lipid laden ATMs. Interestingly, CD11c^{+}CD206^{+} contains more transcript related to lipid handling and lipid oxidation, as well as mRNA coding for lysosomes (J. M. Wentworth et al. 2010). More work needs to be done to determine whether Tim4 is associated with a lysosomal lipolysis signature in human.

The correct degradation of lipids by lysosomes is critical. Lysosomal acid lipase deficiency (LAL-D, also known as Wolman disease) is a genetic disorder in human, arising from a mutation in the *LIPA* gene. It results in accumulation of lipids, notably cholesterol esters and TG, in the liver, arteries, spleen… (Reiner et al. 2014) Indeed, cells can't break down LDL into free cholesterol and FFA and lipids accumulate within lysosomes. LAL-D patients present dyslipidaemia (elevated TG and LDL) and enlarged lipid laden hepatocytes, as hepatocytes can't lyse LDL via their lysosomes, but also lipid laden Kupffer cells. BM transplant had successfully treated few patients with LAL-D but the procedure is risky (Krivit et al. 2000).

However, it suggest the importance of HSC derived cells, and potentially BM derived macrophages in human lipid metabolism via LAL, which was also the case in mouse (Ouimet et al. 2011; Chistiakov, Bobryshev, and Orekhov 2016; S. C.-C. Huang et al. 2014).

Conclusion

In this chapter, I presented preliminary data confirming the existence of Tim4^{+} ATMs in human omentum and SAT. More experiments need to be done to carefully assess the expression of Tim4 on the various ATM subsets previously described in the literature and that I identified. *In vitro* experimentation could be conducted from patient AT explants combined with Tim4 blockade and the measurement of net lipolysis to have an idea of the role of these ATMs in lipid metabolism. The limitation of this chapter is the low number of patients recruited across WHR and sexes.

CHAPTER 7 DISCUSSION

7.1 Summary

In this thesis, I investigated the heterogeneity of ATMs in a murine model and identified several subsets of ATMs expressing distinct surface markers. Notably, these subsets showed a great heterogeneity in the mechanisms controlling their turnover in the AT. After partial body irradiation and i.v. reconstitution with donor mice, I showed that $Tim4^+$ ATMs had a very low input from the donor BM after 8 weeks, contrary to $CD11c^+$ ATM. Therefore, the expression of Tim4 characterised resident ATMs in the mesenteric, subcutaneous and gonadal AT. This newly described subset did not rely on monocyte derived macrophages to increase its pool during HFD induced obesity, but increase in number by proliferation. Even though their number increased during AT expansion, monocyte derived macrophages colonised the tissue and accounted for most of the increase in macrophage number during HFD.

Interestingly, $Tim4^+$ ATMs were lipid laden in lean and obese GAT, raising the question of their role in the control of lipid influx. Indeed, macrophages are known to participate in AT lipolysis and FFA release, via an intracellular process of lysosomal activation and catabolism of lipids taken up by ATM (X. Xu et al. 2013). $Tim4^+$ ATMs had a high lysosomal activity which correlated with their ability to uptake lipids. *In vivo* blockade of Tim4 with monoclonal antibodies affected the levels of FFA in the plasma of mice. Indeed, compared to control mice fed the same HFD for 1 day or 8 weeks, the mice injected with aTim4 blocking antibodies had lower plasmatic FFA levels. Examination of the content and lysosomal activity of $Tim4^+$ macrophages coming from different tissues revealed that blocking Tim4 blocked lipid uptake and reduced lysosomal activity, thus could explain a decrease in lipid catabolism and the decrease on FFA in the plasma. Interestingly, there was some difference in lipid uptake dependent on the tissues from which macrophages were taken, with ATMs and liver macrophages being more efficient at taking up lipids than peritoneal macrophages. The exact mechanism of the involvement of Tim4 and lipid uptake has still to be determined, but it seemed that Tim4 colocalised with lysosomes and might be involved in the internalisation of lipids and formation of phago-lysosomes, maybe in conjunction with other receptors. $Tim4^+$ ATMs were also present in humans (omentum and SAT), in rather large proportions, and did also contain lipids and lysosomes. Their

role in lipid metabolism in human will be of interest as already several GWAS pointed at *timd4* and its association with dyslipidaemia.

The proposed mechanism of action of Tim4 macrophages is summarised in the figure below (Figure 7.1).

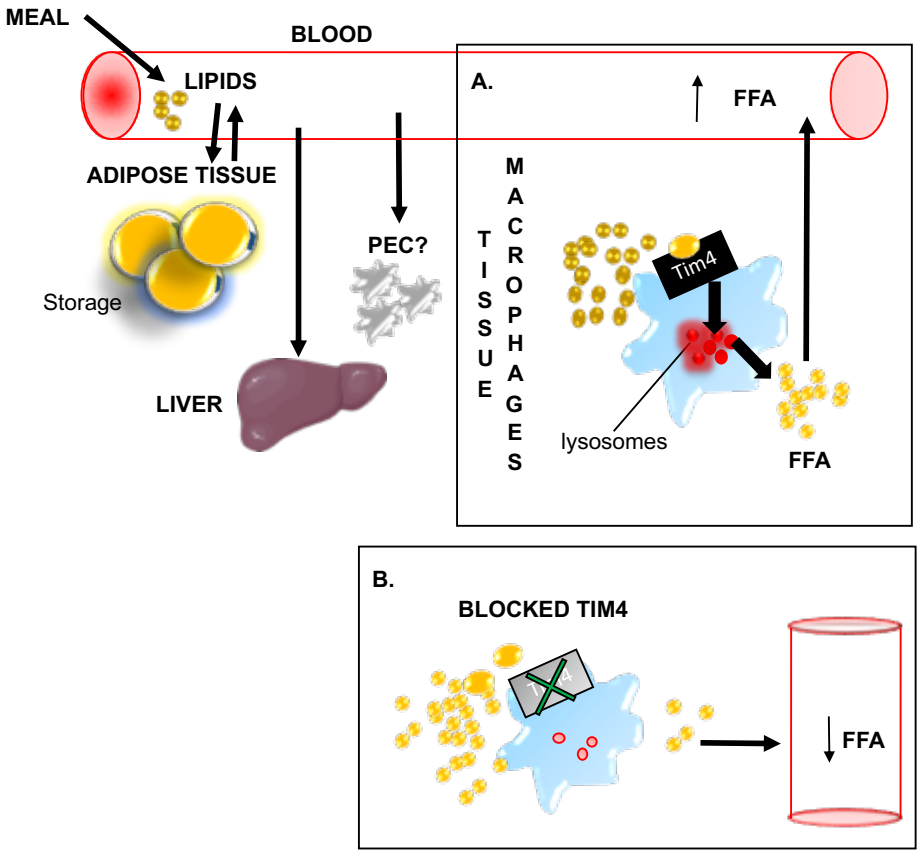

Figure 7.1 Proposed mechanism of action of Tim4^{+} macrophages

After a meal, lipids enter the bloodstream, mainly in the form of TG rich lipoproteins which are taken up by cells to sustain their need for energy and anabolism, while excess TG are stored by adipocytes. **A** Tim4^{+} macrophages in AT and liver are able to pick up excess TG from the environment to buffer TG in the tissue and to release FFA which will become available for other organs. Tim4 is involved in the uptake of lipid particles and their progress to the lysosomes where they are hydrolysed into FFA and released from the tissue to the bloodstream. Blocking Tim4 (**B**) decreases lipid uptake by macrophages and their lysosomal degradation which reduces FFA release in the bloodstream.

7.2 Heterogenous macrophages in AT

Using partial BM chimeras , I showed the heterogeneity of recruitment of ATMs in the tissue. While a number of studies have now shown that ATM can fulfil a number of different and sometimes antagonist functions, there is a critical lack of characterisation of ATM subsets. I hope that my study will contribute to the establishment of a universal gating strategy by flow cytometry for ATMs that would help make future work on ATMs more easily transferable from one lab to another. Amano and colleagues showed that 8 weeks of HFD induce (in male C57Bl/6J) macrophages proliferation (Amano et al. 2014). In their gating strategy they use $CD45^{+}Siglec\text{-}F^{-}CD11b^{+}F4/80^{+}$ to define ATMs. They don't segregate $F4/80^{high}$ or $F4/80^{low}$ ATMs, and in my opinion, missed some ATMs in their gating (notably some $F4/80^{low}$, which, if included, could lower their number of proliferative cells). They do acknowledge that there is a basal ATM proliferation in lean mice (Amano et al. 2014). Adding Tim4 in their study could have revealed that these were the ones proliferating, as well as some $F4/80^{high}$ ATMs. A recent study demonstrated that ATM recruitment was CCR2 independent at the early stage of HFD (2 weeks) and that these $CD11c^{-}$ ATMs were proliferating, as measured by PKH26, a dye injected i.p. that is phagocytosed by macrophages and is diluted with time (Muir et al. 2018). In this thesis, I propose that $Tim4^{+}$ ATMs are a critical subset for the homeostasis of AT, mopping fat spill-over coming from dead adipocytes and high fat rich meals, but that they rapidly become saturated during long term high fat feeding. Excess fat that can't be processed by $Tim4^{+}$ ATMs are taken up by $CD11c^{+}$ ATMs that accumulate progressively more lipids (Carey N Lumeng, Bodzin, and Saltiel 2007; Morris et al. 2013). However Tim4 uptake of lipids could dampen inflammation, as my data show that $MHCII^{low}Tim4^{+}$ ATMs uptake lipids. When put in culture, PEC macrophages from Tim4 KO mice produce more TNFα than WT (K. Wong et al. 2010). The reduced capacity of $Tim4^{+}$ ATMs to buffer lipids in HFD, may be due to their slower turnover compared to BM derived macrophages. The era of single cell sequencing is allowing the definition of more subsets and moving towards defining subset link with specific functions will be critical in the future.

7.3 Tim4 is not unique to ATMs

A number of studies showed that ATMs are involved in lipid trafficking (X. Xu et al. 2013; Reilly and Saltiel 2014; Kosteli et al. 2010a; Prieur et al. 2011). This thesis implies that Tim4 expressing macrophages alone might play a big role in lipid trafficking, as *in vivo* blockade was sufficient to decrease FFA in the plasma of mice after HFD. Tim4 is expressed by a macrophages in various organs but also on other cell types. Dendritic cells (DCs) also express Tim 4 and can become lipid laden in tumour bearing mice (DCs from spleen) and results in default of antigen presentation (Gardner et al. 2014; Pearce and Everts 2015). However no studies have been done on a possible role of DCs in lipid metabolism. Tim4 expressing macrophages are present in several murine organs: for example, spleen, liver, peritoneal cavity, gut and skin (K. Wong et al. 2010; Shaw et al. 2018; Yanagihashi et al. 2017). Other than AT, gut and liver are the organs which have a role in lipid metabolism: the gut for digestion of dietary lipids and formation of chylomicrons and the liver for formation of other lipoproteins and in cholesterol metabolism (Feingold and Grunfeld 2000). Blocking of Tim4 using anti-Tim4 antibodies did not specifically targeted ATMs so I can't attribute the decrease in FFA only to ATMs. Blocking Tim4 *in vivo* targeted the receptor on GAT and PEC macrophages, but also on Kupffer cells (data not shown). Kupffer cells have a transcriptional profile enriched with genes involved in lipid metabolism, and the liver is central in the control of LDL levels in the bloodstream (Remmerie and Scott 2018). Chronic release of FFA by AT can lead to ectopic accumulation of fat in the liver (non-alcoholic fatty liver disease). In the setting of HFD, it would be interesting to test whether blocking Tim4 also affect the amount of fat deposition in the liver.

7.4 Mechanism of lipid uptake by Tim4

Tim4 blockade *in vitro* decreases LDL and CM uptake by ATMs. The fact that less lipids are taken up could explain the decrease in lysotracker activity observed. But *in vivo,* it is not clear what lipids Tim4 ATMs would uptake.

Apoptotic cells

In vivo Tim4 blockade has been performed in *ldlr*$^{-/-}$ mice fed a HFD for 4 weeks. Tim4 blockade increased apoptotic cell numbers in atherosclerotic areas and

as they accumulated, the tissue became necrotic (Foks et al. 2016). Hence $Tim4^+$ macrophages in this setting, seem to be mainly involved in clearance of apoptotic cells containing large amounts of lipids (foam cells) (Foks et al. 2016). No impact on cholesterol or TG levels was observed in the plasma of these mice, however the levels of FFA were not assessed. In addition, the experiments were performed in *ldlr*$^{-/-}$ mice which are highly dyslipidemic which could have masked the effect of blocking Tim4 on lipidemia. It would be interesting to look at atherosclerotic lesions in C57Bl/6 mice after Tim4 blockade. To develop atherosclerosis these mice need 14 weeks of high cholesterol diet (Schreyer, Wilson, and LeBoeuf 1998).

In the atherosclerotic plaque $Tim4^+$ macrophages internalised apoptotic macrophages that had engulfed oxLDL. This could suggest that $Tim4^+$ macrophages acquire their lipids by ingesting lipid laden cells and not LDL directly in this case. In AT, apoptotic adipocytes are surrounded by macrophages (CLS) (Murano et al. 2008). It was demonstrated *in vitro* that macrophages can exocytose their lysosomes to facilitate adipocyte degradation (exophagy) (Haka et al. 2016). Macrophages can then degrade large amount of lipids, and rapidly become foamy (24 hours) (Haka et al. 2016). It is possible that all macrophages are able to uptake apoptotic cells, but it is unclear what becomes of the lipids (degraded via lysosomes or stored as lipid droplet / CE). Either $Tim4^+$ macrophages also become foamy and accumulate lipids or they are present in these areas to clear the foamy cells.

Direct uptake of lipids

PS is a glycerophospholipid recognised by a metal ion-dependent pocket on the N-terminal immunoglobulin-fold extracellular domain of Tim4 (Santiago et al. 2007). Very little has been done on Tim4 signalling. In contrast, other PS receptors, its intracellular domain does not have any tyrosine kinase activity. Lipoproteins naturally contain phospholipids, including PS. Tim4 can interreact with glycerol and fatty acid after PS recognition on dead cells (Santiago et al. 2007). It would be interesting to block PS on lipids and look at their uptake by Tim4 ATMs to identify what is recognised by these macrophages.

Macrophages produce lipase (LpL) to facilitate the uptake of TG rich lipoproteins (Aouadi et al. 2014; M. Takahashi et al. 2013; Babaev et al. 1999). Silencing LpL expression in ob/ob mice ATMs, using siRNA, decreased the amount of lipid laden macrophages and increased FFA levels in the blood as well as glucose intolerance (Aouadi et al. 2014). In addition, LpL silencing reduced CD36 expression on macrophages. Therefore LpL could facilitate lipid uptake by AT and ATMs themselves, and control FFA levels in the blood. Interestingly in this experiment, the fact that LpL was silenced in all macrophages increased FFA levels in the blood whereas blocking Tim4 decreased the amount of FFA. It is possible that lipids that are not taken up by Tim4 are phagocytosed by other macrophages which are unable to process lipids, either due to a lack of lysosomal biogenesis proportional to the amount of lipid taken, or because there metabolism is shifted from OXPHOS, and they don't use FA as a source of energy. Using SeaHorse technology could inform about the mitochondrial activity (OCR) of Tim4 ATMs, in comparison to other subsets.

CD36 expression was higher on $Tim4^{+}$ ATMs challenged with LDL compared to other ATMs, suggesting that these macrophages could be more efficient at lipid uptake. After IL-4 stimulation of BMDM, macrophages (M2) express more CD36 and take up more LDL and VLDL than unstimulated BMDM (M0) (X. Xu et al. 2013). However, BMDM from $CD36^{-/-}$ treated with IL-4 picked up less LDL and VLDL than M2 and M0 macrophages, suggesting the role of CD36 for lipoproteins uptake (X. Xu et al. 2013). These *in vitro* experiments, after differentiation of BMDM, do not integrate the environment "imprinting" that I observed during experiments involving macrophages from the GAT, PEC and liver. It would be interesting to do the same kind of experiments on $CD36^{-/-}$ but using primary macrophage coming from the GAT, PEC and liver, and looking at the differential lipid uptake by the different subsets.

Directed uptake of oxidised lipids

LDL oxidation (oxLDL) or acetylation increase their uptake by macrophages (Miller et al. 2010). These modifications also allow LDL to be scavenged by other receptor than the classical LDL-receptor, which is a receptor ubiquitously expressed (Miller et al. 2010). For example, CD36 is involved in oxLDL uptake (Sheedy et al. 2013; Jay et al. 2015). The presence of a lipoxygenase (12/15LO) on $Tim4^{+}$

macrophages directs apoptotic body uptake to those macrophages (Uderhardt et al. 2012). Indeed, 12/15LO oxidise esterified fatty acids (phosphatidyl ethanolamine PE) which interferes with the ability of other macrophages to bind apoptotic cells by binding MFG-E8. Indeed, MFG-E8 creates a bridge between apoptotic cells and other macrophages, not expressing Tim4 thus enabling them to engulf them. In arachidonate 15 LO (ALOX15) KO mice, the absence of ALOX15 during induced peritonitis, allows the uptake of apoptotic cells by Ly6c^{high} monocytes, via MFG-E8, and enhanced inflammation (Uderhardt et al. 2012). Hypothetically, 12/15 LO could also oxidise lipids such as LDL and enhance a targeted engulfment by Tim4 macrophages, with the help of CD36. 12/15 LO can induce CD36 expression in macrophages after IL-4 stimulation. (J. T. Huang et al. 1999). The need of ALOX15 in ATMs to clear dead cells was also demonstrated recently. Co-culture of F4/80^{+} ATMs with apoptotic adipocytes increased ALOX15 expression and if ALOX15 was pharmacologically inhibited, there was a delay in lipid clearance from adipocytes, by ATMs (Kwon et al. 2016). It is not known if all macrophages express ALOX15, but since the expression of ALOX15 is associated with the expression of Tim4 in peritoneal macrophages, it is possible that the expression of ALOX15 is also restricted to Tim4^{+} ATMs in AT.

7.5 Tim4: good or evil ?

Tim4 blockade limited the amount of FFA release in the bloodstream after HFD (in the non-fasted state). This could potentially improve the metabolic status of patients with dyslipidaemia, as lowering FFA can improve insulin resistance (Boden 2008). SNPs in *TIMD4* in GWAS have been linked with dyslipidaemia. The SNP rs1553318, present in 65% of the studied population, was associated with an increase in TG, LDL and cholesterol in the plasma (Surakka et al. 2015), while other SNPs (rs6882076, rs4704727, rs1501908, rs2036402) were associated with a decrease of the same parameters (Kathiresan et al. 2009b; Spracklen et al. 2017; Teslovich et al. 2010; Willer et al. 2013). None of the SNP found in *Timd4* are found in a coding region and therefore are more likely to affect the gene expression level of Tim4 than its structure (except if the SNP alters the splicing of Timd4 mRNA). Since I found that Tim4 was expressed by the majority of ATM in the 3 obese subjects I studied, it would be critical to study if there are any variability in the frequency of Tim4^{+} ATM or the level of

expression of Tim4 in subjects of varying BMI and metabolic dysfunction and correlate this with the genotype of this subjects. Tim4 and *TIMD4* could be involved in a "lean phenotype" to limit AT expansion by directing lipid efflux to the bloodstream for muscle use after a meal. However, evolution of society and western lipid rich diet means that Tim4 activity may now be more linked to cardiovascular diseases via excess FFA release in the circulation due to our lipid rich diet and their deposition in liver, muscle and arteries.

To conclude, exploring and exploiting the heterogeneity of macrophages in adipose tissue and other compartments could lead to the development of efficient therapeutic treatments targeting lipid metabolism in macrophages to improve dyslipidaemia.

Bibliography

Altintas, Mehmet M., Adiba Azad, Behzad Nayer, Gabriel Contreras, Julia Zaias, Christian Faul, Jochen Reiser, and Ali Nayer. 2011. "Mast Cells, Macrophages, and Crown-like Structures Distinguish Subcutaneous from Visceral Fat in Mice." *Journal of Lipid Research* 52 (3): 480–88. https://doi.org/10.1194/jlr.M011338.

Amano, Shinya U., Jessica L. Cohen, Pranitha Vangala, Michaela Tencerova, Sarah M. Nicoloro, Joseph C. Yawe, Yuefei Shen, Michael P. Czech, and Myriam Aouadi. 2014. "Local Proliferation of Macrophages Contributes to Obesity-Associated Adipose Tissue Inflammation." *Cell Metabolism* 19 (1): 162–71. https://doi.org/10.1016/J.CMET.2013.11.017.

Aouadi, Myriam, Pranitha Vangala, Joseph C. Yawe, Michaela Tencerova, Sarah M. Nicoloro, Jessica L. Cohen, Yuefei Shen, and Michael P. Czech. 2014. "Lipid Storage by Adipose Tissue Macrophages Regulates Systemic Glucose Tolerance." *American Journal of Physiology-Endocrinology and Metabolism* 307 (4): E374–83. https://doi.org/10.1152/ajpendo.00187.2014.

Aparicio-Vergara, Marcela, Ronit Shiri-Sverdlov, Gerald de Haan, and Marten H Hofker. 2010. "Bone Marrow Transplantation in Mice as a Tool for Studying the Role of Hematopoietic Cells in Metabolic and Cardiovascular Diseases." *Atherosclerosis* 213 (2): 335–44. https://doi.org/10.1016/j.atherosclerosis.2010.05.030.

Appari, Mahesh, Keith M Channon, and Eileen McNeill. 2018. "Metabolic Regulation of Adipose Tissue Macrophage Function in Obesity and Diabetes." *Antioxidants & Redox Signaling* 29 (3): 297–312. https://doi.org/10.1089/ars.2017.7060.

Babaev, Vladimir R., Sergio Fazio, Linda A. Gleaves, Kathy J. Carter, Clay F. Semenkovich, and MacRae F. Linton. 1999. "Macrophage Lipoprotein Lipase Promotes Foam Cell Formation and Atherosclerosis in Vivo." *Journal of Clinical Investigation* 103 (12): 1697–1705. https://doi.org/10.1172/JCI6117.

Baghdadi, Muhammad, Akihiro Yoneda, Tsunaki Yamashina, Hiroko Nagao, Yoshihiro Komohara, Shigenori Nagai, Hisaya Akiba, et al. 2013. "TIM-4 Glycoprotein-Mediated Degradation of Dying Tumor Cells by Autophagy Leads to Reduced Antigen Presentation and Increased Immune Tolerance." *Immunity* 39 (6): 1070–81. https://doi.org/10.1016/j.immuni.2013.09.014.

Bain, C C, C L Scott, H Uronen-Hansson, S Gudjonsson, O Jansson, O Grip, M Guilliams, B Malissen, W W Agace, and A McI Mowat. 2013. "Resident and Pro-Inflammatory Macrophages in the Colon Represent Alternative Context-Dependent Fates of the Same Ly6Chi Monocyte Precursors." *Mucosal Immunology* 6 (3): 498–510. https://doi.org/10.1038/mi.2012.89.

Bain, Calum C, Alberto Bravo-Blas, Charlotte L Scott, Elisa Gomez Perdiguero, Frederic Geissmann, Sandrine Henri, Bernard Malissen, Lisa C Osborne, David Artis, and Allan McI Mowat. 2014. "Constant Replenishment from Circulating Monocytes Maintains the Macrophage Pool in the Intestine of Adult Mice." *Nature Immunology* 15 (10): 929–37. https://doi.org/10.1038/ni.2967.

Bain, Calum C, Catherine A Hawley, Hannah Garner, Charlotte L Scott, Anika Schridde, Nicholas J Steers, Matthias Mack, et al. 2016. "Long-Lived Self-Renewing Bone Marrow-Derived Macrophages Displace Embryo-Derived Cells to Inhabit Adult Serous Cavities." *Nature Communications* 7 (June): ncomms11852. https://doi.org/10.1038/ncomms11852.

Bassaganya-Riera, Josep, Sarah Misyak, Amir J. Guri, and Raquel Hontecillas. 2009. "PPAR γ Is Highly Expressed in F4/80hi Adipose Tissue Macrophages and Dampens Adipose-Tissue Inflammation." *Cellular Immunology* 258 (2): 138–46. https://doi.org/10.1016/j.cellimm.2009.04.003.

Beek, Lianne van, Jan B van Klinken, Amanda C M Pronk, Andrea D van Dam, Eline Dirven, Patrick C N Rensen, Frits Koning, Ko Willems van Dijk, and Vanessa van Harmelen. 2015. "The Limited Storage Capacity of Gonadal Adipose Tissue Directs the Development of Metabolic Disorders in Male C57Bl/6J Mice." *Diabetologia* 58 (7): 1601–9. https://doi.org/10.1007/s00125-015-3594-8.

Benezech, C, N T Luu, J A Walker, A A Kruglov, Y Loo, K Nakamura, Y Zhang, et al. 2015. "Inflammation-Induced Formation of Fat-Associated Lymphoid Clusters." *Nat Immunol* 16 (8): 819–28. https://doi.org/10.1038/ni.3215.

Berry, Daniel C, Drew Stenesen, Daniel Zeve, and Jonathan M Graff. 2013. "The Developmental Origins of Adipose Tissue." *Development (Cambridge, England)* 140 (19): 3939–49. https://doi.org/10.1242/dev.080549.

Bigornia, S J, M G Farb, M M Mott, D T Hess, B Carmine, A Fiscale, L Joseph, C M Apovian,

and N Gokce. 2012. “Relation of Depot-Specific Adipose Inflammation to Insulin Resistance in Human Obesity.” *Nutrition & Diabetes* 2 (3): e30–e30. https://doi.org/10.1038/nutd.2012.3.

Boden, Guenther. 2008. “Obesity and Free Fatty Acids.” *Endocrinology and Metabolism Clinics of North America* 37 (3): 635–46, viii–ix. https://doi.org/10.1016/j.ecl.2008.06.007.

Bossche, Jan Van Den, Luke A O ’ Neill, and Deepthi Menon. 2017. “Macrophage Immunometabolism: Where Are We (Going)?” *Trends in Immunology* 38: 395–406. https://doi.org/10.1016/j.it.2017.03.001.

Boutens, Lily, Guido J. Hooiveld, Sourabh Dhingra, Robert A. Cramer, Mihai G. Netea, and Rinke Stienstra. 2018. “Unique Metabolic Activation of Adipose Tissue Macrophages in Obesity Promotes Inflammatory Responses.” *Diabetologia*, January. https://doi.org/10.1007/s00125-017-4526-6.

Boutens, Lily, and Rinke Stienstra. 2016. “Adipose Tissue Macrophages: Going off Track during Obesity.” *Diabetologia* 59 (5): 879–94. https://doi.org/10.1007/s00125-016-3904-9.

Braune, Julia, Ulrike Weyer, Constance Hobusch, Jan Mauer, Jens C Brüning, Ingo Bechmann, and Martin Gericke. 2017. “IL-6 Regulates M2 Polarization and Local Proliferation of Adipose Tissue Macrophages in Obesity.” *Journal of Immunology (Baltimore, Md. : 1950)* 198 (7): 2927–34. https://doi.org/10.4049/jimmunol.1600476.

Catrysse, Leen, and Geert van Loo. 2018. “Adipose Tissue Macrophages and Their Polarization in Health and Obesity.” *Cellular Immunology*, March. https://doi.org/10.1016/J.CELLIMM.2018.03.001.

Chistiakov, Dimitry A, Yuri V Bobryshev, and Alexander N Orekhov. 2016. “Macrophage-Mediated Cholesterol Handling in Atherosclerosis.” *Journal of Cellular and Molecular Medicine* 20 (1): 17–28. https://doi.org/10.1111/jcmm.12689.

Cho, Kae Won, Brian F. Zamarron, Lindsey A. Muir, Kanakadurga Singer, Cara E. Porsche, Jennifer B. DelProposto, Lynn Geletka, Kevin A. Meyer, Robert W. O’Rourke, and Carey N. Lumeng. 2016. “Adipose Tissue Dendritic Cells Are Independent Contributors to Obesity-Induced Inflammation and Insulin Resistance.” *The Journal of Immunology*

197 (9): 3650–61. https://doi.org/10.4049/jimmunol.1600820.

Choe, Sung Sik, Jin Young Huh, In Jae Hwang, Jong In Kim, and Jae Bum Kim. 2016. "Adipose Tissue Remodeling: Its Role in Energy Metabolism and Metabolic Disorders." *Frontiers in Endocrinology* 7 (April): 30. https://doi.org/10.3389/fendo.2016.00030.

Cinti, Saverio, Grant Mitchell, Giorgio Barbatelli, Incoronata Murano, Enzo Ceresi, Emanuela Faloia, Shupei Wang, Melanie Fortier, Andrew S. Greenberg, and Martin S. Obin. 2005. "Adipocyte Death Defines Macrophage Localization and Function in Adipose Tissue of Obese Mice and Humans." *Journal of Lipid Research* 46 (11): 2347–55. https://doi.org/10.1194/jlr.M500294-JLR200.

Cipolletta, Daniela, Markus Feuerer, Amy Li, Nozomu Kamei, Jongsoon Lee, Steven E. Shoelson, Christophe Benoist, and Diane Mathis. 2012. "PPAR-γ Is a Major Driver of the Accumulation and Phenotype of Adipose Tissue Treg Cells." *Nature* 486 (7404): 549–53. https://doi.org/10.1038/nature11132.

Curat, C. A., V. Wegner, C. Sengenès, A. Miranville, C. Tonus, R. Busse, and A. Bouloumié. 2006. "Macrophages in Human Visceral Adipose Tissue: Increased Accumulation in Obesity and a Source of Resistin and Visfatin." *Diabetologia* 49 (4): 744–47. https://doi.org/10.1007/s00125-006-0173-z.

David, Lawrence A., Corinne F. Maurice, Rachel N. Carmody, David B. Gootenberg, Julie E. Button, Benjamin E. Wolfe, Alisha V. Ling, et al. 2014. "Diet Rapidly and Reproducibly Alters the Human Gut Microbiome." *Nature* 505 (7484): 559–63. https://doi.org/10.1038/nature12820.

Davies, John Q, and Siamon Gordon. 2005. "Isolation and Culture of Human Macrophages." *Methods in Molecular Biology (Clifton, N.J.)* 290: 105–16. http://www.ncbi.nlm.nih.gov/pubmed/15361658.

Davies, Luke, Stephen J Jenkins, Judith E Allen, and Philip R Taylor. 2013. "Tissue-Resident Macrophages." *Nature Immunology* 14 (10): 986–95. https://doi.org/10.1038/ni.2705.

Davies, Luke, Marcela Rosas, Paul J. Smith, Donald J. Fraser, Simon A. Jones, and Philip R. Taylor. 2011. "A Quantifiable Proliferative Burst of Tissue Macrophages Restores Homeostatic Macrophage Populations after Acute Inflammation." *European Journal of Immunology* 41 (8): 2155–64. https://doi.org/10.1002/eji.201141817.

Davies, Luke, and Philip R Taylor. 2015. “Tissue-Resident Macrophages: Then and Now.” *Immunology* 144 (4): 541–48. https://doi.org/10.1111/imm.12451.

Do, Ron, Cristen J Willer, Ellen M Schmidt, and Et. Al. 2013. “Common Variants Associated with Plasma Triglycerides and Risk for Coronary Artery Disease.” *Nature Genetics* 45 (11): 1345–52. https://doi.org/10.1038/ng.2795.

Duncan, Robin E, Maryam Ahmadian, Kathy Jaworski, Eszter Sarkadi-Nagy, and Hei Sook Sul. 2007. “Regulation of Lipolysis in Adipocytes.” *Annual Review of Nutrition* 27: 79–101. https://doi.org/10.1146/annurev.nutr.27.061406.093734.

Duran-Struuck, Raimon, and Robert C Dysko. 2009. “Principles of Bone Marrow Transplantation (BMT): Providing Optimal Veterinary and Husbandry Care to Irradiated Mice in BMT Studies.” *Journal of the American Association for Laboratory Animal Science : JAALAS* 48 (1): 11–22. http://www.ncbi.nlm.nih.gov/pubmed/19245745.

Emanuel, Roy, Ismail Sergin, Somashubhra Bhattacharya, Jaleisa Turner, Slava Epelman, Carmine Settembre, Abhinav Diwan, Andrea Ballabio, and Babak Razani. 2014. “Induction of Lysosomal Biogenesis in Atherosclerotic Macrophages Can Rescue Lipid-Induced Lysosomal Dysfunction and Downstream Sequelae.” *Arteriosclerosis, Thrombosis, and Vascular Biology* 34 (9): 1942–52. https://doi.org/10.1161/ATVBAHA.114.303342.

Epelman, Slava, Kory J. Lavine, Anna E. Beaudin, Dorothy K. Sojka, Javier A. Carrero, Boris Calderon, Thaddeus Brija, et al. 2014. “Embryonic and Adult-Derived Resident Cardiac Macrophages Are Maintained through Distinct Mechanisms at Steady State and during Inflammation.” *Immunity* 40 (1): 91–104. https://doi.org/10.1016/j.immuni.2013.11.019.

Epelman, Slava, Kory J Lavine, and Gwendalyn J Randolph. 2014a. “Origin and Functions of Tissue Macrophages.” *Immunity* 41 (1): 21–35. https://doi.org/10.1016/j.immuni.2014.06.013.

———. 2014b. “Origin and Functions of Tissue Macrophages.” *Immunity* 41 (1): 21–35. https://doi.org/10.1016/j.immuni.2014.06.013.

Feingold, Kenneth R, and Carl Grunfeld. 2000. *Introduction to Lipids and Lipoproteins*. *Endotext*. MDText.com, Inc. http://www.ncbi.nlm.nih.gov/pubmed/26247089.

Ferrante, A W. 2013. “The Immune Cells in Adipose Tissue.” *Diabetes, Obesity & Metabolism* 15 Suppl 3 (0 3): 34–38. https://doi.org/10.1111/dom.12154.

Feuerer, Markus, Laura Herrero, Daniela Cipolletta, Afia Naaz, Jamie Wong, Ali Nayer, Jongsoon Lee, et al. 2009. “Lean, but Not Obese, Fat Is Enriched for a Unique Population of Regulatory T Cells That Affect Metabolic Parameters.” *Nature Medicine* 15 (8): 930–39. https://doi.org/10.1038/nm.2002.

Fitzgibbons, Timothy P, and Michael P Czech. 2016. “Emerging Evidence for Beneficial Macrophage Functions in Atherosclerosis and Obesity-Induced Insulin Resistance.” *Journal of Molecular Medicine (Berlin, Germany)* 94 (3): 267–75. https://doi.org/10.1007/s00109-016-1385-4.

Fjeldborg, Karen, Steen B Pedersen, Holger J Møller, Tore Christiansen, Marianne Bennetzen, and Bjørn Richelsen. 2014. “Human Adipose Tissue Macrophages Are Enhanced but Changed to an Anti-Inflammatory Profile in Obesity.” *Journal of Immunology Research* 2014: 309548. https://doi.org/10.1155/2014/309548.

Foks, Amanda C., Daniel Engelbertsen, Felicia Kuperwaser, Noah Alberts-Grill, Ayelet Gonen, Joseph L. Witztum, James Lederer, et al. 2016. “Blockade of Tim-1 and Tim-4 Enhances Atherosclerosis in Low-Density Lipoprotein Receptor-Deficient Mice.” *Arteriosclerosis, Thrombosis, and Vascular Biology* 36 (3): 456–65. https://doi.org/10.1161/ATVBAHA.115.306860.

Fox, Caroline S, Joseph M Massaro, Udo Hoffmann, Karla M Pou, Pal Maurovich-Horvat, Chun-Yu Liu, Ramachandran S Vasan, et al. 2007. “Abdominal Visceral and Subcutaneous Adipose Tissue Compartments: Association with Metabolic Risk Factors in the Framingham Heart Study.” *Circulation* 116 (1): 39–48. https://doi.org/10.1161/CIRCULATIONAHA.106.675355.

Freeman, Gordon J, Jose M Casasnovas, Dale T Umetsu, and Rosemarie H DeKruyff. 2010. “TIM Genes: A Family of Cell Surface Phosphatidylserine Receptors That Regulate Innate and Adaptive Immunity.” *Immunological Reviews* 235 (1): 172–89. https://doi.org/10.1111/j.0105-2896.2010.00903.x.

Fu, Jingyuan, Marten Hofker, and Cisca Wijmenga. 2015. “Apple or Pear: Size and Shape Matter.” *Cell Metabolism* 21 (4): 507–8. https://doi.org/10.1016/j.cmet.2015.03.016.

Fuente-Martín, Esther, Pilar Argente-Arizón, Purificación Ros, Jesús Argente, and Julie A Chowen. 2013. "Sex Differences in Adipose Tissue: It Is Not Only a Question of Quantity and Distribution." *Adipocyte* 2 (3): 128–34. https://doi.org/10.4161/adip.24075.

Furth, R van, and Z A Cohn. 1968. "The Origin and Kinetics of Mononuclear Phagocytes." *The Journal of Experimental Medicine* 128 (3): 415–35. http://www.ncbi.nlm.nih.gov/pubmed/5666958.

Gaber, Timo, Cindy Strehl, and Frank Buttgereit. 2017. "Metabolic Regulation of Inflammation." *Nature Reviews Rheumatology* 13 (5): 267–79. https://doi.org/10.1038/nrrheum.2017.37.

Gardner, Joanne K, Cyril Ds Mamotte, Terrence McGonigle, Danielle E Dye, Connie Jackaman, and Delia J Nelson. 2014. "Lipid-Laden Partially-Activated Plasmacytoid and CD4(-)CD8α(+) Dendritic Cells Accumulate in Tissues in Elderly Mice." *Immunity & Ageing : I & A* 11: 11. https://doi.org/10.1186/1742-4933-11-11.

Geissmann, Frederic, Steffen Jung, and Dan R Littman. 2003. "Blood Monocytes Consist of Two Principal Subsets with Distinct Migratory Properties." *Immunity* 19 (1): 71–82. http://www.ncbi.nlm.nih.gov/pubmed/12871640.

Ginhoux, Florent, Melanie Greter, Marylene Leboeuf, Sayan Nandi, Peter See, Solen Gokhan, Mark F Mehler, et al. 2010. "Fate Mapping Analysis Reveals That Adult Microglia Derive from Primitive Macrophages." *Science (New York, N.Y.)* 330 (6005): 841–45. https://doi.org/10.1126/science.1194637.

Ginhoux, Florent, and Martin Guilliams. 2016. "Tissue-Resident Macrophage Ontogeny and Homeostasis." *Immunity* 44 (3): 439–49. https://doi.org/10.1016/j.immuni.2016.02.024.

Gomez Perdiguero, Elisa, Kay Klapproth, Christian Schulz, Katrin Busch, Emanuele Azzoni, Lucile Crozet, Hannah Garner, et al. 2014. "Tissue-Resident Macrophages Originate from Yolk-Sac-Derived Erythro-Myeloid Progenitors." *Nature* 518 (7540): 547–51. https://doi.org/10.1038/nature13989.

Goudriaan, Jeltje R, Sonia M S Espirito Santo, Peter J Voshol, Bas Teusink, Ko Willems van Dijk, Bart J M van Vlijmen, Johannes A Romijn, Louis M Havekes, and Patrick C N Rensen. 2004. "The VLDL Receptor Plays a Major Role in Chylomicron Metabolism by Enhancing LPL-Mediated Triglyceride Hydrolysis." *Journal of Lipid Research* 45 (8):

1475–81. https://doi.org/10.1194/jlr.M400009-JLR200.

Grijalva, Ambar, Xiaoyuan Xu, and Anthony W Ferrante. 2016. “Autophagy Is Dispensable for Macrophage-Mediated Lipid Homeostasis in Adipose Tissue.” *Diabetes* 65 (4): 967–80. https://doi.org/10.2337/db15-1219.

Grijalva, Ambar, Xiaoyuan Xu, Anthony W Ferrante, and Jr. 2016. “Autophagy Is Dispensable for Macrophage-Mediated Lipid Homeostasis in Adipose Tissue.” *Diabetes* 65 (4): 967–80. https://doi.org/10.2337/db15-1219.

Guilliams, Martin, and Charlotte L. Scott. 2017. “Does Niche Competition Determine the Origin of Tissue-Resident Macrophages?” *Nature Reviews Immunology* 17 (7): 451–60. https://doi.org/10.1038/nri.2017.42.

Gundra, Uma Mahesh, Natasha M Girgis, Dominik Ruckerl, Stephen Jenkins, Lauren N Ward, Zachary D Kurtz, Kirsten E Wiens, et al. 2014. “Alternatively Activated Macrophages Derived from Monocytes and Tissue Macrophages Are Phenotypically and Functionally Distinct.” *Blood* 123 (20): e110-22. https://doi.org/10.1182/blood-2013-08-520619.

Haase, Julia, Ulrike Weyer, Kerstin Immig, Nora Klöting, Matthias Blüher, Jens Eilers, Ingo Bechmann, and Martin Gericke. 2014a. “Local Proliferation of Macrophages in Adipose Tissue during Obesity-Induced Inflammation.” *Diabetologia* 57 (3): 562–71. https://doi.org/10.1007/s00125-013-3139-y.

———. 2014b. “Local Proliferation of Macrophages in Adipose Tissue during Obesity-Induced Inflammation.” *Diabetologia* 57 (3): 562–71. https://doi.org/10.1007/s00125-013-3139-y.

Haka, Abigail S, Valéria C Barbosa-Lorenzi, Hyuek Jong Lee, Domenick J Falcone, Clifford A Hudis, Andrew J Dannenberg, and Frederick R Maxfield. 2016. “Exocytosis of Macrophage Lysosomes Leads to Digestion of Apoptotic Adipocytes and Foam Cell Formation.” *Journal of Lipid Research* 57 (6): 980–92. https://doi.org/10.1194/jlr.M064089.

Harman-Boehm, Ilana, Matthias Blüher, Henry Redel, Netta Sion-Vardy, Shira Ovadia, Eliezer Avinoach, Iris Shai, et al. 2007. “Macrophage Infiltration into Omental *Versus* Subcutaneous Fat across Different Populations: Effect of Regional Adiposity and the Comorbidities of Obesity.” *The Journal of Clinical Endocrinology & Metabolism* 92 (6):

2240–47. https://doi.org/10.1210/jc.2006-1811.

Hashimoto, Daigo, Andrew Chow, Clara Noizat, Pearline Teo, Mary Beth Beasley, Marylene Leboeuf, Christian D Becker, et al. 2013. “Tissue-Resident Macrophages Self-Maintain Locally throughout Adult Life with Minimal Contribution from Circulating Monocytes.” *Immunity* 38 (4): 792–804. https://doi.org/10.1016/j.immuni.2013.04.004.

Heck, A M, J A Yanovski, and K A Calis. 2000. “Orlistat, a New Lipase Inhibitor for the Management of Obesity.” *Pharmacotherapy* 20 (3): 270–79. http://www.ncbi.nlm.nih.gov/pubmed/10730683.

Helming, Laura. 2011. “Inflammation: Cell Recruitment versus Local Proliferation.” *Current Biology* 21 (14): R548–50. https://doi.org/10.1016/J.CUB.2011.06.005.

Hill, Andrea A, W Reid Bolus, and Alyssa H Hasty. 2014. “A Decade of Progress in Adipose Tissue Macrophage Biology.” *Immunological Reviews* 262 (1): 134–52. https://doi.org/10.1111/imr.12216.

Hill, David A, Hee-Woong Lim, Yong Hoon Kim, Wesley Y Ho, Yee Hoon Foong, Victoria L Nelson, Hoang C B Nguyen, et al. 2018. “Distinct Macrophage Populations Direct Inflammatory versus Physiological Changes in Adipose Tissue.” *Proceedings of the National Academy of Sciences of the United States of America* 115 (22): E5096–5105. https://doi.org/10.1073/pnas.1802611115.

Hipolito, Victoria E B, Erika Ospina-Escobar, and Roberto J Botelho. 2018. “Lysosome Remodelling and Adaptation during Phagocyte Activation.” https://doi.org/10.1111/cmi.12824.

Hoeffel, Guillaume, and Florent Ginhoux. 2015. “Ontogeny of Tissue-Resident Macrophages.” *Frontiers in Immunology* 6 (SEP). https://doi.org/10.3389/fimmu.2015.00486.

Hoeffel, Guillaume, Yilin Wang, Melanie Greter, Peter See, Pearline Teo, Benoit Malleret, Marylène Leboeuf, et al. 2012. “Adult Langerhans Cells Derive Predominantly from Embryonic Fetal Liver Monocytes with a Minor Contribution of Yolk Sac–Derived Macrophages.” *The Journal of Experimental Medicine* 209 (6): 1167–81. https://doi.org/10.1084/jem.20120340.

Horton, Jay D, Joseph L Goldstein, and Michael S Brown. 2002. “SREBPs: Activators of the Complete Program of Cholesterol and Fatty Acid Synthesis in the Liver.” *The Journal of Clinical Investigation* 109 (9): 1125–31. https://doi.org/10.1172/JCI15593.

Houben, Tom, Yvonne Oligschlaeger, Albert V. Bitorina, Tim Hendrikx, Sofie M. A. Walenbergh, Marie-Hélène Lenders, Marion J. J. Gijbels, et al. 2017. “Blood-Derived Macrophages Prone to Accumulate Lysosomal Lipids Trigger OxLDL-Dependent Murine Hepatic Inflammation.” *Scientific Reports* 7 (1): 12550. https://doi.org/10.1038/s41598-017-13058-z.

Huang, Jannet T., John S. Welch, Mercedes Ricote, Christoph J. Binder, Timothy M. Willson, Carolyn Kelly, Joseph L. Witztum, Colin D. Funk, Douglas Conrad, and Christopher K. Glass. 1999. “Interleukin-4-Dependent Production of PPAR-γ Ligands in Macrophages by 12/15-Lipoxygenase.” *Nature* 400 (6742): 378–82. https://doi.org/10.1038/22572.

Huang, Stanley Ching-Cheng, Bart Everts, Yulia Ivanova, David O’Sullivan, Marcia Nascimento, Amber M Smith, Wandy Beatty, et al. 2014. “Cell-Intrinsic Lysosomal Lipolysis Is Essential for Alternative Activation of Macrophages.” *Nature Immunology* 15 (9): 846–55. https://doi.org/10.1038/ni.2956.

Huber, Joakim, Florian W. Kiefer, Maximilian Zeyda, Bernhard Ludvik, Gerd R. Silberhumer, Gerhard Prager, Gerhard J. Zlabinger, and Thomas M. Stulnig. 2008. “CC Chemokine and CC Chemokine Receptor Profiles in Visceral and Subcutaneous Adipose Tissue Are Altered in Human Obesity.” *The Journal of Clinical Endocrinology & Metabolism* 93 (8): 3215–21. https://doi.org/10.1210/jc.2007-2630.

Hussaarts, Leonie, Noemí García-Tardón, Lianne van Beek, Mattijs M. Heemskerk, Simone Haeberlein, Gerard C. van der Zon, Arifa Ozir-Fazalalikhan, et al. 2015. “Chronic Helminth Infection and Helminth-Derived Egg Antigens Promote Adipose Tissue M2 Macrophages and Improve Insulin Sensitivity in Obese Mice.” *The FASEB Journal* 29 (7): 3027–39. https://doi.org/10.1096/fj.14-266239.

Jackson-Jones, Lucy H., Sheelagh M. Duncan, Marlène S. Magalhaes, Sharon M. Campbell, Rick M. Maizels, Henry J. McSorley, Judith E. Allen, and Cécile Bénézech. 2016. “Fat-Associated Lymphoid Clusters Control Local IgM Secretion during Pleural Infection and Lung Inflammation.” *Nature Communications* 7 (September): 12651. https://doi.org/10.1038/ncomms12651.

Jaishy, Bharat, and E Dale Abel. 2016. “Lipids, Lysosomes, and Autophagy.” *Journal of Lipid Research* 57 (9): 1619–35. https://doi.org/10.1194/jlr.R067520.

Jay, Anthony G, Alexander N Chen, Miguel A Paz, Justin P Hung, and James A Hamilton. 2015. “CD36 Binds Oxidized Low Density Lipoprotein (LDL) in a Mechanism Dependent upon Fatty Acid Binding.” *The Journal of Biological Chemistry* 290 (8): 4590–4603. https://doi.org/10.1074/jbc.M114.627026.

Jenkins, Stephen J., and David A. Hume. 2014. “Homeostasis in the Mononuclear Phagocyte System.” *Trends in Immunology* 35 (8): 358–67. https://doi.org/10.1016/J.IT.2014.06.006.

Jenkins, Stephen J, Dominik Ruckerl, Peter C Cook, Lucy H Jones, Fred D Finkelman, Nico van Rooijen, Andrew S MacDonald, and Judith E Allen. 2011. “Local Macrophage Proliferation, Rather than Recruitment from the Blood, Is a Signature of TH2 Inflammation.” *Science (New York, N.Y.)* 332 (6035): 1284–88. https://doi.org/10.1126/science.1204351.

Jenkins, Stephen J, Dominik Ruckerl, Graham D Thomas, James P Hewitson, Sheelagh Duncan, Frank Brombacher, Rick M Maizels, David A Hume, and Judith E Allen. 2013a. “IL-4 Directly Signals Tissue-Resident Macrophages to Proliferate beyond Homeostatic Levels Controlled by CSF-1.” *The Journal of Experimental Medicine* 210 (11): 2477–91. https://doi.org/10.1084/jem.20121999.

———. 2013b. “IL-4 Directly Signals Tissue-Resident Macrophages to Proliferate beyond Homeostatic Levels Controlled by CSF-1.” *The Journal of Experimental Medicine* 210 (11): 2477–91. https://doi.org/10.1084/jem.20121999.

Jeon, Sang-Min. 2016. “Regulation and Function of AMPK in Physiology and Diseases.” *Experimental & Molecular Medicine* 48 (7): e245–e245. https://doi.org/10.1038/emm.2016.81.

Jeong, Se Jin, Mi Ni Lee, and Goo Taeg Oh. 2017. “The Role of Macrophage Lipophagy in Reverse Cholesterol Transport.” *Endocrinology and Metabolism (Seoul, Korea)* 32 (1): 41–46. https://doi.org/10.3803/EnM.2017.32.1.41.

Ji, Haofeng, Yuanxing Liu, Yu Zhang, Xiu-da Shen, Feng Gao, Ronald W Busuttil, Vijay K Kuchroo, and Jerzy W Kupiec-Weglinski. 2014. “T-Cell Immunoglobulin and Mucin

Domain 4 (TIM-4) Signaling in Innate Immune-Mediated Liver Ischemia-Reperfusion Injury." *Hepatology (Baltimore, Md.)* 60 (6): 2052–64. https://doi.org/10.1002/hep.27334.

Kanda, Hajime, Sanshiro Tateya, Yoshikazu Tamori, Ko Kotani, Ken-ichi Hiasa, Riko Kitazawa, Sohei Kitazawa, et al. 2006a. "MCP-1 Contributes to Macrophage Infiltration into Adipose Tissue, Insulin Resistance, and Hepatic Steatosis in Obesity." *The Journal of Clinical Investigation* 116 (6): 1494–1505. https://doi.org/10.1172/JCI26498.

———. 2006b. "MCP-1 Contributes to Macrophage Infiltration into Adipose Tissue, Insulin Resistance, and Hepatic Steatosis in Obesity." *The Journal of Clinical Investigation* 116 (6): 1494–1505. https://doi.org/10.1172/JCI26498.

Kanneganti, Thirumala-Devi, and Vishwa Deep Dixit. 2012. "Immunological Complications of Obesity." *Nature Immunology* 13 (8): 707–12. https://doi.org/10.1038/ni.2343.

Kathiresan, Sekar, Cristen J Willer, Gina M Peloso, Serkalem Demissie, Kiran Musunuru, Eric E Schadt, Lee Kaplan, et al. 2009a. "Common Variants at 30 Loci Contribute to Polygenic Dyslipidemia." *Nature Genetics* 41 (1): 56–65. https://doi.org/10.1038/ng.291.

———. 2009b. "Common Variants at 30 Loci Contribute to Polygenic Dyslipidemia." *Nature Genetics* 41 (1): 56–65. https://doi.org/10.1038/ng.291.

Klop, Boudewijn, Jan Willem F Elte, and Manuel Castro Cabezas. 2013. "Dyslipidemia in Obesity: Mechanisms and Potential Targets." *Nutrients* 5 (4): 1218–40. https://doi.org/10.3390/nu5041218.

Kobayashi, Norimoto, Piia Karisola, Victor Peña-Cruz, David M Dorfman, Masahisa Jinushi, Sarah E Umetsu, Manish J Butte, et al. 2007. "TIM-1 and TIM-4 Glycoproteins Bind Phosphatidylserine and Mediate Uptake of Apoptotic Cells." *Immunity* 27 (6): 927–40. https://doi.org/10.1016/j.immuni.2007.11.011.

Komornik, V. 1985. "Some New Estimates for the Eigenfunctions of Higher Order of a Linear Differential Operator." *Acta Mathematica Hungarica* 45 (3–4): 451–57. https://doi.org/10.1038/ncomms2877.

Konrad, Daniel, and Stephan Wueest. 2014. "The Gut-Adipose-Liver Axis in the Metabolic

Syndrome." *Physiology* 29 (5): 304–13. https://doi.org/10.1152/physiol.00014.2014.

Koppaka, S., S. Kehlenbrink, M. Carey, W. Li, E. Sanchez, D.-E. Lee, H. Lee, et al. 2013. "Reduced Adipose Tissue Macrophage Content Is Associated With Improved Insulin Sensitivity in Thiazolidinedione-Treated Diabetic Humans." *Diabetes* 62 (6): 1843–54. https://doi.org/10.2337/db12-0868.

Kosteli, Aliki, Eiji Sugaru, Guenter Haemmerle, Jayne F. Martin, Jason Lei, Rudolf Zechner, and Anthony W. Ferrante. 2010a. "Weight Loss and Lipolysis Promote a Dynamic Immune Response in Murine Adipose Tissue." *Journal of Clinical Investigation* 120 (10): 3466–79. https://doi.org/10.1172/JCI42845.

———. 2010b. "Weight Loss and Lipolysis Promote a Dynamic Immune Response in Murine Adipose Tissue." *Journal of Clinical Investigation* 120 (10): 3466–79. https://doi.org/10.1172/JCI42845.

Krenkel, Oliver, and Frank Tacke. 2017. "Liver Macrophages in Tissue Homeostasis and Disease." *Nature Reviews Immunology*. https://doi.org/10.1038/nri.2017.11.

Kristiansen, Mette, Jonas H. Graversen, Christian Jacobsen, Ole Sonne, Hans-Jürgen Hoffman, S.K. Alex Law, and Søren K. Moestrup. 2001. "Identification of the Haemoglobin Scavenger Receptor." *Nature* 409 (6817): 198–201. https://doi.org/10.1038/35051594.

Krivit, W, C Peters, K Dusenbery, Y Ben-Yoseph, NKC Ramsay, JE Wagner, and R Anderson. 2000. "Wolman Disease Successfully Treated by Bone Marrow Transplantation." *Bone Marrow Transplantation* 26 (5): 567–70. https://doi.org/10.1038/sj.bmt.1702557.

Kunjathoor, Vidya V, Maria Febbraio, Eugene A Podrez, Kathryn J Moore, Lorna Andersson, Stephanie Koehn, Jeongmi S Rhee, Roy Silverstein, Henry F Hoff, and Mason W Freeman. 2002. "Scavenger Receptors Class A-I/II and CD36 Are the Principal Receptors Responsible for the Uptake of Modified Low Density Lipoprotein Leading to Lipid Loading in Macrophages." *The Journal of Biological Chemistry* 277 (51): 49982–88. https://doi.org/10.1074/jbc.M209649200.

Kwon, H-J, S-N Kim, Y-A Kim, and Y-H Lee. 2016. "The Contribution of Arachidonate 15-Lipoxygenase in Tissue Macrophages to Adipose Tissue Remodeling." *Cell Death & Disease* 7 (6): e2285–e2285. https://doi.org/10.1038/cddis.2016.190.

Lee, Yun Sok, Pingping Li, Jin Young Huh, In Jae Hwang, Min Lu, Jong In Kim, Mira Ham, et al. 2011. "Inflammation Is Necessary for Long-Term but Not Short-Term High-Fat Diet-Induced Insulin Resistance." *Diabetes* 60 (10): 2474–83. https://doi.org/10.2337/db11-0194.

Li, Pingping, Min Lu, M T Audrey Nguyen, Eun Ju Bae, Justin Chapman, Daorong Feng, Meredith Hawkins, et al. 2010. "Functional Heterogeneity of CD11c-Positive Adipose Tissue Macrophages in Diet-Induced Obese Mice." *The Journal of Biological Chemistry* 285 (20): 15333–45. https://doi.org/10.1074/jbc.M110.100263.

Lim, Chun-Yan, and Roberto Zoncu. 2016. "The Lysosome as a Command-and-Control Center for Cellular Metabolism." *The Journal of Cell Biology* 214 (6): 653–64. https://doi.org/10.1083/jcb.201607005.

Lumeng, C. N., J. B. DelProposto, D. J. Westcott, and A. R. Saltiel. 2008. "Phenotypic Switching of Adipose Tissue Macrophages With Obesity Is Generated by Spatiotemporal Differences in Macrophage Subtypes." *Diabetes* 57 (12): 3239–46. https://doi.org/10.2337/db08-0872.

Lumeng, C. N., S. M. DeYoung, J. L. Bodzin, and A. R. Saltiel. 2007. "Increased Inflammatory Properties of Adipose Tissue Macrophages Recruited During Diet-Induced Obesity." *Diabetes* 56 (1): 16–23. https://doi.org/10.2337/db06-1076.

Lumeng, Carey N., Stephanie M. Deyoung, and Alan R. Saltiel. 2007. "Macrophages Block Insulin Action in Adipocytes by Altering Expression of Signaling and Glucose Transport Proteins." *American Journal of Physiology-Endocrinology and Metabolism* 292 (1): E166–74. https://doi.org/10.1152/ajpendo.00284.2006.

Lumeng, Carey N, Jennifer L Bodzin, and Alan R Saltiel. 2007. "Obesity Induces a Phenotypic Switch in Adipose Tissue Macrophage Polarization." *The Journal of Clinical Investigation* 117 (1): 175–84. https://doi.org/10.1172/JCI29881.

Lynch, Lydia. 2014. "Adipose Invariant Natural Killer T Cells." *Immunology* 142 (3): 337–46. https://doi.org/10.1111/imm.12269.

Lynch, Lydia, Michael Nowak, Bindu Varghese, Justice Clark, Andrew E. Hogan, Vasillis Toxavidis, Steven P. Balk, Donal O'Shea, Cliona O'Farrelly, and Mark A. Exley. 2012. "Adipose Tissue Invariant NKT Cells Protect against Diet-Induced Obesity and

Metabolic Disorder through Regulatory Cytokine Production." *Immunity* 37 (3): 574–87. https://doi.org/10.1016/j.immuni.2012.06.016.

Mackaness, G B. 1962. "Cellular Resistance to Infection." *The Journal of Experimental Medicine* 116 (3): 381–406. https://doi.org/10.1084/jem.116.3.381.

Martinez-Santibañez, Gabriel, and Carey Nien-Kai Lumeng. 2014. "Macrophages and the Regulation of Adipose Tissue Remodeling." *Annual Review of Nutrition* 34 (1): 57–76. https://doi.org/10.1146/annurev-nutr-071812-161113.

Martinez, Fernando O, and Siamon Gordon. 2014. "The M1 and M2 Paradigm of Macrophage Activation: Time for Reassessment." *F1000prime Reports* 6: 13. https://doi.org/10.12703/P6-13.

Matsuzawa, Y, I Shimomura, T Nakamura, Y Keno, K Kotani, and K Tokunaga. 1995. "Pathophysiology and Pathogenesis of Visceral Fat Obesity." *Obesity Research* 3 Suppl 2 (September): 187S–194S. http://www.ncbi.nlm.nih.gov/pubmed/8581775.

McLaughlin, Tracey, Cindy Lamendola, Alice Liu, and Fahim Abbasi. 2011. "Preferential Fat Deposition in Subcutaneous Versus Visceral Depots Is Associated with Insulin Sensitivity." *The Journal of Clinical Endocrinology & Metabolism* 96 (11): E1756–60. https://doi.org/10.1210/jc.2011-0615.

Metchnikoff, E. 1892. *Lecons Sur La Pathologies Comparee de l'inflammation. Masson*. https://ia800708.us.archive.org/3/items/leonssurlapathol00metc/leonssurlapathol00metc.pdf.

Miller, Yury I., Soo-Ho Choi, Longhou Fang, and Sotirios Tsimikas. 2010. "Lipoprotein Modification and Macrophage Uptake: Role of Pathologic Cholesterol Transport in Atherogenesis." In , 229–51. Springer, Dordrecht. https://doi.org/10.1007/978-90-481-8622-8_8.

Mittendorfer, Bettina. 2011. "Origins of Metabolic Complications in Obesity: Adipose Tissue and Free Fatty Acid Trafficking." *Current Opinion in Clinical Nutrition and Metabolic Care* 14 (6): 535–41. https://doi.org/10.1097/MCO.0b013e32834ad8b6.

Miyanishi, Masanori, Kazutoshi Tada, Masato Koike, Yasuo Uchiyama, Toshio Kitamura, and Shigekazu Nagata. 2007. "Identification of Tim4 as a Phosphatidylserine Receptor."

Nature 450 (7168): 435–39. https://doi.org/10.1038/nature06307.

Moore, Kathryn J, and Mason W Freeman. 2006. "Scavenger Receptors in Atherosclerosis: Beyond Lipid Uptake." *Arteriosclerosis, Thrombosis, and Vascular Biology* 26 (8): 1702–11. https://doi.org/10.1161/01.ATV.0000229218.97976.43.

Morigny, Pauline, Marianne Houssier, Etienne Mouisel, and Dominique Langin. 2016. "Adipocyte Lipolysis and Insulin Resistance." *Biochimie* 125 (June): 259–66. https://doi.org/10.1016/J.BIOCHI.2015.10.024.

Morris, David L., Kae Won Cho, Jennifer L. DelProposto, Kelsie E. Oatmen, Lynn M. Geletka, Gabriel Martinez-Santibanez, Kanakadurga Singer, and Carey N. Lumeng. 2013. "Adipose Tissue Macrophages Function as Antigen Presenting Cells and Regulate Adipose Tissue CD4+ T Cells in Mice." *Diabetes* 62 (MHC II): 2762–72. https://doi.org/10.2337/db12-1404.

Muir, Lindsey A., Samadhi Kiridena, Cameron Griffin, Jennifer B. DelProposto, Lynn Geletka, Gabriel Martinez-Santibañez, Brian F. Zamarron, et al. 2018. "Frontline Science: Rapid Adipose Tissue Expansion Triggers Unique Proliferation and Lipid Accumulation Profiles in Adipose Tissue Macrophages." *Journal of Leukocyte Biology* 103 (4): 615–28. https://doi.org/10.1002/JLB.3HI1017-422R.

Murano, I, G Barbatelli, V Parisani, C Latini, G Muzzonigro, M Castellucci, and S Cinti. 2008. "Dead Adipocytes, Detected as Crown-like Structures, Are Prevalent in Visceral Fat Depots of Genetically Obese Mice." *Journal of Lipid Research* 49 (7): 1562–68. https://doi.org/10.1194/jlr.M800019-JLR200.

Murphy, Jaime, Ross Summer, Andrew A Wilson, Darrell N Kotton, and Alan Fine. 2008. "The Prolonged Life-Span of Alveolar Macrophages." *American Journal of Respiratory Cell and Molecular Biology* 38 (4): 380–85. https://doi.org/10.1165/rcmb.2007-0224RC.

Nakajima, Shotaro, Vivien Koh, Ley-Fang Kua, Jimmy So, Lomanto Davide, Kee Siang Lim, Sven Hans Petersen, Wei-Peng Yong, Asim Shabbir, and Koji Kono. 2016. "Accumulation of CD11c+CD163+ Adipose Tissue Macrophages through Upregulation of Intracellular 11β-HSD1 in Human Obesity." *Journal of Immunology (Baltimore, Md. : 1950)* 197 (9): 3735–45. https://doi.org/10.4049/jimmunol.1600895.

Nawaz, Allah, Aminuddin Aminuddin, Tomonobu Kado, Akiko Takikawa, Seiji Yamamoto,

Koichi Tsuneyama, Yoshiko Igarashi, et al. 2017. “CD206+ M2-like Macrophages Regulate Systemic Glucose Metabolism by Inhibiting Proliferation of Adipocyte Progenitors.” *Nature Communications* 8 (1): 286. https://doi.org/10.1038/s41467-017-00231-1.

Nguyen, Khoa D., Yifu Qiu, Xiaojin Cui, Y. P. Sharon Goh, Julia Mwangi, Tovo David, Lata Mukundan, Frank Brombacher, Richard M. Locksley, and Ajay Chawla. 2011. “Alternatively Activated Macrophages Produce Catecholamines to Sustain Adaptive Thermogenesis.” *Nature* 480 (7375): 104–8. https://doi.org/10.1038/nature10653.

Nguyen, M. T. Audrey, Svetlana Favelyukis, Anh-Khoi Nguyen, Donna Reichart, Peter A. Scott, Alan Jenn, Ru Liu-Bryan, Christopher K. Glass, Jaap G. Neels, and Jerrold M. Olefsky. 2007. “A Subpopulation of Macrophages Infiltrates Hypertrophic Adipose Tissue and Is Activated by Free Fatty Acids via Toll-like Receptors 2 and 4 and JNK-Dependent Pathways.” *Journal of Biological Chemistry* 282 (48): 35279–92. https://doi.org/10.1074/jbc.M706762200.

Nielsen, Thomas Svava, Niels Jessen, Jens Otto L Jørgensen, Niels Møller, and Sten Lund. 2014. “Dissecting Adipose Tissue Lipolysis: Molecular Regulation and Implications for Metabolic Disease.” *Journal of Molecular Endocrinology* 52 (3): R199-222. https://doi.org/10.1530/JME-13-0277.

Nishi, Chihiro, Satoshi Toda, Katsumori Segawa, and Shigekazu Nagata. 2014. “Tim4- and MerTK-Mediated Engulfment of Apoptotic Cells by Mouse Resident Peritoneal Macrophages.” *Molecular and Cellular Biology* 34 (8): 1512–20. https://doi.org/10.1128/MCB.01394-13.

O’Neill, Luke A. J., Rigel J. Kishton, and Jeff Rathmell. 2016. “A Guide to Immunometabolism for Immunologists.” *Nature Reviews Immunology* 16 (9): 553–65. https://doi.org/10.1038/nri.2016.70.

Odegaard, Justin I, Roberto R Ricardo-Gonzalez, Matthew H Goforth, Christine R Morel, Vidya Subramanian, Lata Mukundan, Alex Red Eagle, et al. 2007. “Macrophage-Specific PPARgamma Controls Alternative Activation and Improves Insulin Resistance.” *Nature* 447 (7148): 1116–20. https://doi.org/10.1038/nature05894.

Osborn, Olivia, and Jerrold M Olefsky. 2012. “The Cellular and Signaling Networks Linking the Immune System and Metabolism in Disease.” *Nature Medicine* 18 (3): 363–74.

https://doi.org/10.1038/nm.2627.

Ouimet, Mireille, Vivian Franklin, Esther Mak, Xianghai Liao, Ira Tabas, and Yves L. Marcel. 2011. "Autophagy Regulates Cholesterol Efflux from Macrophage Foam Cells via Lysosomal Acid Lipase." *Cell Metabolism* 13 (6): 655–67. https://doi.org/10.1016/J.CMET.2011.03.023.

Park, Daeho, Amelia Hochreiter-Hufford, and Kodi S. Ravichandran. 2009. "The Phosphatidylserine Receptor TIM-4 Does Not Mediate Direct Signaling." *Current Biology* 19 (4): 346–51. https://doi.org/10.1016/J.CUB.2009.01.042.

Patel, Amit A, Yan Zhang, James N Fullerton, Lies Boelen, Anthony Rongvaux, Alexander A Maini, Venetia Bigley, et al. 2017. "The Fate and Lifespan of Human Monocyte Subsets in Steady State and Systemic Inflammation." *The Journal of Experimental Medicine* 214 (7): 1913–23. https://doi.org/10.1084/jem.20170355.

Patsouris, David, Ping-Ping Li, Divya Thapar, Justin Chapman, Jerrold M. Olefsky, and Jaap G. Neels. 2008a. "Ablation of CD11c-Positive Cells Normalizes Insulin Sensitivity in Obese Insulin Resistant Animals." *Cell Metabolism* 8 (4): 301–9. https://doi.org/10.1016/j.cmet.2008.08.015.

Pearce, Edward J, and Bart Everts. 2015. "Dendritic Cell Metabolism." *Nature Reviews. Immunology* 15 (1): 18–29. https://doi.org/10.1038/nri3771.

Perdiguero, Elisa Gomez, and Frederic Geissmann. 2016. "The Development and Maintenance of Resident Macrophages." *Nature Immunology* 17 (1): 2–8. https://doi.org/10.1038/ni.3341.

Pereira, Solange S., and Jacqueline I. Alvarez-Leite. 2014. "Low-Grade Inflammation, Obesity, and Diabetes." *Current Obesity Reports* 3 (4): 422–31. https://doi.org/10.1007/s13679-014-0124-9.

Prieur, Xavier, Crystal Y.L. Mok, Vidya R. Velagapudi, Vanessa Núñez, Lucía Fuentes, David Montaner, Ko Ishikawa, et al. 2011. "Differential Lipid Partitioning Between Adipocytes and Tissue Macrophages Modulates Macrophage Lipotoxicity and M2/M1 Polarization in Obese Mice." *Diabetes* 60 (3): 797–809. https://doi.org/10.2337/db10-0705.

Qiu, Yifu, Khoa D. Nguyen, Justin I. Odegaard, Xiaojin Cui, Xiaoyu Tian, Richard M.

Locksley, Richard D. Palmiter, and Ajay Chawla. 2014. “Eosinophils and Type 2 Cytokine Signaling in Macrophages Orchestrate Development of Functional Beige Fat.” *Cell* 157 (6): 1292–1308. https://doi.org/10.1016/j.cell.2014.03.066.

Rader, Daniel J., and Ellen Puré. 2005. “Lipoproteins, Macrophage Function, and Atherosclerosis: Beyond the Foam Cell?” *Cell Metabolism* 1 (4): 223–30. https://doi.org/10.1016/J.CMET.2005.03.005.

Reilly, Shannon M., and Alan R. Saltiel. 2014. “A Complex Role for Adipose Tissue Macrophages.” *Nature Reviews Endocrinology* 10 (4): 193–94. https://doi.org/10.1038/nrendo.2014.12.

———. 2017. “Adapting to Obesity with Adipose Tissue Inflammation.” *Nature Reviews Endocrinology* 13 (11): 633–43. https://doi.org/10.1038/nrendo.2017.90.

Reiner, Željko, Ornella Guardamagna, Devaki Nair, Handrean Soran, Kees Hovingh, Stefano Bertolini, Simon Jones, et al. 2014. “Lysosomal Acid Lipase Deficiency--an under-Recognized Cause of Dyslipidaemia and Liver Dysfunction.” *Atherosclerosis* 235 (1): 21–30. https://doi.org/10.1016/j.atherosclerosis.2014.04.003.

Remmerie, Anneleen, and Charlotte L. Scott. 2018. “Macrophages and Lipid Metabolism.” *Cellular Immunology*, February. https://doi.org/10.1016/J.CELLIMM.2018.01.020.

Ricardo-Gonzalez, Roberto R, Alex Red Eagle, Justin I Odegaard, Hani Jouihan, Christine R Morel, Jose E Heredia, Lata Mukundan, Davina Wu, Richard M Locksley, and Ajay Chawla. 2010. “IL-4/STAT6 Immune Axis Regulates Peripheral Nutrient Metabolism and Insulin Sensitivity.” *Proceedings of the National Academy of Sciences of the United States of America* 107 (52): 22617–22. https://doi.org/10.1073/pnas.1009152108.

Rosas, M., L. C. Davies, P. J. Giles, C.-T. Liao, B. Kharfan, T. C. Stone, V. B. O’Donnell, D. J. Fraser, S. A. Jones, and P. R. Taylor. 2014. “The Transcription Factor Gata6 Links Tissue Macrophage Phenotype and Proliferative Renewal.” *Science* 344 (6184): 645–48. https://doi.org/10.1126/science.1251414.

Samuel, Varman T, Zhen-Xiang Liu, Xianqin Qu, Benjamin D Elder, Stefan Bilz, Douglas Befroy, Anthony J Romanelli, and Gerald I Shulman. 2004. “Mechanism of Hepatic Insulin Resistance in Non-Alcoholic Fatty Liver Disease.” *The Journal of Biological Chemistry* 279 (31): 32345–53. https://doi.org/10.1074/jbc.M313478200.

Santiago, César, Angela Ballesteros, Laura Martínez-Muñoz, Mario Mellado, Gerardo G. Kaplan, Gordon J. Freeman, and José M. Casasnovas. 2007. "Structures of T Cell Immunoglobulin Mucin Protein 4 Show a Metal-Ion-Dependent Ligand Binding Site Where Phosphatidylserine Binds." *Immunity* 27 (6): 941–51. https://doi.org/10.1016/j.immuni.2007.11.008.

Schipper, Henk S., Berent Prakken, Eric Kalkhoven, and Marianne Boes. 2012. "Adipose Tissue-Resident Immune Cells: Key Players in Immunometabolism." *Trends in Endocrinology & Metabolism* 23 (8): 407–15. https://doi.org/10.1016/J.TEM.2012.05.011.

Schlitzer, Andreas, and Joachim L Schultze. 2017. "Tissue-Resident Macrophages - How to Humanize Our Knowledge." *Immunology and Cell Biology* 95 (2): 173–77. https://doi.org/10.1038/icb.2016.82.

Schreyer, S A, D L Wilson, and R C LeBoeuf. 1998. "C57BL/6 Mice Fed High Fat Diets as Models for Diabetes-Accelerated Atherosclerosis." *Atherosclerosis* 136 (1): 17–24. https://doi.org/10.1016/S0021-9150(97)00165-2.

Schulz, C., E. G. Perdiguero, L. Chorro, H. Szabo-Rogers, N. Cagnard, K. Kierdorf, M. Prinz, et al. 2012a. "A Lineage of Myeloid Cells Independent of Myb and Hematopoietic Stem Cells." *Science* 336 (6077): 86–90. https://doi.org/10.1126/science.1219179.

Scotland, R. S., M. J. Stables, S. Madalli, P. Watson, and D. W. Gilroy. 2011. "Sex Differences in Resident Immune Cell Phenotype Underlie More Efficient Acute Inflammatory Responses in Female Mice." *Blood* 118 (22): 5918–27. https://doi.org/10.1182/blood-2011-03-340281.

Scott, Charlotte L, and Martin Guilliams. 2018. "The Role of Kupffer Cells in Hepatic Iron and Lipid Metabolism." *Journal of Hepatology* 0 (0). https://doi.org/10.1016/j.jhep.2018.02.013.

Scott, Charlotte L, Fang Zheng, Patrick De Baetselier, Liesbet Martens, Yvan Saeys, Sofie De Prijck, Saskia Lippens, et al. 2016. "Bone Marrow-Derived Monocytes Give Rise to Self-Renewing and Fully Differentiated Kupffer Cells." *Nature Communications* 7 (January): 10321. https://doi.org/10.1038/ncomms10321.

Serbina, Natalya V, and Eric G Pamer. 2006. "Monocyte Emigration from Bone Marrow

during Bacterial Infection Requires Signals Mediated by Chemokine Receptor CCR2." *Nature Immunology* 7 (3): 311–17. https://doi.org/10.1038/ni1309.

Shapiro, Hagit, Tal Pecht, Ruthy Shaco-Levy, Ilana Harman-Boehm, Boris Kirshtein, Yael Kuperman, Alon Chen, Matthias Blüher, Iris Shai, and Assaf Rudich. 2013. "Adipose Tissue Foam Cells Are Present in Human Obesity." *The Journal of Clinical Endocrinology & Metabolism* 98 (3): 1173–81. https://doi.org/10.1210/jc.2012-2745.

Shaw, Tovah N, Stephanie A Houston, Kelly Wemyss, Hayley M Bridgeman, Thomas A Barbera, Tamsin Zangerle-Murray, Patrick Strangward, et al. 2018. "Tissue-Resident Macrophages in the Intestine Are Long Lived and Defined by Tim-4 and CD4 Expression." *The Journal of Experimental Medicine* 215 (6): 1507–18. https://doi.org/10.1084/jem.20180019.

Sheedy, Frederick J, Alena Grebe, Katey J Rayner, Parisa Kalantari, Bhama Ramkhelawon, Susan B Carpenter, Christine E Becker, et al. 2013. "CD36 Coordinates NLRP3 Inflammasome Activation by Facilitating Intracellular Nucleation of Soluble Ligands into Particulate Ligands in Sterile Inflammation." *Nature Immunology* 14 (8): 812–20. https://doi.org/10.1038/ni.2639.

Sheng, Jianpeng, Christiane Ruedl, and Klaus Karjalainen. 2015. "Most Tissue-Resident Macrophages Except Microglia Are Derived from Fetal Hematopoietic Stem Cells." *Immunity* 43 (2): 382–93. https://doi.org/10.1016/J.IMMUNI.2015.07.016.

Shi, Chao, and Eric G Pamer. 2011. "Monocyte Recruitment during Infection and Inflammation." *Nature Reviews. Immunology* 11 (11): 762–74. https://doi.org/10.1038/nri3070.

Shin, Kyung Cheul, Injae Hwang, Sung Sik Choe, Jeu Park, Yul Ji, Jong In Kim, Gha Young Lee, et al. 2017. "Macrophage VLDLR Mediates Obesity-Induced Insulin Resistance with Adipose Tissue Inflammation." *Nature Communications* 8 (1): 1087. https://doi.org/10.1038/s41467-017-01232-w.

Smith, Ulf. 2015. "Abdominal Obesity: A Marker of Ectopic Fat Accumulation." *Journal of Clinical Investigation* 125 (5): 1790–92. https://doi.org/10.1172/JCI81507.

Spracklen, Cassandra N., Peng Chen, Young Jin Kim, Xu Wang, Hui Cai, Shengxu Li, Jirong Long, et al. 2017. "Association Analyses of East Asian Individuals and Trans-Ancestry

Analyses with European Individuals Reveal New Loci Associated with Cholesterol and Triglyceride Levels." *Human Molecular Genetics* 26 (9): 1770–84. https://doi.org/10.1093/hmg/ddx062.

Stein, M, S Keshav, N Harris, and S Gordon. 1992. "Interleukin 4 Potently Enhances Murine Macrophage Mannose Receptor Activity: A Marker of Alternative Immunologic Macrophage Activation." *The Journal of Experimental Medicine* 176 (1): 287–92. http://www.ncbi.nlm.nih.gov/pubmed/1613462.

Stern, Jennifer H, Joseph M Rutkowski, and Philipp E Scherer. 2016. "Cell Metabolism Review Adiponectin, Leptin, and Fatty Acids in the Maintenance of Metabolic Homeostasis through Adipose Tissue Crosstalk." https://doi.org/10.1016/j.cmet.2016.04.011.

Surakka, Ida, Momoko Horikoshi, Reedik Mägi, Antti Pekka Sarin, Anubha Mahajan, Vasiliki Lagou, Letizia Marullo, et al. 2015. "The Impact of Low-Frequency and Rare Variants on Lipid Levels." *Nature Genetics* 47 (6): 589–97. https://doi.org/10.1038/ng.3300.

Takahashi, K, F Yamamura, and M Naito. 1989. "Differentiation, Maturation, and Proliferation of Macrophages in the Mouse Yolk Sac: A Light-Microscopic, Enzyme-Cytochemical, Immunohistochemical, and Ultrastructural Study." *Journal of Leukocyte Biology* 45 (2): 87–96. http://www.ncbi.nlm.nih.gov/pubmed/2536795.

Takahashi, Manabu, Hiroaki Yagyu, Fumiko Tazoe, Shuichi Nagashima, Taichi Ohshiro, Kenta Okada, Jun-ichi Osuga, Ira J. Goldberg, and Shun Ishibashi. 2013. "Macrophage Lipoprotein Lipase Modulates the Development of Atherosclerosis but Not Adiposity." *Journal of Lipid Research* 54 (4): 1124–34. https://doi.org/10.1194/jlr.M035568.

Tamoutounour, Samira, Sandrine Henri, Hugues Lelouard, Béatrice de Bovis, Colin de Haar, C. Janneke van der Woude, Andrea M. Woltman, et al. 2012. "CD64 Distinguishes Macrophages from Dendritic Cells in the Gut and Reveals the Th1-Inducing Role of Mesenteric Lymph Node Macrophages during Colitis." *European Journal of Immunology* 42 (12): 3150–66. https://doi.org/10.1002/eji.201242847.

Teslovich, Tanya M., Kiran Musunuru, Albert V. Smith, Andrew C. Edmondson, Ioannis M. Stylianou, Masahiro Koseki, James P. Pirruccello, et al. 2010. "Biological, Clinical and Population Relevance of 95 Loci for Blood Lipids." *Nature* 466 (7307): 707–13. https://doi.org/10.1038/nature09270.

Thomas, Dylan, and Caroline Apovian. 2017. “Macrophage Functions in Lean and Obese Adipose Tissue.” *Metabolism* 72 (July): 120–43. https://doi.org/10.1016/J.METABOL.2017.04.005.

Tiemessen, M. M., A. L. Jagger, H. G. Evans, M. J. C. van Herwijnen, S. John, and L. S. Taams. 2007. “CD4+CD25+Foxp3+ Regulatory T Cells Induce Alternative Activation of Human Monocytes/Macrophages.” *Proceedings of the National Academy of Sciences* 104 (49): 19446–51. https://doi.org/10.1073/pnas.0706832104.

Tontonoz, P, L Nagy, J G Alvarez, V A Thomazy, and R M Evans. 1998. “PPARgamma Promotes Monocyte/Macrophage Differentiation and Uptake of Oxidized LDL.” *Cell* 93 (2): 241–52. http://www.ncbi.nlm.nih.gov/pubmed/9568716.

Tsou, Chia-Lin, Wendy Peters, Yue Si, Sarah Slaymaker, Ara M Aslanian, Stuart P Weisberg, Matthias Mack, and Israel F Charo. 2007. “Critical Roles for CCR2 and MCP-3 in Monocyte Mobilization from Bone Marrow and Recruitment to Inflammatory Sites.” *The Journal of Clinical Investigation* 117 (4): 902–9. https://doi.org/10.1172/JCI29919.

Uderhardt, Stefan, Martin Herrmann, Olga V. Oskolkova, Susanne Aschermann, Wolfgang Bicker, Natacha Ipseiz, Kerstin Sarter, et al. 2012. “12/15-Lipoxygenase Orchestrates the Clearance of Apoptotic Cells and Maintains Immunologic Tolerance.” *Immunity* 36 (5): 834–46. https://doi.org/10.1016/J.IMMUNI.2012.03.010.

Wang, Qiong A, Philipp E Scherer, and Rana K Gupta. 2014. “Improved Methodologies for the Study of Adipose Biology: Insights Gained and Opportunities Ahead.” *Journal of Lipid Research* 55 (4): 605–24. https://doi.org/10.1194/jlr.R046441.

Wang, Qiong A, Caroline Tao, Rana K Gupta, and Philipp E Scherer. 2013. “Tracking Adipogenesis during White Adipose Tissue Development, Expansion and Regeneration.” *Nature Medicine* 19 (10): 1338–44. https://doi.org/10.1038/nm.3324.

Weisberg, Stuart P, Daniel McCann, Manisha Desai, Michael Rosenbaum, Rudolph L Leibel, Anthony W Ferrante, and Jr. 2003. “Obesity Is Associated with Macrophage Accumulation in Adipose Tissue.” *The Journal of Clinical Investigation* 112 (12): 1796–1808. https://doi.org/10.1172/JCI19246.

Weissglas-Volkov, Daphna, Carlos A Aguilar-Salinas, Elina Nikkola, Kerry A Deere, Ivette Cruz-Bautista, Olimpia Arellano-Campos, Linda Liliana Muñoz-Hernandez, et al. 2013.

"Genomic Study in Mexicans Identifies a New Locus for Triglycerides and Refines European Lipid Loci." *Journal of Medical Genetics* 50 (5): 298–308. https://doi.org/10.1136/jmedgenet-2012-101461.

Wentworth, J. M., G. Naselli, W. A. Brown, L. Doyle, B. Phipson, G. K. Smyth, M. Wabitsch, P. E. O'Brien, and L. C. Harrison. 2010. "Pro-Inflammatory CD11c+CD206+ Adipose Tissue Macrophages Are Associated With Insulin Resistance in Human Obesity." *Diabetes* 59 (7): 1648–56. https://doi.org/10.2337/db09-0287.

Wentworth, John M, Gaetano Naselli, Wendy A Brown, Lisa Doyle, Belinda Phipson, Gordon K Smyth, Martin Wabitsch, Paul E O'Brien, and Leonard C Harrison. 2010. "Pro-Inflammatory CD11c+CD206+ Adipose Tissue Macrophages Are Associated with Insulin Resistance in Human Obesity." *Diabetes* 59 (7): 1648–56. https://doi.org/10.2337/db09-0287.

"WHO | Obesity and Overweight." 2018. *WHO*. http://www.who.int/mediacentre/factsheets/fs311/en/.

"WHO | Waist Circumference and Waist–Hip Ratio." 2018. *WHO*.

Willer, Cristen J, Ellen M Schmidt, Sebanti Sengupta, Gonçalo R Abecasis, and Global Lipids Genetics Consortium. 2013. "Discovery and Refinement of Loci Associated with Lipid Levels." *Nature Genetics* 45 (11): 1274–83. https://doi.org/10.1038/ng.2797.

Wong, K. L., J. J.-Y. Tai, W.-C. Wong, H. Han, X. Sem, W.-H. Yeap, P. Kourilsky, and S.-C. Wong. 2011. "Gene Expression Profiling Reveals the Defining Features of the Classical, Intermediate, and Nonclassical Human Monocyte Subsets." *Blood* 118 (5): e16–31. https://doi.org/10.1182/blood-2010-12-326355.

Wong, Kit, Patricia A Valdez, Christine Tan, Sherry Yeh, Jo-Anne Hongo, and Wenjun Ouyang. 2010. "Phosphatidylserine Receptor Tim-4 Is Essential for the Maintenance of the Homeostatic State of Resident Peritoneal Macrophages." *Proceedings of the National Academy of Sciences of the United States of America* 107 (19): 8712–17. https://doi.org/10.1073/pnas.0910929107.

Wu, D., A. B. Molofsky, H.-E. Liang, R. R. Ricardo-Gonzalez, H. A. Jouihan, J. K. Bando, A. Chawla, and R. M. Locksley. 2011. "Eosinophils Sustain Adipose Alternatively Activated Macrophages Associated with Glucose Homeostasis." *Science* 332 (6026):

243–47. https://doi.org/10.1126/science.1201475.

Wynn, Thomas A, and Kevin M Vannella. 2016. “Macrophages in Tissue Repair, Regeneration, and Fibrosis.” *Immunity* 44 (3): 450–62. https://doi.org/10.1016/j.immuni.2016.02.015.

Xu, Haiyan, Glenn T. Barnes, Qing Yang, Guo Tan, Daseng Yang, Chieh J. Chou, Jason Sole, et al. 2003. “Chronic Inflammation in Fat Plays a Crucial Role in the Development of Obesity-Related Insulin Resistance.” *Journal of Clinical Investigation* 112 (12): 1821–30. https://doi.org/10.1172/JCI19451.

Xu, Xiaoyuan, Ambar Grijalva, Alicja Skowronski, Marco van Eijk, Mireille J. Serlie, and Anthony W. Ferrante. 2013. “Obesity Activates a Program of Lysosomal-Dependent Lipid Metabolism in Adipose Tissue Macrophages Independently of Classic Activation.” *Cell Metabolism* 18 (6): 816–30. https://doi.org/10.1016/J.CMET.2013.11.001.

Yanagihashi, Yuichi, Katsumori Segawa, Ryota Maeda, Yo-Ichi Nabeshima, and Shigekazu Nagata. 2017. “Mouse Macrophages Show Different Requirements for Phosphatidylserine Receptor Tim4 in Efferocytosis.” *Proceedings of the National Academy of Sciences of the United States of America* 114 (33): 8800–8805. https://doi.org/10.1073/pnas.1705365114.

Ye, Jianping. 2013. “Mechanisms of Insulin Resistance in Obesity.” *Frontiers of Medicine* 7 (1): 14–24. https://doi.org/10.1007/s11684-013-0262-6.

Yona, Simon, Ki-Wook Kim, Yochai Wolf, Alexander Mildner, Diana Varol, Michal Breker, Dalit Strauss-Ayali, et al. 2013. “Fate Mapping Reveals Origins and Dynamics of Monocytes and Tissue Macrophages under Homeostasis.” *Immunity* 38 (1): 79–91. https://doi.org/10.1016/j.immuni.2012.12.001.

Zeyda, M, D Farmer, J Todoric, O Aszmann, M Speiser, G Györi, G J Zlabinger, and T M Stulnig. 2007. “Human Adipose Tissue Macrophages Are of an Anti-Inflammatory Phenotype but Capable of Excessive pro-Inflammatory Mediator Production.” *International Journal of Obesity* 31 (9): 1420–28. https://doi.org/10.1038/sj.ijo.0803632.

Zhang, Weiyu, Xianling Zhang, Huan Wang, Xin Guo, Honggui Li, Ying Wang, Xin Xu, et al. 2012. “AMP-Activated Protein Kinase A1 Protects Against Diet-Induced Insulin Resistance and Obesity.” https://doi.org/10.2337/db11-1373doi:10.2337/db11-1373/-

/DC1.

Zhang, Xia, Ricardo Goncalves, and David M Mosser. 2008. “The Isolation and Characterization of Murine Macrophages.” *Current Protocols in Immunology* Chapter 14 (November): Unit 14.1. https://doi.org/10.1002/0471142735.im1401s83.

Zheng, C, Q Yang, J Cao, N Xie, K Liu, P Shou, F Qian, Y Wang, and Y Shi. 2016a. “Local Proliferation Initiates Macrophage Accumulation in Adipose Tissue during Obesity.” *Cell Death & Disease* 7 (3): e2167. https://doi.org/10.1038/cddis.2016.54.

Zigmond, E., S. Samia-Grinberg, M. Pasmanik-Chor, E. Brazowski, O. Shibolet, Z. Halpern, and C. Varol. 2014. “Infiltrating Monocyte-Derived Macrophages and Resident Kupffer Cells Display Different Ontogeny and Functions in Acute Liver Injury.” *The Journal of Immunology* 193 (1): 344–53. https://doi.org/10.4049/jimmunol.1400574.